HÍ | UMHVERFIS- OG BYGGINGARVERKFRÆÐIDEILD

Stífni- og sveiflueiginleikar íslensks jarðvegs og jarðsniða

Characterization of the dynamic properties of Icelandic soil materials

Lokaskýrsla (vegna áranna 2023 og 2024)

Verkefni styrkt af Rannsóknasjóði Vegagerðarinnar

Verkefnisstjóri: Elín Ásta Ólafsdóttir, HÍ

Samstarfsaðilar: Bjarni Bessason, HÍ, Sigurður Erlingsson, HÍ

Dagsetning: 29. mars 2025

1. Inngangur

Jarðfræðilegar aðstæður á Íslandi eru að mörgu leyti sérstakar. Setlög hérlendis eru jarðfræðilega ung, að stórum hluta mynduð í hamfaraatburðum og oft lausþjöppuð [1]. Upplýsingar um aflfræðilega eiginleika þeirra verða því ekki eingöngu sóttar í erlendar rannsóknaniðurstöður heldur þarf að afla þeirra með staðbundnum hætti.

Yfirborðsbylgjumælingar (*surface wave methods*) eru skilvirk og hagkvæm leið til þess að ákvarða stífnieiginleika (skúfbylgjuhraða og skúfstuðul) jarðvegs. Framkvæmd yfirborðsbylgjumælinga raskar ekki jarðveginum sem mældur er (*non-invasive testing*) og krefst einungis létts mælibúnaðar. Rannsakendur við Umhverfis- og byggingarverkfræðideild HÍ hafa framkvæmt aktífar yfirborðsbylgjumælingar (*active-source surface wave analysis*) hérlendis frá árinu 1996, fyrst SASW mælingar (*Spectral Analysis of Surface Waves*) [2–3] en MASW mælingar (*Multichannel Analysis of Surface Waves*) frá 2013 [4]. Framkvæmd MASW yfirborðsbylgjumælinga er lýst á mynd 1. Slíkar mælingar fara þannig fram að yfirborðsbylgjur eru framkallaðar með höggi á yfirborð jarðar og útbreiðsla þeirra skráð með röð hraðanema. MASW mælingar skila að jafnaði upplýsingum um stífnieiginleika jarðvegs niður á 10–30 m dýpi. Passífar MAM yfirborðsbylgjumælingar (*Microtremour Array Measurements*) byggja á greiningu umhverfistitrings sem skráður er með tvívíðu neti hraðanema sem komið er fyrir á yfirborði. Árið 2020 var slíkum mælingum beitt í fyrsta sinn hérlendis [5]. Í samanburði við aktífar yfirborðsbylgjumælingar skila passífar mælingar auknu könnunardýpi við mat á skúfbylgjuhraða, þó á kostnað nákvæmni næst yfirborði. Að auki geta passífar mælingar gefið upplýsingar um grunntíðni jarðsniða.

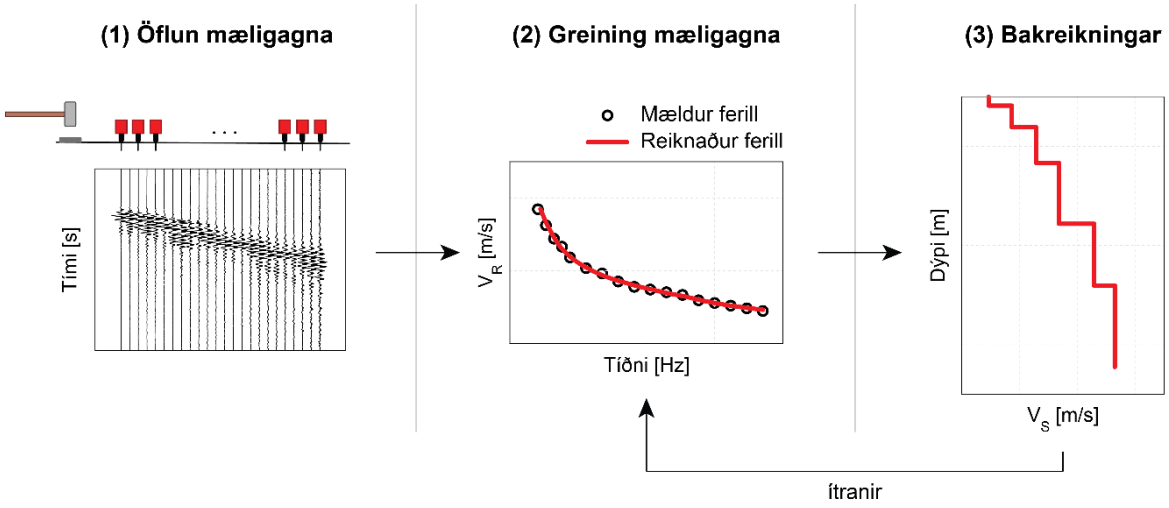

Mynd 1: *Framkvæmd aktífra yfirborðsbylgjumælinga. 1) Öflun mæligagna í felti. 2) Greining mæligagna. Mat á tvístrunarferli prófunarstaðar sem lýsir útbreiðsluhraða Rayleigh bylgna sem fall af tíðni. 3) Bakreikningar til að ákvarða skúfbylgjuhraða sem fall af dýpi. Mynd: Elín Ásta Ólafsdóttir o.fl. [6].*

Yfirborðsbylgjumælingar hafa gefið góða raun við íslenskar aðstæður, þar með talið til prófana í grófum eða samlímdum jarðvegi. Ólíkt borholumælingum og kóníska mælingum (CPT, *Cone Penetration Tests*) skila yfirborðsbylgjumælingar meðaltalsstífnieiginleikum þess svæðis þar sem mælinemum er komið fyrir. Úrvinnsla og greining mæligagna byggir á lagskiptu líkani með láréttum jarðlögum. Yfirborðsbylgjumælingar henta því síður á stöðum þar sem breytileiki innan jarðlagastaflans er mikill og víkur verulega frá láréttri lagskiptingu. Þá er þekkt að aktífar yfirborðsbylgjuaðferðir, svo sem MASW mælingar, henta illa við aðstæður þar sem stíf jarðlög (t.d. hraun- eða kargalög) liggja ofan á lausum jarðlögum (með mun lægri skúfbylgjuhraða). Við slíkar aðstæður er nær ómögulegt að örva þau jarðlög sem liggja undir stífa laginu með höggálagi á yfirborði.

Þekking á staðbundnum eiginleikum jarðefna er meðal annars nauðsynleg við hönnun og mat á áhrifum jarðskjálfta á mannvirki. Á stöðum þar sem ekki gætir áhrifa frá óreglulegu landslagi (*topographic and basin effects*) er tölulegt mat á staðbundinni sveiflumögnun með „equivalent linear“ (EQL) aðferð byggt á upplýsingum um stífni og heildarþykkt jarðlaga, ásamt ólínulegum stífni- og dempunareiginleikum jarðvegs við hærri streitu [7]. Yfirborðsbylgjumælingar skila upplýsingum um stífnieiginleika jarðefna við lága streitu auk upplýsinga um þykkt einstakra laga en upplýsingar um dýnamíska hegðun jarðefna við hærri streitu þarf að ákvarða með prófunum á rannsóknarstofu. Samhliða aukinni þróun efnislíkana (*advanced non-linear soil constitutive models*) [t.d. 8–12], sem lýsa spennu-streitu sambandi fyrir ólíkar gerðir jarðvegs, hefur töluleg greining á sveiflumögnunaráhrifum og ysjunarhegðun (*soil liquefaction behaviour*) með ólínulegum aðferðum rutt sér rúms í auknum mæli erlendis á undanförnum árum. Til þess að ólínuleg greining skili raunsæjum niðurstöðum (miðað við þá gerð jarðefnis sem á í hlut) er þó nauðsynlegt að kvarða stika hvers efnislíkans að eiginleikum einstakra jarðefna.

Meginmarkmið verkefnisins *Stífni- og sveiflueiginleikar íslensks jarðvegs og jarðsniða* voru:

1) Að byggja upp reynslu og þekkingu á samþættri notkun aktífra og passífra yfirborðsbylgjumælinga við íslenskar aðstæður. Áhersla er lögð á þróun aðferða sem henta til ákvörðunar á skúfbylgjuhraða og lagskiptingum á svæðum þar sem setlög eru þykk (meira en 15–30 m).
2) Að kortleggja náttúrulega tíðni mælistaða og þykkt setlaga með samþættri notkun HVSR-tækni og yfirborðsbylgjumælinga. Niðurstöður nýtast til að aðlaga reynslulíkingar, sem tengja saman náttúrulega tíðni setlagastafla og dýpi á fast, að eiginleikum íslenskra jarðefna.
3) Að meta styrk-, stífni- og dempunareiginleika íslenskra jarðefna með tilraunastofuprófunum.
4) Að kvarða valin efnislíkön sem lýsa ólínulegu spennu-streitu sambandi jarðvegs við hærri streitu (*soil constitutive models*) að eiginleikum íslenskra jarðefna.
5) Að greina staðbundna sveiflumögnun (*seismic site amplification*) valinna jarðsniða með tölulegum aðferðum.
6) Að byggja upp og viðhalda opnum gagnagrunni sem gerir hönnuðum, rannsakendum og öðrum mögulegt að nálgast og bera saman niðurstöður mælinga frá mismunandi stöðum.

2. Samantekt á helstu niðurstöðum

Verkefnið *Stífni- og sveiflueiginleikar íslensks jarðvegs og jarðsniða* skiptist í fjóra meginverkþætti (VÞ1−VÞ4). VÞ1 og VÞ2 sneru að mati á sveiflufræðilegum eiginleikum jarðvegs með felt- og tilraunastofumælingum. Í VÞ3 voru niðurstöður mælinga nýttar, ásamt öðrum fyrirliggjandi gögnum, til tölulegrar greiningar á sveiflumögnun jarðlagastafla. VÞ4 sneri að opnu aðgengi að mæliniðurstöðum og hugbúnaði. Meginafrakstur verkefnisins er:

- Öflug mæliaðferð, byggð á samþættri greiningu aktífra og passífra yfirborðsbylgna, til ákvörðunar á skúfbylgjuhraða/skúfstuðli jarðvegssniða, lagþykktum og dýpi á fast/stíf jarðlög á allt að 150−200 m dýpi. [VÞ1]
- Reynslulíkingar, sem aðlagaðar hafa verið að íslenskum jarðvegsaðstæðum og sem má nota til þess að (i) meta skúfbylgjuhraða/hágildi skúfstuðuls ólíkra jarðvegsgerða og (ii) meta dýpi niður á fast út frá upplýsingum um náttúrulega tíðni setlagastafla. [VÞ1]
- Greining á styrk og spennu-streitu sambandi sandsýna frá bakka Ölfusár fyrir ólík statísk og dýnamísk álagstilfelli (*monotonic and cyclic loading*), ásamt mati á ysjunarhegðun (*liquefaction characteristics*) efnisins. [VÞ2]
- Töluleg efnislíkön sem lýsa ólínulegu spennu-streitu sambandi jarðvegs við hærri streitu (*soil constitutive models*) sem hafa verið kvörðuð að eiginleikum íslenskra jarðefna. [VÞ2]
- Rannsóknaniðurstöður á sveiflueiginleikum jarðsniða með tilliti til jarðskjálftaálags á völdum stöðum. [VÞ3]
- Gagnagrunnur með mældum skúfbylgjuhraðaferlum prófunarstaða sem er aðgengilegur á opinni vefsíðu (https://serice.hi.is/#/velocity-profiles). [VÞ4]
- Opinn hugbúnaður fyrir yfirborðsbylgjumælingar og gagnaúrvinnslu. [VÞ4]

Niðurstöður verkefnisins hafa verið kynntar í ritrýndum vísindatímaritum og á ráðstefnum í jarðskjálftaverkfræði og jarðtækni. Enn fremur hefur áhersla verið lögð á að kynna niðurstöður verkefnisins á innlendum vettvangi, svo sem með erindi á Rannsóknaráðstefnu Vegagerðarinnar í nóvember 2024 og með grein í Verktækni, tímariti Verkfræðingafélags Íslands. Hér að neðan má sjá yfirlit yfir birtar niðurstöður verkefnisins. Nánar er greint frá niðurstöðum hvers verkþáttar í köflum 2.1−2.4, sem og í viðaukum þessarar skýrslu.

Birtar tímaritsgreinar og tímaritsgreinar í ritrýningarferli

Elín Ásta Ólafsdóttir, Bjarni Bessason, Sigurður Erlingsson og Amir M. Kaynia. (2024). A Tool for Processing and Inversion of MASW Data and a Study of Inter-Session Variability of MASW. *Geotechnical Testing Journal*, 47(5), 1006−1025. https://doi.org/10.1520/GTJ20230380

Elín Ásta Ólafsdóttir, Bjarni Bessason og Sigurður Erlingsson. (2023). Gagnagrunnur fyrir skúfbylgjuhraða í jarðsniðum byggður á yfirborðsbylgjumælingum. *Icelandic Journal of Engineering (Verktækni - Tímarit Verkfræðingafélags Íslands)*, 29(1). https://doi.org/10.33112/ije.29.3

Elín Ásta Ólafsdóttir, Sigurður Erlingsson og Bjarni Bessason. (2023). Hybrid non-invasive characterization of soil strata at sites with and without embedded lava rock layers in the South Iceland Seismic Zone. *Bulletin of Engineering Geology and the Environment*, 82(4), 146. https://doi.org/10.1007/s10064-023-03136-0

Seyed Javad Fattahi, Yaser Jafarian, Maria Konstadinou, Elín Ásta Ólafsdóttir, Sigurður Erlingsson, Bjarni Bessason og Rajesh Rupakhety. Liquefaction assessment of Icelandic Basaltic Sand through Monotonic and Cyclic Direct Simple Shear Tests. Grein í ritrýningu hjá *International Journal of Geotechnical Engineering*.

Birtar ráðstefnugreinar

Elín Ásta Ólafsdóttir, Bjarni Bessason og Sigurður Erlingsson. (2024). MASWavesPy: A Python package for analysis of MASW data. Birt í ráðstefnuriti *19th Nordic Geotechnical Meeting (NGM 2024)*, 18.–20. september 2024, Gautaborg, Svíþjóð. Grein kynnt með fyrirlestri á ráðstefnunni.

Elín Ásta Ólafsdóttir, Sigurður Erlingsson og Bjarni Bessason. (2024). Geotechnical seismic site characterization of deep alluvial sand sites in the South Iceland Lowland. Birt í ráðstefnuriti *XVIII European Conference on Soil Mechanics and Geotechnical Engineering*, 26.–30. ágúst 2024, Lissabon, Portúgal. Grein kynnt með fyrirlestri á ráðstefnunni.

Elín Ásta Ólafsdóttir, Sigurður Erlingsson og Bjarni Bessason. (2024). Database of measured shear wave velocity profiles for Icelandic soil sites. Birt í ráðstefnuriti *XVIII European Conference on Soil Mechanics and Geotechnical Engineering*, 26.–30. ágúst 2024, Lissabon, Portúgal. Grein kynnt með veggspjaldi á ráðstefnunni.

Elín Ásta Ólafsdóttir, Bjarni Bessason og Sigurður Erlingsson. (2024). Non-invasive seismic site characterization of sandwiched lava-rock/sedimentary sites in Iceland. Birt í ráðstefnuriti *18th World Conference on Earthquake Engineering (WCEE2024)*, 30. júní til 5. júlí 2024, Mílanó, Ítalíu. Grein kynnt með fyrirlestri á ráðstefnunni.

Seyed Javad Fattahi, Yaser Jafarian, Maria Konstadinou, Elín Ásta Ólafsdóttir, Sigurður Erlingsson, Bjarni Bessason og Rajesh Rupakhety. (2023). Model calibration and nonlinear site response analysis for medium compacted saturated volcanic sand. *Proceedings of the 9th International Conference on Computational Methods in Structural Dynamics and Earthquake Engineering (COMPDYN 2023)*, bls. 4189–4196.

Enn fremur er greint frá niðurstöðum verkþátta VÞ2 og VÞ3 í tímaritsgrein sem ráðgert er að send verði til ritrýningar á árinu 2025. Þá hefur útdrætti að ráðstefnugrein, þar sem fjallað er um niðurstöður verkefnisins, verið skilað til mögulegrar birtingar í ráðstefnuriti alþjóðlegu jarðtækniráðstefnunnar, *21st International Conference on Soil Mechanics and Geotechnical Engineering 2026*.

2.1. Yfirborðsbylgjumælingar og þróun greiningaraðferða [VÞ1]

Eins og áður var getið skila MASW mælingar að jafnaði upplýsingum um stífnieiginleika jarðvegs niður á 10–30 m dýpi. Könnunardýpið takmarkast af lengstu bylgjulengd Rayleigh bylgna sem unnt er að framkalla og greina hverju sinni, nokkuð sem er einkum háð staðbundnum jarðvegsaðstæðum. Enn fremur er þekkt að MASW yfirborðsbylgjumælingar henta illa þar sem stíf jarðlög liggja ofan á lausum jarðlögum. Því eru aktífar MASW mælingar einar og sér ekki alltaf fullnægjandi til að rannsaka jarðvegsaðstæður hér á landi. Til að bregðast við þessu hefur VÞ1 miðað að því að samþætta notkun aktífra MASW mælinga með öðrum feltmæliaðferðum, sér í lagi svokölluðum passífum yfirborðsbylgjumælingum. Með samþættri greiningu á gögnum frá aktífum og passífum mælingum má nýta kosti beggja aðferðanna, þ.e. auka könnunardýpi mælingarinnar án þess að skerða nákvæmi hennar nálægt yfirborði.

Yfirlit yfir aðferð til slíkrar samþættrar greiningar, sem var þróuð sem hluti verkefnisins og lýst í tímaritsgrein sem birtist í *Bulletin of Engineering Geology and the Environment* [13], má sjá á mynd 2.

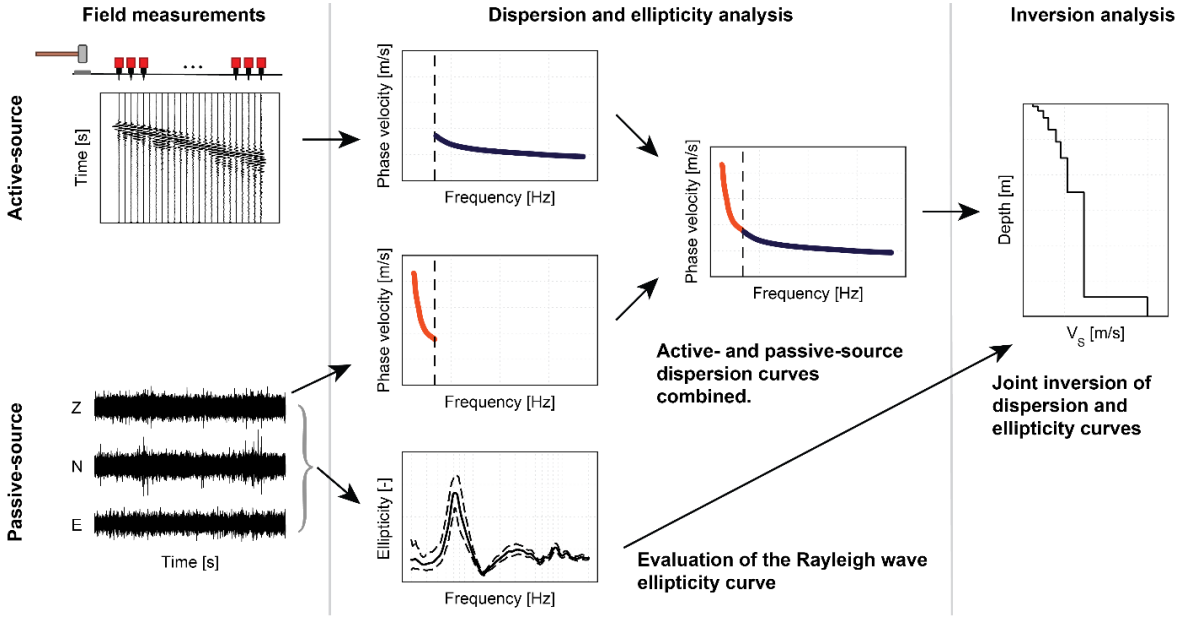

Mynd 2: *Aðferð til samþættrar greining aktífra og passífra yfirborðsbylgna við mat á skúfbylgjuhraða þykkra setlaga. 1) Öflun mæligagna í felti (field measurements). 2) Greining mæligagna (dispersion and ellipticity analysis). Mat á tvístrunarferli prófunarstaðar með aktífum MASW og passífum MAM mælingum. Mat á ellipsuferli prófunarstaðar með þríása mælingum á umhverfisóróa. 3) Bakreikningar til að ákvarða skúfbylgjuhraða sem fall af dýpi (inversion analysis). Mynd: Elín Ásta Ólafsdóttir o.fl. [13].*

Aðferðin byggir á samþættri greiningu gagna sem aflað er með MASW og MAM yfirborðsbylgjumælingum, auk mælinga á umhverfisóróa með frístandandi jarðskjálftamæli (eða þríása hröðunarnema). MASW og MAM mælingar skila upplýsingum um tvístrunarferli prófunarstaðar (*dispersion curve*) á mismunandi tíðnibilum. Þá gefa þríása mælingar á umhverfisóróa mat á ellipsuferli (*Rayleigh wave ellipticity curve*) prófunarstaðarins [14] en lögun hans stjórnast af skúfbylgjuhraða og heildarþykkt setlaga. Í framhaldi er bakreikningum (*joint inversion of dispersion and ellipticity curves*) beitt til þess að meta skúfbylgjuhraða frá yfirborði og niður á klöpp. Niðurstöður verkefnisins gefa til kynna að þessi greiningaraðferð

henti vel til mælinga hérlendis þar sem setlög eru þykk, svo sem á Suðurlandsundirlendinu þar sem hún hefur gert kleift að ákvarða skúfbylgjuhraða niður á allt að 200 m dýpi. Mynd 3 sýnir dæmi um niðurstöður mælingar sem framkvæmd var í námunda við Markarfljótsbrú. Gefa þær til kynna þykk setlög (heildarþykkt 140–155 m) þar sem mældur skúfbylgjuhraði eykst með dýpi frá 130–160 m/s nálægt yfirborði upp í um 600 m/s.

Enn fremur hefur þessi aðferð til samþættrar greiningar aktífra og passífra yfirborðsbylgna gert það mögulegt að meta skúfbylgjuhraða og mörk jarðlaga á stöðum þar sem stíft lag (t.d. hraunlag eða kargalag) er klemmt á milli mýkri setlaga. Mynd 4 sýnir niðurstöður mælinga sem framkvæmdar voru við norðausturenda brúarinnar yfir Stóru-Laxá. Boranir (mynd 4d) sýna stíft lag við dýpi á milli um 5,5 m og 12–13 m. Ber því vel saman við mælda skúfbylgjuhraðaferla sem sýna mikla aukningu á skúfbylgjuhraða á því dýptarbili. Á Íslandi eru aðstæður sem þessar nokkuð algengar, til dæmis þar sem hraun hefur runnið yfir svæði sem þakið var setlögum. Auka þessar niðurstöður því notkunarmöguleika yfirborðsbylgjuaðferða til muna hérlendis.

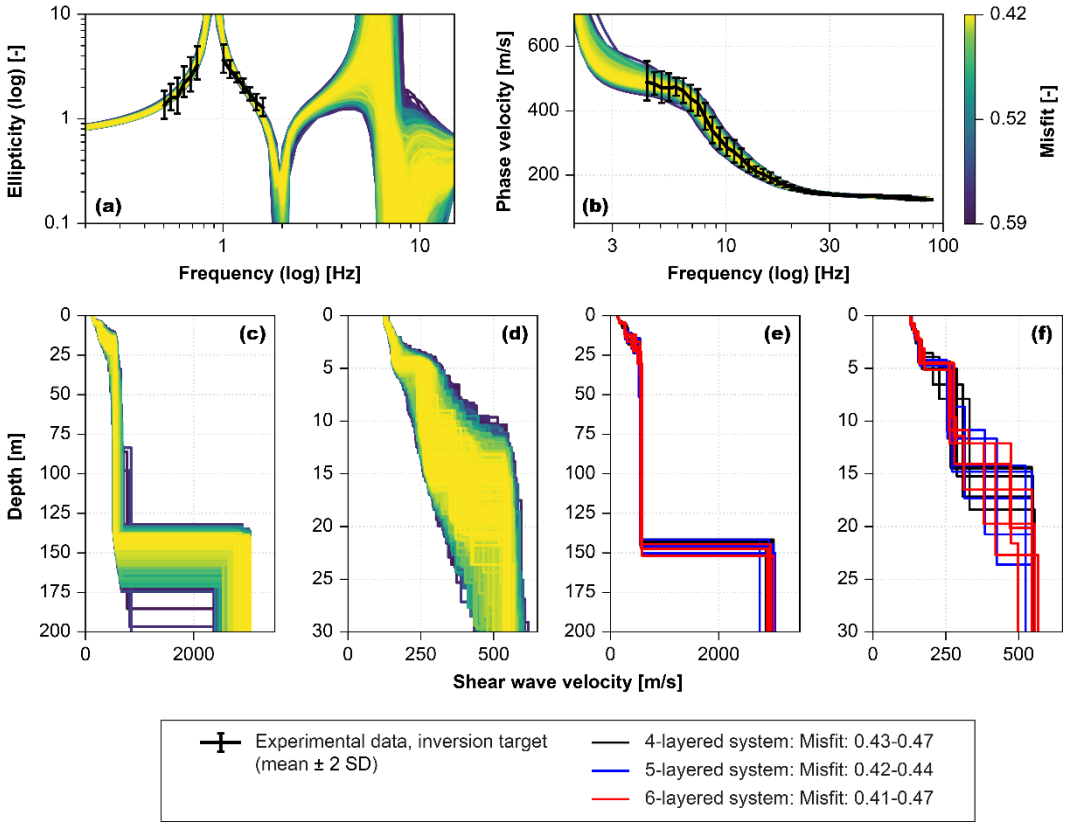

Mynd 3: *Dæmi um samþætta greiningu aktífra og passífra yfirborðsbylgna. Niðurstöður mælinga á skúfbylgjuhraða og dýpi á fast sem framkvæmdar voru í námunda við Markarfljótsbrú. Mynd: Elín Ásta Ólafsdóttir o.fl. [13].*

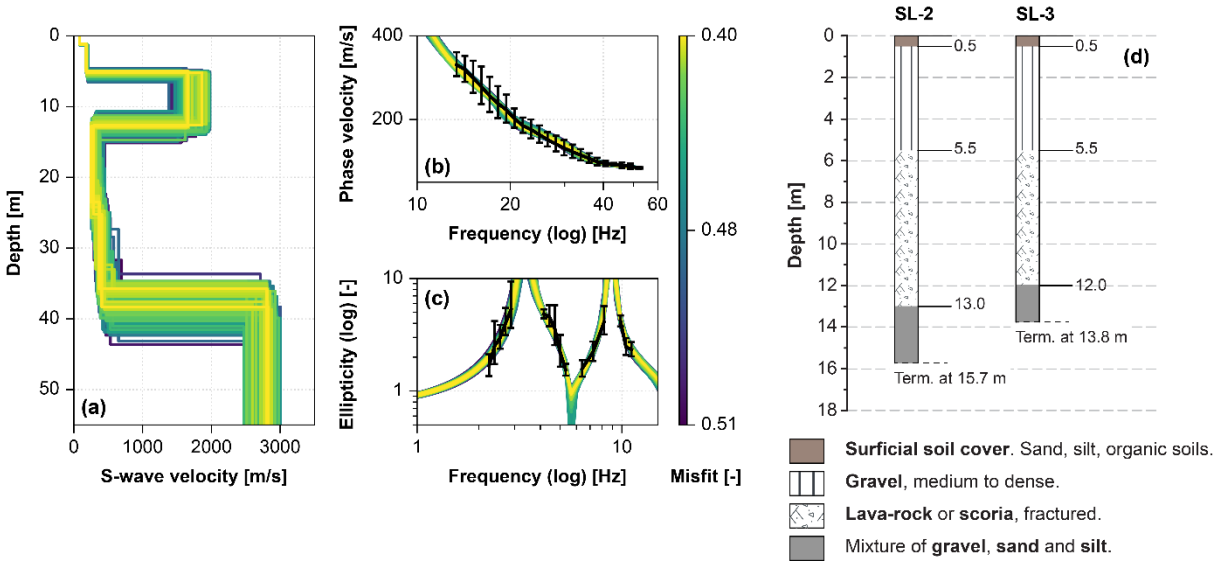

Mynd 4: *(a-c) Niðurstöður mælinga á skúfbylgjuhraða og mörkum jarðlaga við norðausturenda brúarinnar yfir Stóru-Laxá. (d) Borholusnið fyrir mælistaðinn. Mynd: Elín Ásta Ólafsdóttir o.fl. [13], samsett.*

Í framhaldi af þróun aðferðarinnar var framkvæmd nákvæm greining (*geotechnical seismic site characterization*) á svæði meðfram Markarfljóti, frá Markarfljótsbrú í norðri og að Landeyjahöfn í suðri, þar sem byggt var á mælingum á umhverfisóróa með fristandandi jarðskjálftanemum og samþættri greiningu gagna sem aflað var með MASW og MAM yfirborðsbylgjumælingum. Samþætt greining aktífra og passífra yfirborðsbylgna var notuð til að ákvarða skúfbylgjuhraða og heildarþykkt setlaga og niðurstöður bornar saman við fyrirliggjandi borholumælingar, CPT prófanir og bylgjubrotsmælingar. Nánar er greint frá niðurstöðum greiningarinnar í ráðstefnugrein sem kynnt var á ráðstefnu evrópska jarðtæknifélagsins (XVIII ECSMGE 2024) í Portúgal í ágúst sl. og birt í ráðstefnuriti ráðstefnunnar [15], og sem finna má í viðauka A með þessari skýrslu.

Þá var náttúruleg tíðni jarðlagastaflans á mismunandi stöðum innan prófunarsvæðisins metin með HVSR-tækni (*Horizontal-to-Vertical Spectral Ratio*) [16]. Þessar mælingar voru jafnframt liður í því að safna gögnum til að aðlaga líkingar, sem tengja saman náttúrulega tíðni setlagastafla (f_0) og dýpi á fast (H), að eiginleikum íslenskra jarðefna. Markmið þeirrar vinnu er að nýta megi HVSR mælingar á f_0 til að fá gróft mat á dýpi á fast berg. Fyrstu niðurstöður benda til þess að jafna (1) geti hentað til að lýsa aðstæðum á því svæði í Landeyjum nú þegar hefur verið tekið til skoðunar.

$$H = \frac{\overline{V}_S}{4f_0} \tag{1}$$

þar sem $\overline{V}_S$ (meðaltals skúfbylgjuhraði setlaga) er skilgreindur bilinu 300–500 m/s (mynd 5). Frekari mælingar eru þó nauðsynlegar til þess að kanna hve vel jafna (1) hentar til þess að lýsa aðstæðum á öðrum svæðum hérlendis þar sem setlög eru þykk.

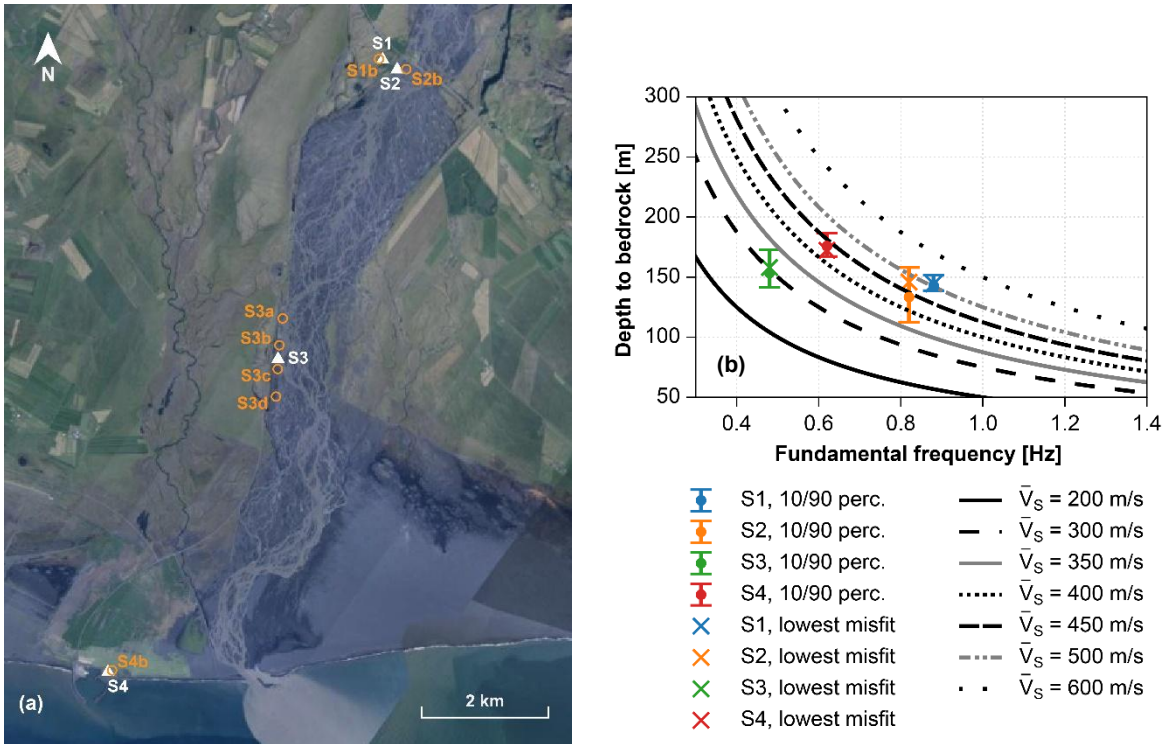

Mynd 5: *(a) Staðsetning prófunarstaða S1–S4 meðfram Markarfljóti. (b) Samanburður mælds dýpis á fast og gilda fengnum með jöfnu (1) þar sem $\overline{V}_S$ (meðaltals skúfbylgjuhraði setlaga) er á bilinu 200–600 m/s. Mynd: Elín Ásta Ólafsdóttir o.fl. [15], samsett.*

2.2. Mat á stífni, styrk og dempunareiginleikum íslensks jarðvegs með statískum og dýnamískum prófunum [VÞ2]

Annar verkþáttur verkefnisins (VÞ2) miðaði að mati á streituháðri hegðun (*strain-dependent properties*) og ysjunareiginleikum (*liquefaction behaviour*) sendinna jarðefna með tilraunastofuprófunum. Sökum þess að ysjunar varð vart við Arnarbæli við bakka Ölfusár í kjölfar Suðurlandsskjálftans 2008 var sá staður valinn sem megin könnunarstaður í VÞ2.

Jarðvegssýnum var safnað við bakka Ölfusár og statísk og dýnamísk DSS skúfboxpróf (*monotonic and cyclic direct simple shear tests*) framkvæmd á þeim á jarðtæknitilraunastofu Deltares í Delft í Hollandi. Gagnasettið inniheldur sex statískar mælingar og 32 dýnamískar mælingar fyrir mismunandi álagstilfelli og mismunandi þjöppun jarðvegssýna. Er þetta í fyrsta skipti sem slíkar mælingar eru framkvæmdar á íslenskum jarðefnum. Í tengslum við þennan verkþátt voru feltmælingar, þ.e. CPT mælingar og passífar yfirborðsbylgjumælingar, einnig framkvæmdar í Arnarbæli (VÞ1). Þá voru niðurstöður DSS skúfboxprófananna nýttar til að meta ysjunareiginleika efnisins með *stress-based* og *energy-based* greiningaraðferðum. Til samanburðar við niðurstöður tilraunastofuprófananna var mótstaða efnisins gegn ysjun (þ.e. dýnamískt mótstöðuhlutfall, CRR) einnig metin með aðferðum sem grundvallast á CPT mælingum og mældum skúfbylgjuhraðaferlum. Greint er frá niðurstöðum DSS prófananna og mati á ysjunareiginleikum efnisins í tímaritsgrein sem nú er í ritrýningarferli [17].

Seyed Javad Fattahi, Yaser Jafarian, Maria Konstadinou, Elín Ásta Ólafsdóttir, Sigurður Erlingsson, Bjarni Bessason og Rajesh Rupakhety. Liquefaction assessment of Icelandic Basaltic Sand through Monotonic and Cyclic Direct Simple Shear Tests. Grein í ritrýningu hjá *International Journal of Geotechnical Engineering*.

Samhliða þeirri vinnu voru niðurstöður DSS skúfboxprófananna nýttar til að kvarða valin töluleg efnislíkön (*advanced soil constitutive models*), sem lýsa spennu-streitu sambandi og ysjunarhegðun jarðvegs, og aðlaga þau að eiginleikum íslenskra jarðefna. Slík kvörðun er nauðsynleg til þess að unnt sé að framkvæma sveiflufræðilega greiningu á jarðlögunum með ólínulegum aðferðum, t.d. í tengslum við mat á áhrifum jarðskjálfta, eins og greint er frá í umfjöllun um þriðja verkþátt verkefnisins.

Fyrsti fasi þeirrar vinnu, sem unnin var á árinu 2023, miðaðist að því að kvarða UBC3D-PLM jarðvegslíkanið [8] þannig að það henti til þess að lýsa efnishegðun sendinna jarðlaga við bakka Ölfusár. Í því skyni var þróaður sérstakur leitaralgóritmi til bestunar á efnisstikum líkansins. Dæmi um niðurstöður er sýnt á mynd 6. Þar eru bornar saman mæliniðurstöður úr statísku DSS prófi (hlutfallslegur þéttleiki sýnis $D_r = 60\%$ og lóðrétt upphafsspenna $\sigma'_{v,o} = 100$ kPa) og reiknaðir ferlar sem fengnir eru með kvarðaðri útgáfu UBC3D-PLM jarðvegslíkansins [18].

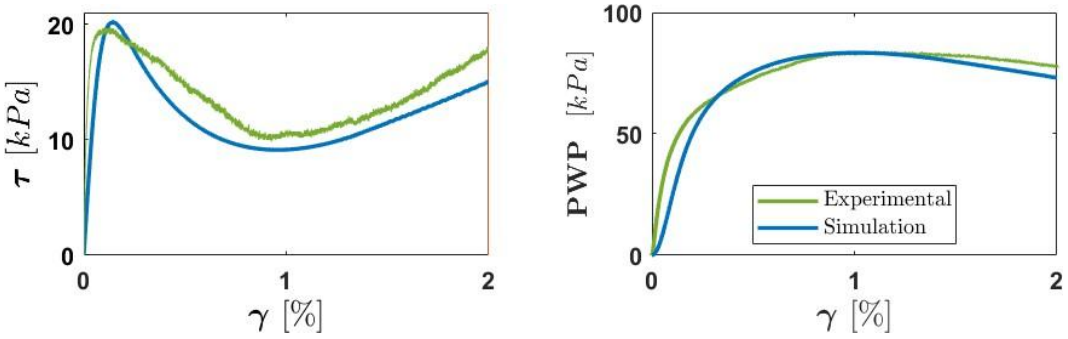

Mynd 6: *Samanburður á mæliniðurstöðum úr statísku DSS skúfboxprófi (constant volume conditions) og niðurstöðum tölulegs líkans sem byggir á kvaðaðri útgáfu UBC3D-PLM líkansins. (a) Samband spennu og streitu. (b) Uppbygging póruvatnsþrýstings (pore water pressure generation, PWP) með streitu. Mynd: Seyed Javad Fattahi o.fl. [18].*

Síðari fasi vinnu við kvörðun efnislíkana miðaðist að þróaðri líkönum, þ.e. PM4Sand [9] og SANISAND [10,11] efnislíkönunum, sem fyrirliggjandi niðurstöður gefa til kynna að gefi raunsærri mynd af streituháðri hegðun jarðefnisins undir dýnamíksu álagi en kvörðuð útgáfa UBC3D-PLM líkansins. Gerð er grein fyrir niðurstöðum þessarar vinnu í tímaritsgrein (ISI), sem nú er í vinnslu og áætlað er að send verði til ritrýningar árið 2025.

2.3. Mat á sveiflumögnun jarðlagastafla

Í þriðja verkþætti verkefnisins voru niðurstöður felt- og tilraunastofumælinga (úr VÞ1 og VÞ2), ásamt öðrum fyrirliggjandi gögnum, nýttar til tölulegrar greiningar á sveiflumögnun jarðlagastafla (*site response analysis*) með „equivalent-linear“ (EQL) og ólínulegum (NL) aðferðum.

Fyrri hluti þeirrar vinnu var sérstaklega miðaður að jarðvegssniðum sem einkennast af því að stakt hraunlag sé yfir eða á milli lausra setlaga. Slík jarðsnið falla illa að þeirri jarðlagagerð sem Evrópustaðallinn Eurocode 8 miðast við. Staðbundin greining er því nauðsynleg. Niðurstöður mælinga á skúfbylgjuhraða (úr VÞ1), ásamt fyrirliggjandi borholusniðum, voru notaðar til að kvarða tölvulíkön fyrir tölulega greiningu á sveiflumögnun á tveimur stöðum (þ.e. við brúna yfir Stóru-Laxá og á Óseyrartanga) þar sem borholusnið sýna 5–10 m þykkt hraunlag á um 5–6 m dýpi frá yfirborði (mynd 7). Mældar jarðskjálftatímaraðir (mynd 8) voru nýttar við tölulega greiningu á sveiflueiginleikum og bylgjumögnun jarðvegssniðanna (þrír PGA flokkar) auk greiningar á áhrifum þess að nýta mismunandi greiningaraðferðir við módelreikningana, þ.e. EQL greiningu og NL greiningu þar sem gengið var út frá mismunandi efnislíkönum fyrir sendnu jarðefnin undir hraunlaginu. Mynd 9 sýnir niðurstöður greiningarinnar miðað við þá jarðlagagerð sem er að finna við brúna yfir Stóru-Laxá. Gefa þær til kynna mögnunaráhrif við meðallangan til langan sveiflutíma fyrir alla þrjá PGA flokkana, á meðan dvínunaráhrifa gætir við styttri sveiflutíma (þ.e. $T < 0{,}2$–$0{,}3$ s) fyrir þá tvo flokka þar sem $PGA \geq 0{,}2$g. Nánar er fjallað um niðurstöður þessarar vinnu í ráðstefnugrein sem kynnt var á *18th World Conference on Earthquake Engineering* (WCEE2024) [19] og sem finna má í viðauka B með þessari skýrslu.

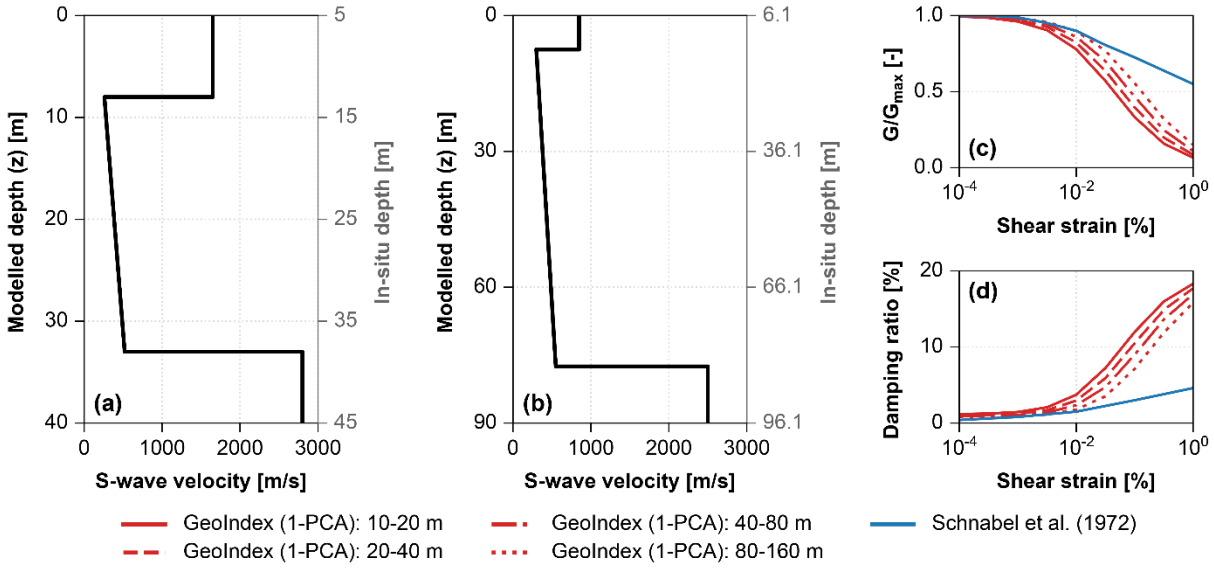

***Mynd** 7: Einfaldaðir skúfbylgjuhraðaferlar sem notaðir voru við sveiflufræðilega greiningu á jarðvegsaðstæðum við (a) brúna yfir Stóru-Laxá og (b) Óseyrartanga. (c,d) Streituháðir skúfstyrks- og dempunareiginleikar efnisins (modulus reduction and damping properties) sem miðað var við í greiningunni. Mynd: Elín Ásta Ólafsdóttir o.fl. [19].*

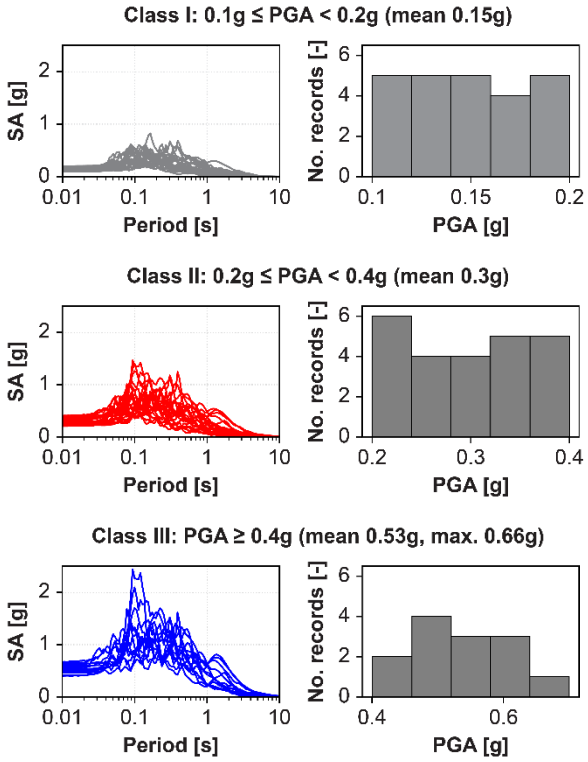

***Mynd 8**: (Vinsri) Hröðunarróf (acceleration response spectra) tímaraðanna sem notaðar voru við sveiflufræðilega greiningu við brúna yfir Stóru-Laxá og á Óseyrartanga. (Hægri) Tímaröðunum var skipt í þrjá flokka eftir hágildi yfirborðshröðunar (PGA) til að unnt væri að meta ákefðarháða sveiflumögnun jarðsniðanna. Tímaraðirnar voru skalaðar á þann hátt að dreifing PGA innan hvers flokks væri sem jöfnust. Mynd: Elín Ásta Ólafsdóttir o.fl. [19].*

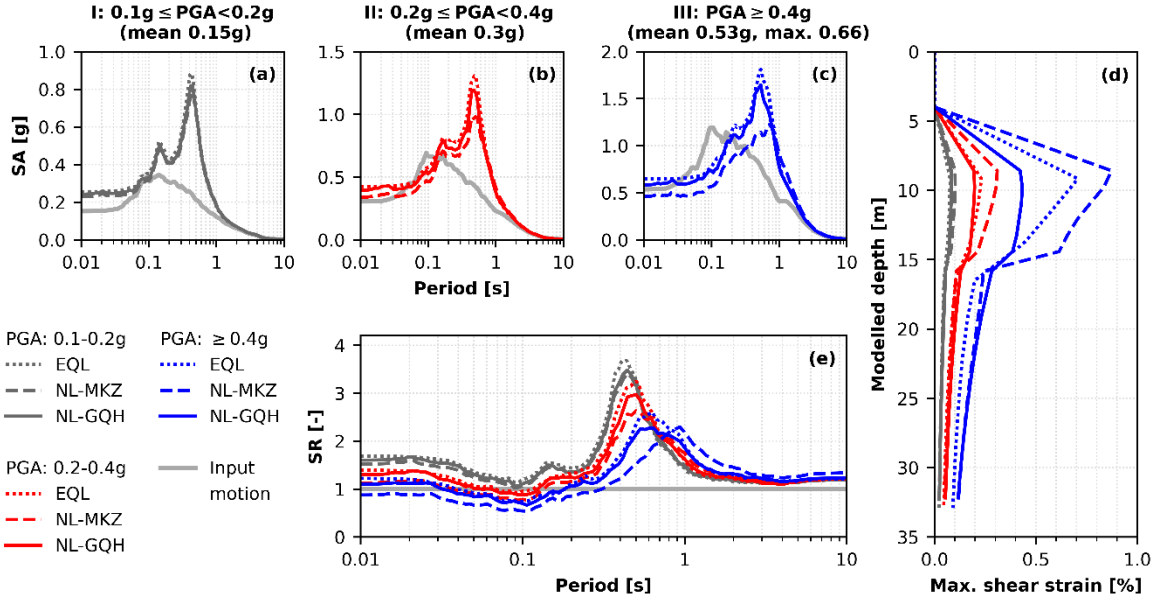

***Mynd 9**: Niðurstöður EQL og NL greiningar á sveiflumögnunaráhrifum við brúna yfir Stóru-Laxá. Reiknuð hröðunarróf (SA, 5% dempun) fyrir (a) PGA-flokk I, (b) PGA-flokk II og (c) PGA-flokk III. (d) Hámarks skúfstreita. (e) Hlutfallsleg mögnun (spectral amplification ratio, skilgreint sem $SR = SA_{yfirborð}/SA_{klöpp}$). Mynd: Elín Ásta Ólafsdóttir o.fl. [19].*

Síðari þáttur vinnu við VÞ3 miðaði að tölulegu mati á sveiflumögnun og ysjun jarðlaga við bakka Ölfusár. Feltmælingar (úr VÞ1) voru nýttar við gerð reiknilíkans fyrir jarðvegsaðstæður í nágrenni Arnarbælis og kvörðuð efnislíkön (úr VP2) nýtt við mat á ysjunarhættu með PLAXIS hugbúnaðinum (sem byggir á einingaaðferðinni). Greint var frá fyrstu niðurstöðum þessarar vinnu, sem fengnar voru með því að nota kvarðaða útgáfu UBC3D-PLM líkansins, í grein sem birt var í ráðstefnuriti *9th International Conference on Computational Methods in Structural Dynamics and Earthquake Engineering* [18]. Niðurstöður gáfu til kynna ysjun jarðlaga næst yfirborði, sem er í samræmi við athuganir á staðnum í kjölfar Suðurlandsskjálftans í maí 2008. Greint er frá niðurstöðum ýtarlegri greiningar, þar sem kvörðuð efnislíkön eru nýtt við greiningu á sveiflumögnun á völdum svæðum á Suðurlandsundirlendinu, í tímaritsgrein sem áætlað er að send verði til ritrýningar á árinu 2025. Niðurstöður eru bornar saman við greiningu með EQL aðferð þar sem gengið er út frá mældri streituháðri hegðun efnisins (úr VÞ2) og ákefðarháða mögnunarstuðla sem skilgreindir eru í nýrri útgáfu Eurocode 8.

2.4. Uppbygging gagnagrunns með mæliniðurstöðum og opið aðgengi að hugbúnaði [VÞ4]

Niðurstöður þeirra MASW yfirborðsbylgjumælinga sem framkvæmdar hafa verið hérlendis hafa verið teknar saman og birtar í opnum gagnagrunni með samræmdum hætti. Alls inniheldur gagnagrunnurinn nú niðurstöður mælinga frá nítján stöðum, samtals 30 skúfbylgjuhraðaferla. Má nálgast hann á slóðinni http://serice.hi.is/#/velocity-profiles.

Í gagnagrunninum eru niðurstöður frá hverjum stað settar fram á formi mældra tvístrunarferla (*dispersion curves*) og skúfbylgjuhraðasniða (*median shear wave velocity*). Enn fremur eru niðurstöður sýndar á formi meðalskúfbylgjuhraða ($V_{S,z}$, *time-averaged shear wave velocity*) í samræmi við hagnýtingu mælinga á skúfbylgjuhraða í núgildandi útgáfu Eurocode 8 við flokkun byggingarstaða í jarðvegsflokka, sem og í væntanlegri uppfærðri útgáfu staðalsins. Notendaviðmót gagnagrunnsins byggist á kortagrunni sem sýndur er á myndum 10 og 11. Í gagnagrunninum gefst tæknifólki og rannsakendum ekki aðeins kostur á því að nálgast fyrrgreindar mæliniðurstöður, heldur einnig að bera saman niðurstöður mælinga frá mismunandi svæðum með einföldum hætti.

Á grunni þeirra MASW mælinga sem liggja fyrir hefur mælistöðunum verið skipt í fjóra flokka eftir gerð þeirra jarðlaga sem þar er að finna: (I) mýrlendi og mýrarkenndur jarðvegur, (II) laus sand- og/eða malarkennd setlög, (III) manngerðar fyllingar, jarðstíflur og (IV) samlímdur jarðvegur og móhella. Niðurstöður mælinga sýna að umtalsverð líkindi eru meðal skúfbylgjuhraðaferlanna innan hvers flokks, á meðan greinilegur munur er á milli flokka (mynd 12). Marka þessar mælingar því fyrstu skrefin í átt að því að ákvarða einkennandi skúfbylgjuhraða fyrir helstu flokka íslenskra jarðefna.

Nánar er greint frá gagnagrunninum í ráðstefnugrein sem birtist í ráðstefnuriti XVIII ECSMGE 2024 (*XVIII European Conference on Soil Mechanics and Geotechnical Engineering*) [20] sem finna má í viðauka C með þessari skýrslu. Gagnagrunninum er enn fremur lýst í grein sem birt var í *Verktækni – Tímariti verkfræðingafélags Íslands* [6]. Þar eru einnig settar fram einfaldar reynslulíkingar fyrir skúfstuðul sem byggðar eru á mældum skúfbylgjuhraðaferlum fyrir hvern ofangreindra jarðvegsflokka. Slíkar líkingar nýtast til að meta skúfstuðul eða skúfbylgjuhraða

á stöðum þar sem mælingar hafa ekki verið framkvæmdar en upplýsingar um jarðvegsgerð liggja fyrir. Þær má einnig nota til að framreikna mæliniðurstöður í tilfellum þar sem könnunardýpi mældra skúfbylgjuhraðaferla er ekki nægjanlegt.

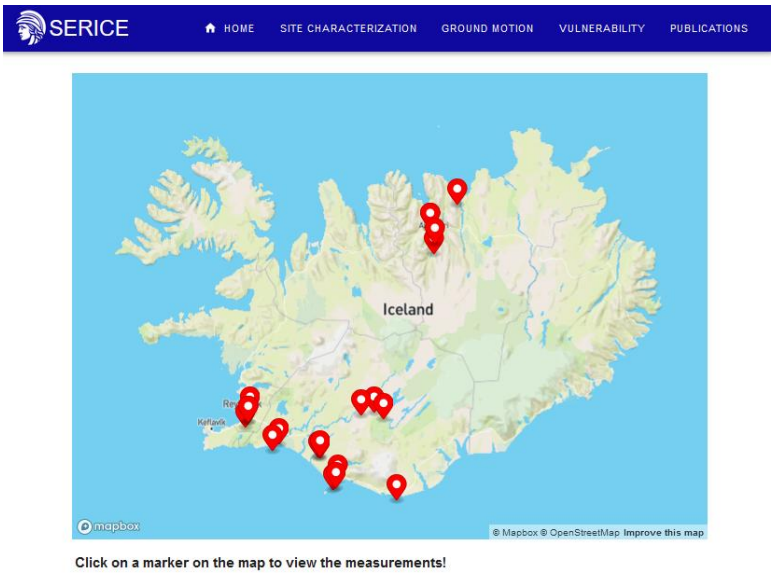

Mynd 10: *Kortagrunnur með niðurstöðum MASW mælinga. Rauð merki sýna þau svæði þar sem mælingar hafa verið framkvæmdar. Mynd: Elín Ásta Ólafsdóttir o.fl. [6].*

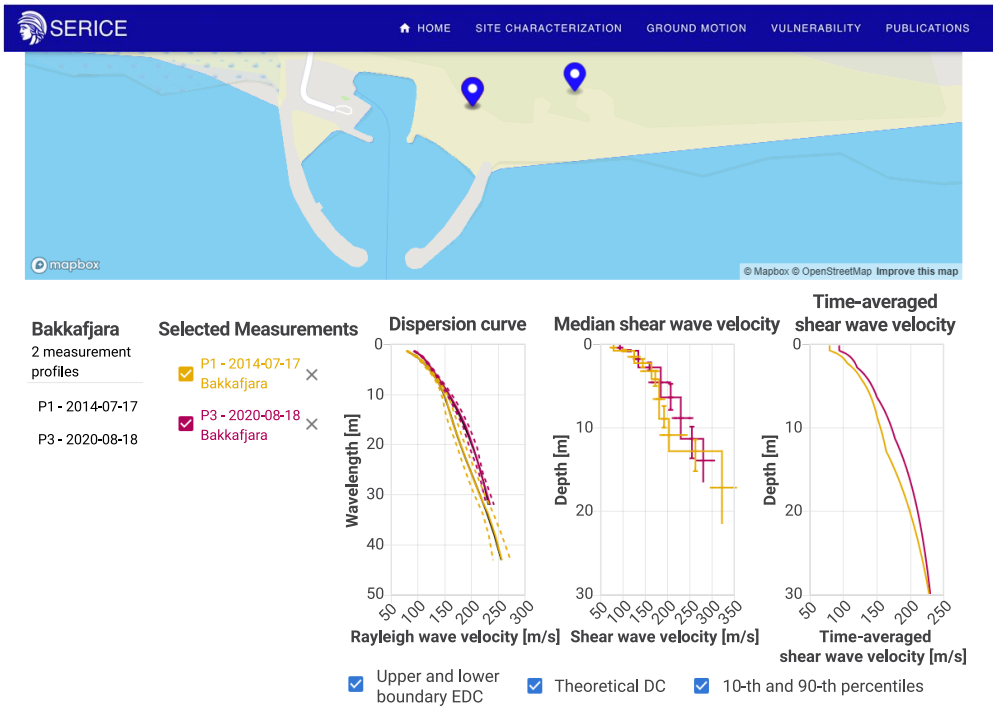

Mynd 11: *Kortagrunnur með niðurstöðum MASW mælinga. Dæmi um framsetningu mæliniðurstaðna. Mynd: Elín Ásta Ólafsdóttir o.fl. [20].*

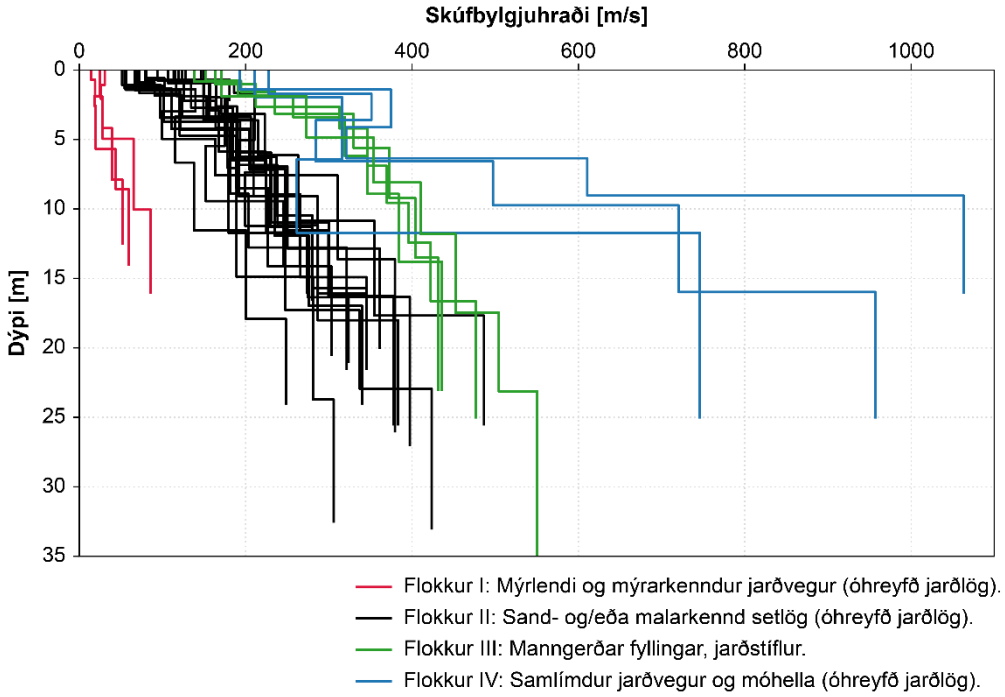

Mynd 12: *Mældir skúfbylgjuhraðaferlar fyrir þá mælistaði sem gagnagrunnurinn inniheldur. Mælistöðunum er skipt í fjóra flokka eftir jarðvegsgerð. Mynd: Elín Ásta Ólafsdóttir o.fl. [6].*

MASWavesPy, Python hugbúnaður til greiningar á MASW mæligögnum og mati á skúfbylgjuhraða með bakreikningum, var gerður aðgengilegur á pakkavefnum PyPI (https://pypi.org/project/maswavespy/) ásamt notendaleiðbeiningum. Mynd 13 sýnir flæðirit með helstu hlutum MASWavesPy pakkans og virkni þeirra. Uppbyggingu hugbúnaðarins er nánar lýst í ráðstefnugrein sem birt var í ráðstefnuriti NGM 2024 [21] (*19th Nordic Geotechnical Meeting*) og finna má í viðauka D. Þá var hugbúnaðurinn og þróun hans kynnt með grein í tímaritinu Geotechnical Testing Journal [22].

Niðurstöður sem hugbúnaðurinn skilar hafa verið sannreyndar með mælingum á jarðtækniprófunarstöðum í Noregi, þar sem þær voru bornar saman við niðurstöður mælinga á skúfbylgjuhraða sem framkvæmdar voru með borholumælingum, öðrum gerðum yfirborðsbylgjumælinga og prófunum á tilraunastofu. Niðurstöður þess samanburðar eru teknar saman á mynd 14 en nánar er fjallað um þær í viðauka D.

Mynd 13: *Yfirlit yfir helstu hluta MASWavesPy hugbúnaðarins. Mynd: Elín Ásta Ólafsdóttir o.fl. [22].*

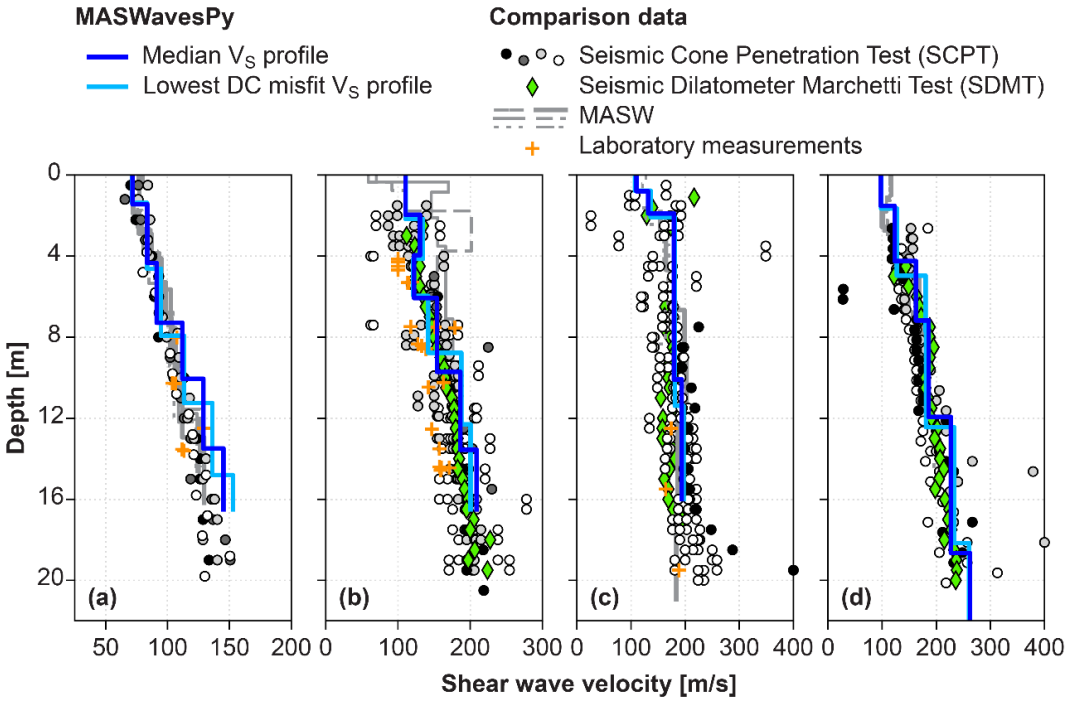

Mynd 14: *Samanburður á mældum skúfbylgjuhraðaferlum (MASWavesPy greining) og niðurstöðum mælinga á skúfbylgjuhraða sem framkvæmdar voru með borholuaðferðum (SCPT og SDMT), öðrum útfærslum MASW yfirborðsbylgjumælinga og mælingum á tilraunastofu (Bender element prófanir á jarðvegssýnum) á fjórum jarðtækniprófunarstöðum í Noregi. Mynd: Elín Ásta Ólafsdóttir o.fl. [21].*

3. Lokaorð

Rannsóknir undanfarinna ára á þessu fagsviði hafa skilað greiningartækni og hugbúnaði til að ákvarða skúfbylgjuhraða setlaga sem fall af dýpi. Slíkar mælingar gagnast meðal annars við hönnun á undirstöðum mannvirkja, við ákvörðun á jarðskjálftaálagi og við mat á staðbundnum jarðskjálftaáhrifum. Frekari þróun greiningartækninnar hefur gert það mögulegt að greina mýkri setlög sem eru klemmd á milli stífari laga (t.d. hraun- eða kargalaga) ofarlega í jarðsniði, sem og gert kleift að áætla þykkt setlaga og þar með dýpi niður á fast berg eða jafngildi þess (*engineering bedrock*). Greiningartæknin byggir á yfirborðsmælingum með léttum mælibúnaði og notar ekki bortæki eða annan þungan vélbúnað sem skilur eftir sig umhverfisspor. Niðurstöðum mælinga hefur verið safnað saman í gagnagrunn í opnu aðgengi, en tilgangur þess er að hönnuðir, rannsakendur og aðrir geti nálgast mæliniðurstöður og borið saman ólíka mælistaði með einföldum hætti.

Sem hluti af verkefninu voru statísk og dýnamísk DSS skúfboxpróf framkvæmd í fyrsta sinn á íslenskum jarðefnum. Niðurstöður prófananna gefa upplýsingar um stífni og styrk jarðefnisins undir skúfáraun, sem og upplýsingar um sveiflufræðilega eiginleika hans. Íslenskur jarðvegur er að mörgu leyti sérstæður þegar miðað er við nágrannalönd okkar. Er hann yfirleitt basískur að uppruna og yfirborðsfletir hans oft glerkenndir. Hefur stór hluti hans myndast á síðasta jökulskeiði í hamfaraatburðum, svo sem eldsumbrotum eða jökulhlaupum og er hann því oft lítið þjappaður eða samlímdur. Þetta setur mark sitt á efniseiginleika jarðvegsins. Því er ekki alltaf sjálfgefið að hægt sé að finna nákvæm/lýsandi gildi á efniseiginleikum í erlendum rannsóknum. Verkefnið er því liður í því að afla aukinna upplýsinga um efnishegðun hérlendra jarðefna.

Niðurstöður DSS skúfboxprófana voru nýttar til að kvarða valin töluleg efnislíkön, sem lýsa spennu-streitu sambandi og ysjunarhegðun jarðvegs, og aðlaga þau að eiginleikum íslenskra jarðefna. Slík kvörðun er nauðsynleg til þess að unnt sé að framkvæma sveiflufræðilega greiningu á jarðlögunum með ólínulegum aðferðum, t.d. í tengslum við mat á áhrifum jarðskjálfta og ysjunarhættu. Nýtast slík líkön einnig á breiðari grunni, svo sem við mat á sveifluvíxlverkunaráhrifum á milli jarðvegs og undirstaðna við hönnun mannvirkja.

4. Heimildir

[1] Sigurður Erlingsson. (2019). Geotechnical challenges in Iceland. *Proceedings of the XVII European Conference on Soil Mechanics and Geotechnical Engineering, ECSMGE-2019*. https://doi.org/10.32075/17ECSMGE-2019-1109

[2] Bjarni Bessason. (1998). Yfirborðsbylgjumælingar við ákvörðun á skúfbylgjuhraða í jarðvegi. *Árbók VFÍ/TFÍ 1997/98*, 10, 293–303.

[3] Bjarni Bessason, Sigurður Erlingsson. (2011). Shear wave velocity in surface sediments. *Jökull*, 61, 51–64.

[4] Elín Ásta Ólafsdóttir. (2019). *Multichannel analysis of surface waves for soil site characterization* [Doktorsritgerð]. Háskóli Íslands.

[5] Elín Ásta Ólafsdóttir, Bjarni Bessason, Sigurður Erlingsson. (2022). Non-invasive active- and passive-source stiffness characterization at a loose sand site. *Proceedings of the 20th International Conference on Soil Mechanics and Geotechnical Engineering*, 501–506.

[6] Elín Ásta Ólafsdóttir, Bjarni Bessason, Sigurður Erlingsson. (2023). Gagnagrunnur fyrir skúfbylgjuhraða í jarðsniðum byggður á yfirborðsbylgjumælingum. *Icelandic Journal of Engineering // Verktækni*, 29(1). https://doi.org/10.33112/ije.29.3

[7] Kramer, S. L. (2014). *Geotechnical earthquake engineering*. Pearson Education Limited.

[8] Petalas, A., Galavi, V. (2012). *Plaxis Liquefaction Model UBC3D-PLM*. Plaxis.

[9] Boulanger, R. W., Ziotopoulou, K. (2017). *PM4Sand (Version 3.1): a sand plasticity model for earthquake engineering applications. Report No. UCD/CGM-17/01*. University of California at Davis, Davis, CA.

[10] Dafalias, Y. F., Manzari, M. T. (2004). Simple plasticity sand model accounting for fabric change effects. *Journal of Engineering Mechanics*, 130(6), 622–634. https://doi.org/10.1061/(ASCE)0733-9399(2004)130:6(622)

[11] Yang, M., Taiebat, M., Dafalias, Y. F. (2022). SANISAND-MSf: a sand plasticity model with memory surface and semifluidised state. *Géotechnique*, 72(3), 227–246. https://doi.org/10.1680/jgeot.19.P.363

[12] Khosravifar, A., Elgamal, A., Lu, J., Li, J. (2018). A 3D model for earthquake-induced liquefaction triggering and post-liquefaction response. *Soil Dynamics and Earthquake Engineering*, 110, 43–52. https://doi.org/10.1016/j.soildyn.2018.04.008

[13] Elín Ásta Ólafsdóttir, Sigurður Erlingsson, Bjarni Bessason. (2023). Hybrid non-invasive characterization of soil strata at sites with and without embedded lava rock layers in the South Iceland Seismic Zone. *Bulletin of Engineering Geology and the Environment*, 82(4), 146. https://doi.org/10.1007/s10064-023-03136-0

[14] Hobiger, M., Bard, P. Y., Cornou, C., Le Bihan N. (2009). Single station determination of Rayleigh wave ellipticity by using the random decrement technique (RayDec). *Geophysical Research Letters*, 36: L14303. https://doi.org/10.1029/2009GL038863

[15] Elín Ásta Ólafsdóttir, Sigurður Erlingsson, Bjarni Bessason. (2024). Geotechnical seismic site characterization of deep alluvial sand sites in the South Iceland Lowland. *Proceedings of*

the XVIII European Conference on Soil Mechanics and Geotechnical Engineering, 26.–30. ágúst 2024, Lissabon, Portúgal.

[16] SESAME. (2004). *Guidelines for the implementation of the H/V spectral ratio technique on ambient vibrations: measurements, processing, and interpretations*. SESAME European research project (WP12 – Deliverable D23.12).

[17] Seyed Javad Fattahi, Yaser Jafarian, Maria Konstadinou, Elín Ásta Ólafsdóttir, Sigurður Erlingsson, Bjarni Bessason, Rajesh Rupakhety. Liquefaction assessment of Icelandic Basaltic Sand through Monotonic and Cyclic Direct Simple Shear Tests. Grein í ritrýningu hjá *International Journal of Geotechnical Engineering*.

[18] Seyed Javad Fattahi, Yaser Jafarian, Maria Konstadinou, Elín Ásta Ólafsdóttir, Sigurður Erlingsson, Bjarni Bessason, Rajesh Rupakhety. (2023). Model calibration and nonlinear site response analysis for medium compacted saturated volcanic sand. *Proceedings of the 9th International Conference on Computational Methods in Structural Dynamics and Earthquake Engineering (COMPDYN 2023)*, bls. 4189–4196.

[19] Elín Ásta Ólafsdóttir, Bjarni Bessason, Sigurður Erlingsson. (2024). Non-invasive seismic site characterization of sandwiched lava-rock/sedimentary sites in Iceland. Birt í ráðstefnuriti *18th World Conference on Earthquake Engineering (WCEE2024)*, 30. júní til 5. júlí 2024, Mílanó, Ítalíu.

[20] Elín Ásta Ólafsdóttir, Sigurður Erlingsson, Bjarni Bessason. (2024). Database of measured shear wave velocity profiles for Icelandic soil sites. Birt í ráðstefnuriti *XVIII European Conference on Soil Mechanics and Geotechnical Engineering*, 26.–30. ágúst 2024, Lissabon, Portúgal.

[21] Elín Ásta Ólafsdóttir, Bjarni Bessason, Sigurður Erlingsson. (2024). MASWavesPy: A Python package for analysis of MASW data. Birt í ráðstefnuriti *19th Nordic Geotechnical Meeting (NGM 2024)*, 18.–20. september 2024, Gautaborg, Svíþjóð.

[22] Elín Ásta Ólafsdóttir, Bjarni Bessason, Sigurður Erlingsson, Amir M. Kaynia. (2024). A Tool for Processing and Inversion of MASW Data and a Study of Inter-Session Variability of MASW. *Geotechnical Testing Journal*, 47(5), 1006-1025. https://doi.org/10.1520/GTJ20230380

Viðauki A

Elín Ásta Ólafsdóttir, Sigurður Erlingsson og Bjarni Bessason. (2024). Geotechnical seismic site characterization of deep alluvial sand sites in the South Iceland Lowland. Birt í ráðstefnuriti *XVIII European Conference on Soil Mechanics and Geotechnical Engineering*, 26.–30. ágúst 2024, Lissabon, Portúgal.

Proceedings of the XVIII ECSMGE 2024
GEOTECHNICAL ENGINEERING CHALLENGES
TO MEET CURRENT AND EMERGING NEEDS OF SOCIETY

ISBN 978-1-032-54816-6
DOI 10.1201/9781003431749-226

ECSMGE 24
XVIII EUROPEAN CONFERENCE ON SOIL MECHANICS AND GEOTECHNICAL ENGINEERING

Geotechnical seismic site characterization of deep alluvial sand sites in the South Iceland Lowland

Caractérisation géotechnique sismique des sites de sables alluviaux profonds dans les basses terres du sud de l'Islande

E.A. Olafsdottir*, S. Erlingsson, B. Bessason
Faculty of Civil and Environmental Engineering, University of Iceland, Reykjavik, Iceland
**elinasta@hi.is*

ABSTRACT: Thick deposits of post-glacial sediments are widely found along the coastline and close to main riverbeds in South Iceland. This work studies the feasibility of using a joint inversion of dispersion and ellipticity curves to characterize deep alluvial sand sites in the South Iceland Lowland. For this purpose, MASW (Multichannel Analysis of Surface Waves), small-aperture MAM (Microtremor Array Measurements) and MHVSR (Microtremor Horizontal-to-Vertical Spectral Ratio) field tests were conducted at selected locations along the Markarfljót River. The results provide the V_S profiles of the tested sites down to bedrock level at 120–190 m depth, along with the fundamental frequency (f_0) of the soil strata. Furthermore, simple correlations between f_0 and bedrock depth are evaluated against the measurement results, in order to identify suitable relationships for preliminary assessment of bedrock depths based on MHVSR measurements in South Iceland.

RÉSUMÉ: D'épais dépôts de sédiments post-glaciaires sont largement répandus le long du littoral et à proximité des principaux lits des rivières du sud de l'Islande. Ce travail étudie la faisabilité de l'utilisation d'une inversion conjointe des courbes de dispersion et d'ellipticité pour caractériser les sites de sable alluvionnaire profond dans les basses terres du sud de l'Islande. À cette fin, des tests sur le terrain MASW, MAM à petite ouverture et MHVSR ont été menés à des endroits sélectionnés le long de la rivière Markarfljót. Les résultats fournissent les profils V_S des sites testés jusqu'au niveau du substrat rocheux à 120–190 m de profondeur, ainsi que la fréquence fondamentale (f_0) des strates du sol. De plus, des corrélations simples entre f_0 et la profondeur du substrat rocheux sont évaluées par rapport aux résultats de mesure afin d'identifier les relations appropriées pour une évaluation préliminaire des profondeurs du substrat rocheux sur la base des mesures MHVSR dans le sud de l'Islande.

Keywords: Non-invasive site characterization; shear wave velocity; bedrock depth; South Iceland Lowland.

1 INTRODUCTION

The South Iceland Lowland is characterized by strike-slip earthquake activity and a geological environment shaped by volcanism and glacial impacts. Thick deposits of post-glacial sediments, resulting from repeated glacial outburst floods and accumulation of volcanic-originated materials, are widely found along the South Iceland coast and close to main riverbeds. The local soils are mostly normally consolidated coarse-grained basaltic materials and are often loosely compacted due to a rapid sediment build-up in catastrophic events.

This work focuses on an area along the Markarfljót River in South Iceland, between the Markarfljót Bridge and the Landeyjar Harbor (Figure 1a). The area is close to the eastern boundary of the South Iceland Seismic Zone (SISZ). The soil deposits along the glacier fed river primarily consist of sand and sandy gravel and were mainly created in outburst events. The river is highly dynamic with the river mouth moving in a cyclical pattern along a few-kilometre wide part of the coastline. It carries an estimated 100,000–200,000 m^3 of sand to the coastal zone annually (Pétursson et al., 2020).

Borehole logs for a site around 4.5 km east of the current study area indicate layers of sand and gravel down to a depth of 80 m and unspecified sedimentary layers down to 168 m. The borings were terminated before reaching competent bedrock. Seismic refraction surveys conducted in the 1970s (Mott MacDonald and Línuhönnun, 2004) further showed thick sediment formations in the area. The minimum sediment thickness was estimated as 40–50 m near the farm Kross, ca. 12 km west of the current study area. The depth to bedrock was then found to increase towards east, reaching up to 250 m near the farm Bakki, 2-3 km west of the Markarfljót River. No data exists for the sites considered in this work.

Non-invasive methods, specifically Multichannel Analysis of Surface Waves (MASW), Microtremor Array Measurements (MAM) and single-station microtremor measurements, are used to evaluate the shear wave velocity (V_S), depth to bedrock (H) and fundamental frequency (f_0) for selected sites within the area. Subsequently, simple equations relating f_0 and H are evaluated against the results to identify suitable correlations for preliminary assessment of bedrock depths for deep soil sites in South Iceland.

2 SITE CHARACTERIZATION

The surface wave tests in the Markarfljót area (Figure 1a) consisted of four MASW arrays (at S1–S4), two small-aperture MAM arrays (at S1 and S4) and single-station measurements at several locations, including S2 and in the vicinity of S3. This section provides an overview of the data acquisition (DAQ) and analysis. A more comprehensive description is given in Olafsdottir et al. (2023).

2.1 In-situ data acquisition

The MASW data was acquired using an array of twenty-four 4.5 Hz vertical geophones (receiver spacing of 0.5–2 m) and a 6.3 kg sledgehammer to generate the impact load. Repeated shots were collected along the same survey line whilst changing the receiver spacing, source offset and shot position. The MAM measurements were conducted using four Lennartz 5 s seismometers, each coupled with a Reftek digitizer. The seismometers were arranged in triangular-shaped arrays (circumradius of 12 m and 24 m) whose centroid was located at the midpoint of the respective MASW array. The single-station measurements at locations S2, S2b and S3a–d by the bridge and along the river (Figure 1a) were conducted using ETNA 2 accelerographs. As prior studies have recommended against the use of accelerometers for HVSR analysis (e.g., Guillier et al., 2008), the data acquisition was repeated at stations S1 and S1a using the ETNA 2 accelerographs and the resulting MHVSR compared (Figure 1b). The results show that comparable H/V ratios were obtained with both instruments, which is considered to support the use of the ETNA 2 accelerographs in this work.

2.2 Evaluation of f_0, V_S and H

The MHVSR (Microtremor Horizontal-to-Vertical Spectral Ratio) technique was used for evaluation of f_0. For each site, the three-component record (duration 50–100 min) was split into 50 s windows. The Fourier spectra of each component was smoothed using the Konno-Ohmachi function (with b = 40) and the H/V-ratio subsequently obtained by dividing the geometric mean of the horizontal spectra by the vertical spectrum. The resulting MHVSR curves are given in Figures 1b–e.

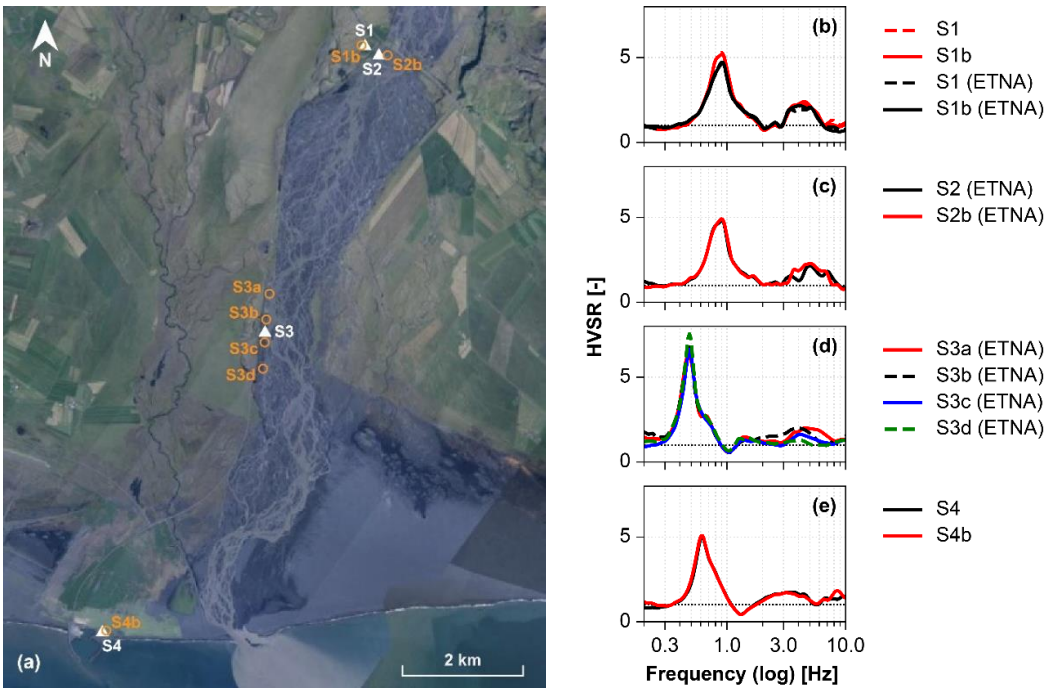

Figure 1. (a) Aerial image of the survey area along the Markarfljót River showing the test site locations. S1-S4: Evaluation of S-wave velocity profile, fundamental site frequency and depth to bedrock. S1b, S2b, S3a-d, S4b: Evaluation of fundamental site frequency. (b-e) Lognormal-median MHVSR curves for individual measurement stations.

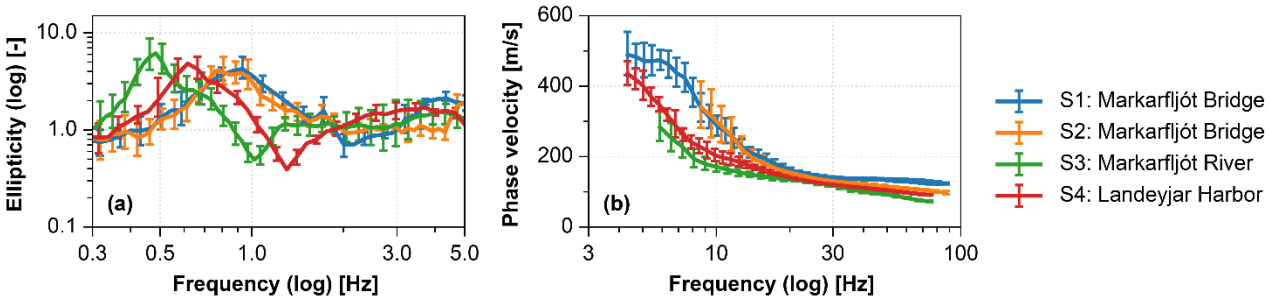

Figure 2. Experimental R-wave (a) ellipticity and (b) dispersion curves for sites S1-S4.

A joint R-wave dispersion-ellipticity inversion was used to evaluate V_S and H for sites S1–S4. The dispersion curve (DC) for each site was obtained from the active-source (MASW) and, where available, the passive-source (MAM) data. Each MASW shot gather was processed using the dispersion tool in MASWaves (Olafsdottir et al., 2018). The MAM data was processed using the MSPAC toolbox in Geopsy (Wathelet et al., 2020), with the 50–60 min recordings split into 12.5–15 min windows and each sub-record processed separately. An average DC (Figure 2b) was finally obtained by binning the dispersion data within log-spaced frequency bands.

The RayDec technique (Hobiger et al., 2009) was used to evaluate the R-wave ellipticity (Figure 2a), with the recorded microtremors split into 8–10 min windows. For S1 and S4, the ellipticity curves specified as inversion targets were obtained using the recordings of the central stations of the MAM arrays. For S2, a single-station measurement was conducted at the location of the MASW survey. The HVSR curves for stations S3a–d show limited variability (Figure 1d), thus indicating small variations in soil stratigraphy for the 1.2 km segment between S3a and S3d. Hence, the ellipticity for site S3 was estimated as the average ellipticity of S3b and S3c.

The inversion was conducted as described in Olafsdottir et al. (2023) using the Dinver module in Geopsy (Wathelet et al., 2020). The layer thicknesses and V_S in each layer were treated as unknowns to be established by the inversion, whilst the mass density was fixed as 2000 kg/m^3 and the Poisson's ratio confined to the range of 0.2–0.5 in lack of site-specific data. The inversion scheme was initiated five times with 75,000–90,000 models sampled in each initiation.

Following each inversion initiation, 100 models were randomly selected from the subset of sampled models whose dispersion-ellipticity misfit (m) fulfils $m \leq 1.25m_{min}$, with m_{min} being the minimum misfit value. The resulting collections of inverted velocity profiles, along with the associated ellipticity and dispersion curves, are shown in Figure 3 (sites S1, S2) and Figure 4 (sites S3, S4). Figure 5 illustrates the variation of the sediment V_S down to bedrock level and within the upper-most 30 m. Also shown is the lowest misfit model for each site.

The analysis points to a broadly similar velocity structure at all four sites along the river. Specifically, for the sandy and gravelly sediments, the developed velocity profiles indicate an increase in V_S from 70–130 m/s at surface to around 350–600 m/s.

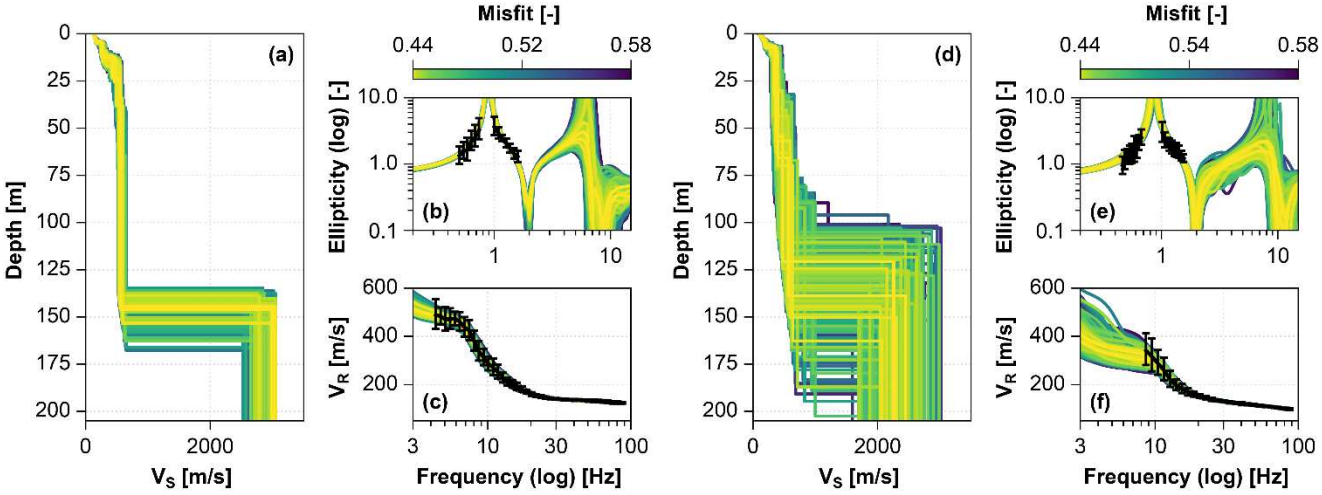

Figure 3. Joint dispersion-ellipticity curve inversion for Markarfljót Bridge sites (a-c) S1 and (d-f) S2. (a,d) Set of V_S profiles whose misfit values fulfil $m \leq 1.25m_{min}$. The associated theoretically computed ellipticity (b,e) and dispersion (c,f) curves are compared to the experimental data points specified as inversion targets.

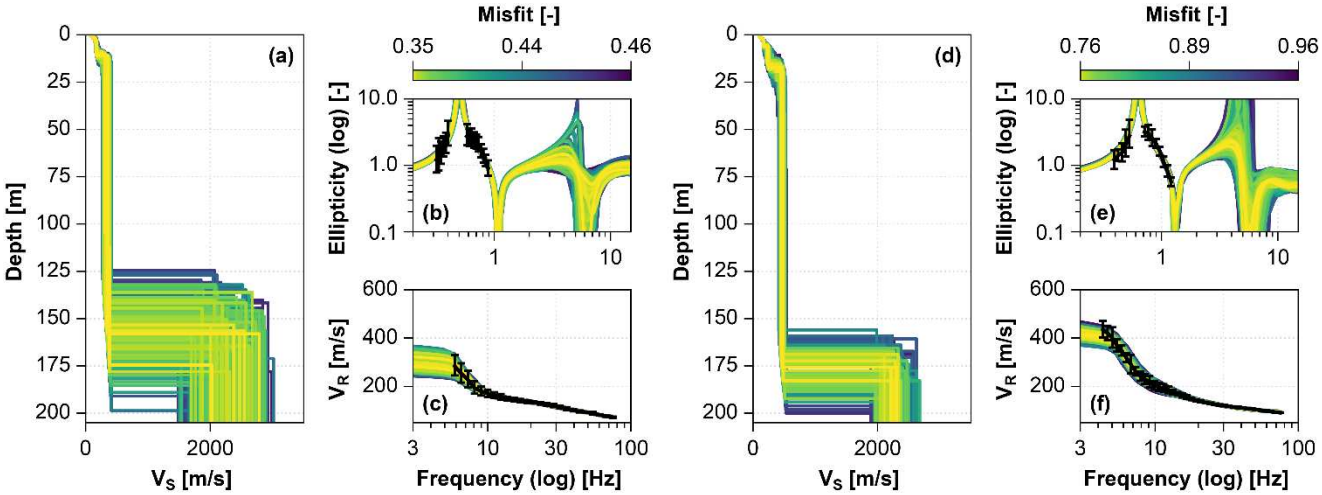

Figure 4. Joint dispersion-ellipticity curve inversion for (a-c) Markarfljót River site S3 and (d-f) Landeyjar Harbor site S4.

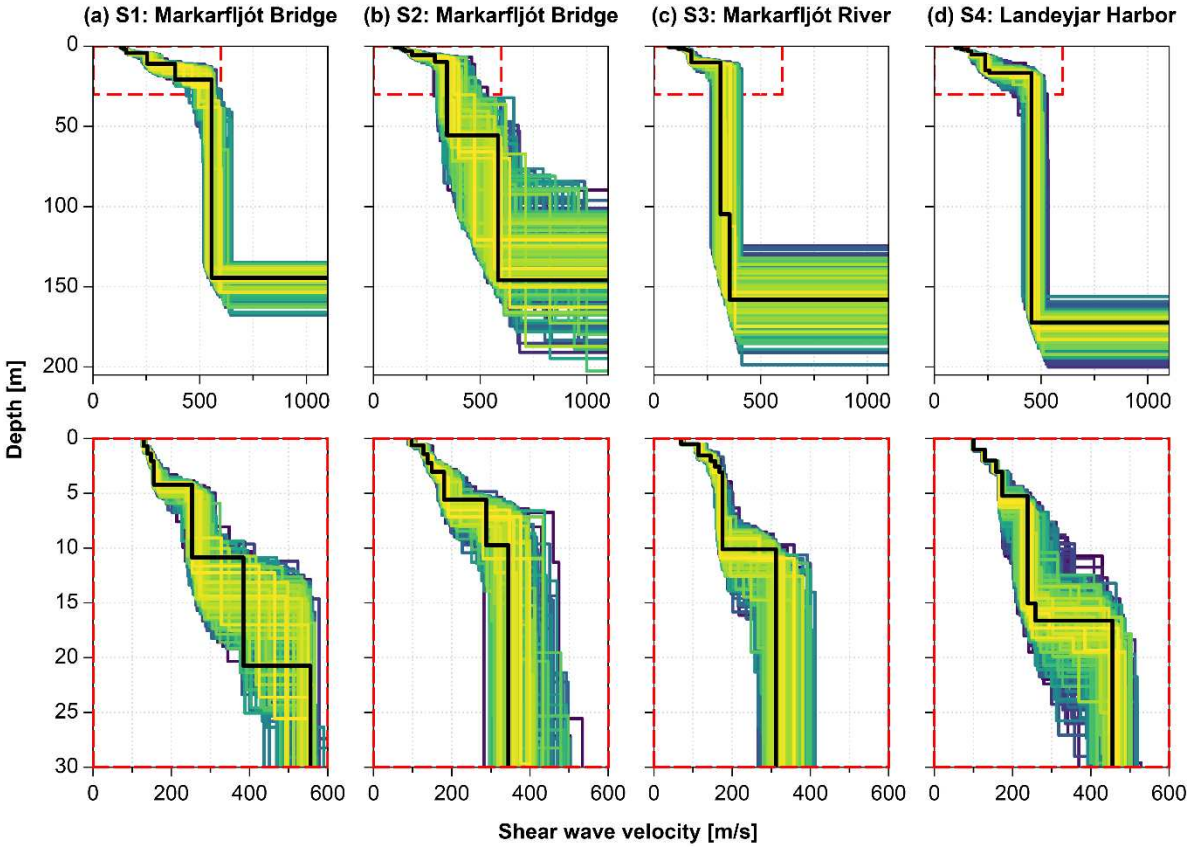

Figure 5. Variation of the sediment shear wave velocity predicted for sites (a) S1, (b) S2, (c) S3, and (d) S4 down to bedrock level (upper row) and down to a depth of 30 m (lower row). The colour scale used for each site refers to the misfit values in Figures 3 and 4. The lowest misfit shear wave velocity profile for each site is shown as a black line.

The strong impedance contrast at a depth of around 120–190 m is interpreted as depth to bedrock. However, the predicted bedrock velocity (>2000 m/s) may be affected by the uncertainty of the obtained data at depth. The time-averaged V_S for the top-most 30 m ($V_{S,30}$) is found to be in the range of 230–320 m/s. Down to bedrock level, the time-averaged V_S ($V_{S,H}$) is estimated as 290–480 m/s. Sediment thickness well exceeding 100 m is in line with available information on the Markarfljót area. It is noted that depth to bedrock was only retrieved at four locations. However, based on the results in Figure 5, a picture of increasing sediment thickness from north towards the sea emerges. Measurements at additional locations along the river are, however, required to conclude on this point.

The inversion results for the two sites by the Markarfljót Bridge (S1 and S2, Figures 3 and 5ab)

reveal a significantly more variation within the set of S2 V_S models as compared to those for S1. This is both observed in the predicted location of the sediment-bedrock interface, which is much better constrained for S1 than S2, as well as in the velocity estimates, particularly at depth. The observed difference is attributed to the narrower frequency range of the S2 dispersion curve, which results in a wider frequency gap between the right flank of the ellipticity peak and the experimental DC, as compared to that of S1. The lower surficial V_S for S2 (Figures 5ab) is consistent with prior expectations, as the surficial soil at S1 consisted of slightly compacted gravel whilst it was loose basalt sand at S2.

The results in Figures 4 and 5cd present a comparable trend for sites S3 and S4, as previously described for S1 and S2. Particularly, the lack of low-frequency components in the S3 DC (which results in a gap in the experimental data at 0.9–5.9 Hz) leads to increased difficulties in constraining the depth to bedrock. The effects of the lack of low-frequency DC components are also observed in the velocity estimates at depth, which are slightly less constrained at S3 than at S4. As shown in Figure 2b, the S3 DC presents the lowest phase velocity values out of the four experimental DCs, thus suggesting a somewhat softer surficial soil profile than at the other sites. However, the lack of data to constrain the theoretically computed DCs below 6 Hz is considered to affect the reliability of the velocity estimates for S3 at depth, possibly biasing the inverted V_S estimates to lower values and thereby also affecting the predicted bedrock depth. It would, therefore, be of value to gather MAM data at S3 in order to extend the experimental DC to lower frequencies. Consequently, the current estimate of the depth to bedrock and the corresponding value of $V_{S,H}$ for site S3 are considered more uncertain than those for S4.

3 SIMPLIFIED ESTIMATE OF H

In lack of site-specific measurements of velocity profiles or deep borehole logs, simple relationships providing a link between f_0 and H may be used to estimate depth to bedrock (or engineering bedrock) based on MHVSR measurements without inversion. Power-law regression models, i.e., $H = a \cdot f_0^b$, have been proposed by many authors, with the regression parameters a and b reflecting regional and geological characteristics. Thus, local calibration using data from multiple sites is required.

Assuming a one-dimensional soil model consisting of a soft sedimentary layer above bedrock, Eq. (1) relates f_0 and the average V_S of the sedimentary layer ($\overline{V}_S$) with H following a quarter-wavelength approach (Lachetl and Bard, 2011). A value of $\overline{V}_S$ = 300 m/s has previously been suggested to estimate sediment thickness based on measurements of f_0 (Nelson and McBride, 2019):

$$H = \frac{\overline{V}_S}{4 f_0} \quad (1)$$

Figure 6 compares the measurement results (i.e., MHVSR estimates of f_0 and the depth to bedrock level established based on the joint inversion) with values computed using Eq. (1) with $\overline{V}_S$ in the range of 200–600 m/s. For the softest site (S3), $\overline{V}_S$ = 300 m/s is found to provide an estimate of H that is consistent with the measured values. However, for S1, S2 and S4 a value of 300 m/s would lead to a significant underestimation of the depth to bedrock, with a $\overline{V}_S$ value in the range of 400–500 m/s seeming more appropriate. These results are consistent with the estimated $V_{S,H}$ for the four sites, i.e., around 300 m/s for S3, 410–420 m/s for S2 and S4, and up to 480 m/s for S1. This further correlates with the $V_{S,30}$ for the respective sites, which was estimated at around 230 m/s for S3 but showed values in the range of 260–280 m/s for S2 and S4 and exceeding 300 m/s for S1.

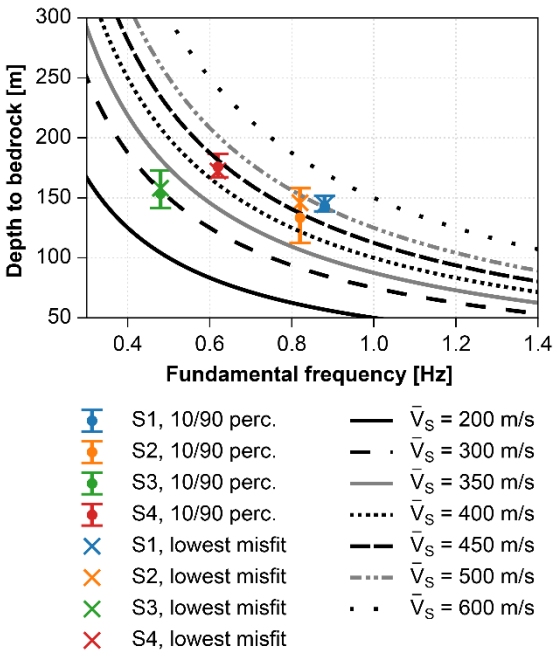

Figure 6. Comparison of measured values of depth to bedrock and values computed using Eq. (1) with $\overline{V}_S$ in the range of 200–600 m/s. For each site, the measured values are given as the 10th to 90th percentiles of the inverted bedrock depths (error bars) and the depth indicated by the lowest misfit velocity profile (crosses).

4 CONCLUSIONS

This study points at a joint dispersion-ellipticity inversion as a feasible method to retrieve the V_S distribution and depth to bedrock at deep soil sites in the South Iceland Lowland. For the conditions described here, a composite use of MASW and small-aperture MAM is further found highly beneficial to reduce the frequency gap between the experimental dispersion and ellipticity data, thus providing a more refined estimate of the sediment V_S and depth to bedrock. The bedrock depths estimated in this work are in line with available information on the wider Markarfljót area. However, existing data is limited to a few surveys, thus, comparison with direct measurements, e.g., deep boreholes, is considered beneficial for further verification of the results.

The results suggest that the quarter-wavelength approach (Eq. (1)) with $\overline{V}_S$ in the range of 300–500 m/s could be used for initial assessment of bedrock depths in the area based on MHVSR measurements of f_0. However, this study only includes data from four sites along the Markarfljót River. Further verification based on data from a larger number of sites is therefore required before general conclusions can be drawn. Future steps may also include calibration of power-law regression models relating f_0 and H to describe the local characteristics.

ACKNOWLEDGEMENTS

This work was supported by the Icelandic Research Fund (grants no. 206793-053, 218149-053), the Icelandic Road and Coastal Administration, and the Energy Research Fund of the National Power Company of Iceland.

REFERENCES

Guillier, B., Atakan, K., Chatelain, J.-L., Havskov, J., Ohrnberger, M., Cara, F., Duval, A.-M., Zacharopoulos, S., Teves-Costa, P., the SESAME team. (2008). Influence of instruments on the H/V spectral ratios of ambient vibrations. *Bulletin of Earthquake Engineering*, 6, pp. 3-31. https://doi.org/10.1007/s10518-007-9039-0.

Hobiger, M., Bard, P. Y., Cornou, C., Le Bihan, N. (2009). Single station determination of Rayleigh wave ellipticity by using the random decrement technique (RayDec), *Geophysical Research Letters*, 36, L14303. https://doi.org/10.1029/2009GL038863.

Lachetl, C., Bard, P.-Y. (2011) Numerical and theoretical investigations on the possibilities and limitations of Nakamura's technique. *Journal of Physics of the Earth*, 42(5), pp. 377–397. https://doi.org/10.4294/jpe1952.42.377.

Mott MacDonald, Línuhönnun. (2004). Independent Review of a Tunnel Connection to Vestmannaeyjar. Technical Report.

Nelson, S., McBride, J. (2019). Application of HVSR to estimating thickness of laterite weathering profiles in basalt. *Earth Surface Processes and Landforms*, 44(7), pp. 1365–1376. https://doi.org/10.1002/esp.4580.

Olafsdottir, E. A., Erlingsson, S., Bessason, B. (2018). Tool for analysis of multichannel analysis of surface waves (MASW) field data and evaluation of shear wave velocity profiles of soils, *Canadian Geotechnical Journal*, 55(2), pp. 217–233. https://doi.org/10.1139/cgj-2016-0302.

Olafsdottir, E. A., Erlingsson S., Bessason, B. (2023). Hybrid non-invasive characterization of soil strata at sites with and without embedded lava rock layers in the South Iceland Seismic Zone, *Bulletin of Engineering Geology and the Environment*, 82, 146. https://doi.org/10.1007/s10064-023-03136-0.

Pétursson, G. S., van Rijn, L., Pálmarsson, S. Ó., Myer, E. M., Ragnarsson, E. (2020). Landeyjahöfn harbour preliminary independent evaluation. Data review and assessment of harbour utilization, Ministry of Transport and Local Government, Reykjavik, Iceland, Rep. 20.07 / 2020-L-I.

Wathelet, M., Chatelain, J. L., Cornou, C., Di Giulio, G., Guillier, B., Ohrnberger, M., Savvaidis, A. (2020). Geopsy: A User-Friendly Open-Source Tool Set for Ambient Vibration Processing, *Seismological Research Letters*, 91(3), pp. 1878-1889. https://doi.org/10.1785/0220190360.

Viðauki B

Elín Ásta Ólafsdóttir, Bjarni Bessason og Sigurður Erlingsson. (2024). Non-invasive seismic site characterization of sandwiched lava-rock/sedimentary sites in Iceland. Birt í ráðstefnuriti *18th World Conference on Earthquake Engineering (WCEE2024)*, 30. júní til 5. júlí 2024, Mílanó, Ítalíu. Grein kynnt með fyrirlestri á ráðstefnunni.

18TH WORLD CONFERENCE ON EARTHQUAKE ENGINEERING
WCEE2024
MILAN

MILAN, ITALY
30TH JUNE - 5TH JULY 2024
www.wcee2024.it

NON-INVASIVE SEISMIC SITE CHARACTERIZATION OF SANDWICHED LAVA-ROCK/SEDIMENTARY SITES IN ICELAND

E.A. Olafsdottir[1], B. Bessason[2] & S. Erlingsson[2]

[1] Faculty of Civil and Environmental Engineering, University of Iceland, Reykjavik, Iceland, elinasta@hi.is

[2] Faculty of Civil and Environmental Engineering, University of Iceland, Reykjavik, Iceland

Abstract: *The geological setting of the South Iceland Seismic Zone (SISZ) is shaped by a combination of volcanic activity, glacial drift, and sea level variations through the ages. In large areas, layers of fractured basaltic lava-rock are embedded in or overlying softer sandy/gravelly sediments, resulting in strong velocity reversals with depth. Such conditions are not represented in the site categorization criteria defined in both the current and forthcoming versions of Eurocode 8, thus requiring site-specific analysis. This work presents initial efforts to characterize sandwiched lava-rock/sedimentary sites in the SISZ using geophysical techniques. Active- and passive-source surface wave analysis (MASW, MAM) and single-station microtremor measurements were conducted at two sites in the SISZ where a-priori information indicates a layer of lava-rock between soft sediments in the upper-most 10–20 m. The S-wave velocity (V_S) profile for each site was obtained with a composite inversion of the retrieved dispersion and ellipticity curves. The predicted depth and thickness of the lava-rock agrees with available geotechnical information and existing boreholes. The estimated range in V_S for the underlying sediments is further consistent with measured values for comparable soil types in other locations in the SISZ. Further is MHVSR (Microtremor Horizontal-to-Vertical Spectral Ratio) found to be a highly valuable tool to differentiate between sedimentary sites with and without an embedded lava-rock layer. Equivalent linear and non-linear ground response analysis is subsequently used to study the effects of the granular sediments, underlying the lava-rock, on ground motion amplifications for expected hazard scenarios in South Iceland. Conventional practice for major construction works is to remove the surficial soils and found structures on the underlying rock. Hence, the subsurface models used for the site response quantification are defined as 'stiff-soft-stiff' structures based on the retrieved velocity profiles. The ground motion variability is considered by using three sets of recorded rock motions (PGA of 0.1–0.2g, 0.2–0.4g, and ≥0.4g) from recent earthquakes in the SISZ as seismic inputs. Based on the available data, each set consists of 13 or 24 accelerograms. Hence, initial steps are taken towards a more general seismic characterization of sandwiched lava-rock/sedimentary sites in the SISZ.*

1 Introduction

Iceland is the most seismically active part of Northern Europe, with the largest earthquakes occurring within two complex fracture zones: the South Iceland Seismic Zone (SISZ) and the Tjörnes Fracture Zone (TFZ). The SISZ, located in the South Iceland Lowland, crosses the largest and most populated agricultural region in the country, whereas the TFZ is in the north-east, mostly offshore. The earthquakes occurring within these two zones are primarily shallow (<10 km) strike-slip quakes and have reached magnitudes of M_w 7 (Einarsson, 2008; Jónasson et al., 2021). Following the current Eurocode 8 (CEN, 2004) and its Icelandic National Annexes (IST, 2010), the 475-year mean return period PGA is 0.5g for both the SISZ and TFZ. The most recent major

earthquakes in the SISZ struck in the early 2000s. Two events of magnitudes M_w 6.5 and M_w 6.4 occurred in June 2000 and were followed by an M_w 6.3 quake in May 2008. The three earthquakes all caused damage to structures in the region along with liquefaction, landslides, and rock fall, but there was no collapse of residential buildings and no fatalities (Bessason et al., 2022).

The characteristics of soil sites in the SISZ are shaped by a combination of volcanism and glacial impacts, including sub-glacier outburst floods (Atakan et al., 1997; Erlingsson, 2019). Soil deposits in the South Iceland Lowland, and along the southern coast, are mainly composed of normally consolidated black basalt materials that have usually been carried off the highlands by aerial, fluvial, glacial or glaciofluvial processes in Holocene times. The sediments are primarily characterized by coarse silty particles, sand, and coarser grains, and are often loosely compacted due to the rapid sediment build-up. In many areas, the soil deposits are overlaid by Holocene lava formations, thus creating structures with layers of fractured lava-rock on top of or embedded in the softer sediments. These result in strong velocity reversals with depth.

Previous studies (Bessason and Kaynia, 2002; Rahpeyma et al., 2016; Sigurðsson et al., 2017) have reported a significantly intensified ground motion at composite lava-rock/sedimentary sites in the SISZ, as compared to rock conditions. The overall response is predominantly controlled by the soil layers. Hence, the average S-wave velocity from surface down to depth z ($V_{S,z}$) becomes largely irrelevant as a site effect proxy. Such conditions are, therefore, not well represented in the site categorization criteria defined in the current and forthcoming versions of Eurocode 8 (CEN, 2004; CEN/TC 250/SC 8, 2021), highlighting the need for site-specific analysis based on local geotechnical information. However, a lack of measured values of S-wave velocity (V_S) for soil deposits underlying lava-rock in the SISZ, as well as information on their strain-dependent behaviour, has restricted the use of numerical techniques for evaluation of ground motion amplifications in said locations.

This paper presents a case study for two locations in the SISZ where an approximately 5–10 m thick layer of lava-rock is embedded in soft sediments within the uppermost 10–20 m. The V_S profile for each site is retrieved using active- and passive-source surface wave analysis, combined with single-station microtremor analysis, and shown to be consistent with available borehole data and other geological information. Equivalent linear (EQL) and non-linear (NL) ground response analysis is subsequently used to study the effects of the soft sandy/gravelly sediments, underlying the lava-rock, on ground motion amplifications for different hazard scenarios. Consistent with conventional construction practise, where the surficial soils overlying the lava-rock are removed and structures founded on the underlying rock, the subsoil models used in the analysis are defined as ‘stiff-soft-stiff’ structures based on the retrieved velocity profiles.

2 Survey locations – Stóra-Laxá Bridge and Óseyri Bridge

The first site is located by the north-eastern abutment of the Stóra-Laxá Bridge, around 3 km north of the fault rupture of the M_w 6.5 June 17, 2000 South Iceland Earthquake (Fig. 1a). The Stóra-Laxá Bridge is a 145 m long four-span RC base-isolated bridge that was constructed between 2021 and 2023. The surface wave measurements described in Section 3 were conducted in 2020, before earthworks at the site began. Four geotechnical boreholes (SL-1 to SL-4) were drilled at the location of the north-eastern abutment in 2020 during the design phase of the bridge. The boreholes all indicate a layer of scoria (i.e., vesicular igneous rock) between depths of 5.5–6 m and 11–13 m at the site (Fig. 1b). Below are soil layers comprised of a mixture of gravel, sand, and silt. The borings were terminated at a depth of between 13.8 m and 23.7 m before reaching bedrock or another lava-rock layer. Therefore, no information on soil layering is available for depths exceeding 23.7 m.

The second survey location is at the estuary of the Ölfus River close to the western abutment of the Óseyri Bridge and less than 2 km from the western fault rupture of the May 2008 M_w 6.3 Ölfus Earthquake (Fig. 1a). The Óseyri Bridge was built in 1988 and is a 370 m long base-isolated, continuous post-tensioned two-beam concrete bridge built in eight spans. The surficial deposits by the bridge are comprised of loose black basalt sand that, based on a borehole drilled by the western abutment (OB-1), extends down to a depth of 6 m (Fig. 1c). Beneath the sand, a layer of lava-rock was found. However, the boring was terminated at 11.7 m depth before reaching the bottom of the lava-rock. Borings conducted both east and west of the Óseyri Bridge site, i.e., in the town of Þorlákshöfn, the village of Eyrarbakki, and on the eastern bank of the Ölfus River (Fig. 1a), show the presence of a second sand layer beneath the lava-rock. Nonetheless, based on the available data, the thickness of the presumed lava-rock layer at the Óseyri Bridge site is unknown.

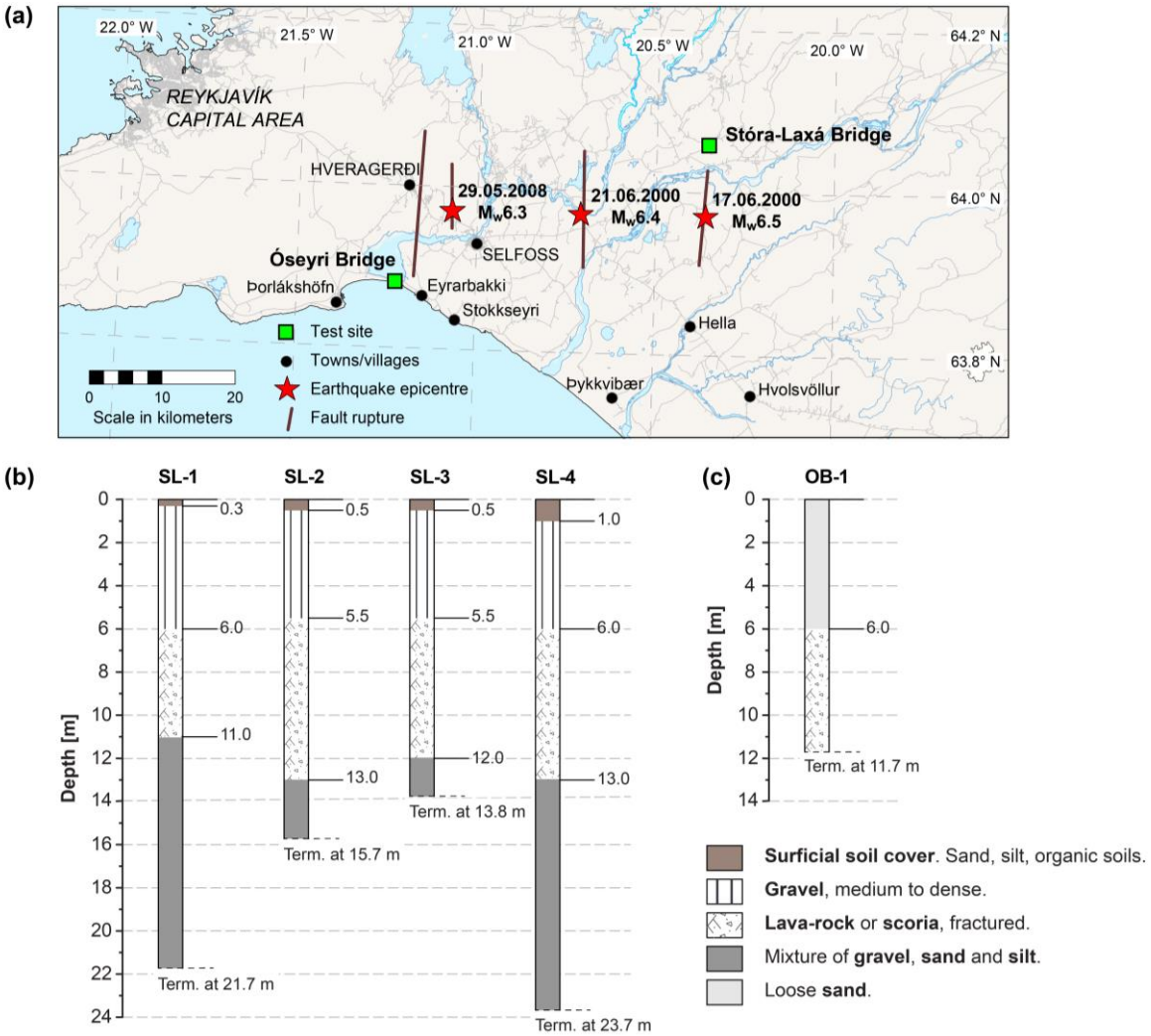

Figure 1. (a) Locations of the Stóra-Laxá Bridge and Óseyri Bridge sites relative to the epicentres and fault ruptures of the June 2000 South Iceland Earthquakes and the May 2008 Ölfus Earthquake. Borehole logs for (b) Stóra-Laxá Bridge (SL-1, SL-2, SL-3, SL-4) and (c) Óseyri Bridge (OB-1).

3 Non-invasive measurements at lava-rock/sedimentary sites

The surface wave measurements at the two sites consisted of active-source MASW (Multichannel Analysis of Surface Waves) and passive-source MAM (Microtremor Array Measurements). The passive-source data were further analysed using the MHVSR technique (Microtremor Horizontal-to-Vertical Spectral Ratio) to assess the fundamental site frequencies, and the RayDec method for evaluation of R-wave ellipticity. A joint dispersion-ellipticity inversion was subsequently implemented for evaluation of the V_S profile for each site, including the depth and thickness of the embedded lava-rock layer. This section provides a brief overview of the in-situ data acquisition and analysis. A more comprehensive description is provided in Olafsdottir et al. (2023).

3.1 In-situ data acquisition

The MASW testing was conducted using twenty-four 4.5 Hz vertical geophones (GS-11D from Geospace Technologies) arranged in an equally spaced linear array and connected to custom data acquisition (DAQ) hardware and software (with receiver spacings of 0.5 m and 1 m for Stóra-Laxá Bridge, and 1 m and 2 m for Óseyri Bridge). The seismic source was a 6.3 kg sledgehammer that was struck on a metallic plate, in-line with the receivers. At each site, repeated shots were collected along the same survey line with varying receiver spacing, source offsets and shot positions (forward or reverse shot gathers). The duration of each shot gather was 2.2 s, including a 0.2 s pre-trigger, with a sampling rate of 1000 Hz. The passive-source DAQ was conducted using a set of four broadband three-component Lennartz 5 s seismometers each coupled with a Reftek digitizer. The seismometers were arranged in triangular-shaped arrays (circumradius of 6 m for Stóra-

Laxá Bridge, and 6 m, 12 m, and 24 m for Óseyri Bridge) whose centroid was located as close as possible to the midpoint of the MASW survey line. The DAQ was conducted under favourable weather conditions (low wind and no rain) and the recording duration for each array was 50–60 min with a sample rate of 200 Hz.

3.2 Microtremor Horizontal-to-Vertical Spectral Ratio

The MHVSR for each station was computed following the recommendations presented in the SESAME (2004) report. The recorded microtremors were split into 50 s windows and the Fourier spectra of the horizontal and vertical components smoothed using the Konno-Ohmachi (1998) function with b = 40. The HVSR of each window was subsequently obtained by dividing the geometric mean of the horizontal spectra by the spectrum for the vertical component. The resulting lognormal-median MHVSR curves for the stations of the triangular-shaped arrays at the Stóra-Laxá Bridge and Óseyri Bridge sites are shown in Figs. 2a and 2b, respectively.

As established by the geotechnical borings by the Stóra-Laxá Bridge, the second (higher frequency) peak in Fig. 2a is presumably caused by the impedance contrast between the gravel layer and the lava-rock at about 5.5 m depth (Fig. 1b). Similarly, for the Óseyri Bridge site, the second HVSR peak is most likely related to the impedance contrast between the surficial sand layer and the lava-rock found approximately 6 m below ground level (Fig. 1c). The fact that the observed MHVSR for the Óseyri Bridge site displays two distinct peaks is further considered to support prior evaluations indicating the presence of a second sand layer beneath the encountered lava-rock at the site. The mean frequency of each peak ($f_{0,HV}$ for the first peak and $f_{1,HV}$ for the second peak) and the associated standard deviations (std) are marked with vertical line segments in Fig. 2. It is worth noting that only HVSR peaks that fulfil the clarity criteria of SESAME (2004), and are therefore considered reliable, are used for evaluation of $f_{0,HV}$ and $f_{1,HV}$.

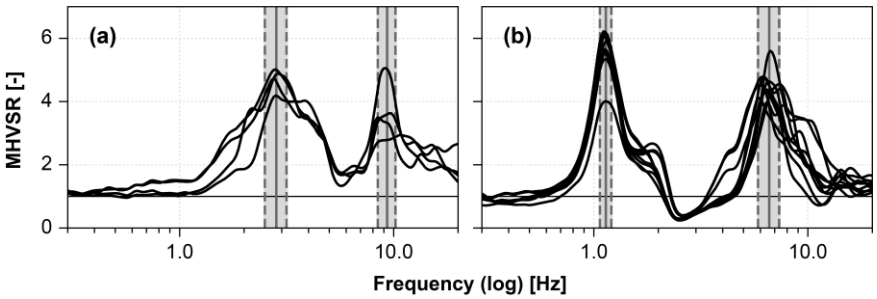

Figure 2. Lognormal-median MHVSR for individual stations of the passive-source arrays at (a) Stóra-Laxá Bridge and (b) Óseyri Bridge. The vertical lines show the mean ± std frequencies of the HVSR peaks.

3.3 Experimental dispersion and ellipticity curves

The R-wave dispersion curve for each site was obtained using the acquired MASW and MAM data. The active-source data was processed using the phase shift method as implemented in the MASWaves code (Olafsdottir et al., 2018) with each shot gather processed separately. The passive-source registrations were analysed using the Modified Spatial Autocorrelation (MSPAC) toolbox of the Geopsy package (Wathelet et al., 2020). To calculate standard deviation values, the 50–60 min recordings from each triangular array were split into windows of 12.5–15 min and each sub-record analysed independently. The resulting collections of dispersion curves are presented in Figs. 3a and 4a for the Stóra-Laxá Bridge and Óseyri Bridge sites, respectively. The MASW and MAM dispersion curve data points overlap in the frequency range of 12.7–25 Hz for Stóra-Laxá Bridge and 9.1–13.9 Hz for Óseyri Bridge, indicating a good agreement between the different types of analysis and that the active- and passive-source branches can be reasonably combined into a single broadband curve. The resulting arithmetic mean dispersion curves, obtained by binning the data points in Figs. 3a and 4a within logarithmically spaced frequency bands, are shown in Figs. 3d and 4d, for the two sites respectively. The upper and lower boundaries also shown correspond to two standard deviations from the mean curve. No systematic difference was observed between dispersion curves obtained from shots applied at different ends of the MASW receiver array, therefore, not indicating significant lateral variations in soil stratigraphy at shallow depth beneath the linear array. This observation is consistent with the similar-shaped MHVSR at the individual MAM stations (Fig. 2). Hence, a 1-D analysis was considered sufficient in the following.

The R-wave ellipticity curve for each station of the MAM arrays was computed with the RayDec technique (Hobiger et al., 2009). The microtremor recordings were split into six 8–10 min windows that were analysed

separately to obtain standard deviations for the experimental ellipticity. The ellipticity curves for each station were finally averaged by assuming a lognormal distribution. The resulting sets of lognormal-median curves for the Stóra-Laxá Bridge and Óseyri Bridge sites are shown in Figs. 3b and 4b, respectively. The analysis results for both sites show bimodal curves with peak frequencies consistent with those indicated by the MHVSR (Fig. 2). Furthermore, the calculated ellipticity is close to the MHVSR, suggesting that the recorded wavefield is primarily composed of R-waves. The segments of the ellipticity curves that were used in the joint R-wave dispersion and ellipticity curve inversion (see Section 3.4) are shown with upper and lower boundaries corresponding to two standard deviations in Figs. 3e and 4e.

3.4 Inversion for S-wave velocity

The V_S profiles for the two sites were obtained by jointly inverting the identified dispersion and ellipticity curves using the Dinver module of Geopsy (Wathelet et al., 2004; 2020). The inversion was conducted in the same manner as described in Olafsdottir et al. (2023). However, the layering parameterization was changed to allow for evaluation of the variation in V_S within the granular layer underlying the lava-rock. That is, the Stóra-Laxá Bridge site was modelled as a five-layered system over a half-space, and the Óseyri Bridge site as six layers over a half-space. In both cases, a velocity reversal was permitted between layers three and four. The layer thicknesses and the S-wave velocity in each layer were treated as unknown parameters to be established by the inversion, with search ranges defined based on available geological and geotechnical data. The material density has a small effect on the theoretically computed curves and was therefore fixed to reduce the number of inversion parameters. The Poisson's ratio (confined to the range of 0.2–0.5) was used to link the S- and P-wave velocities in each layer to prevent soil models with physically impossible combinations of V_S and V_P. Additionally, for soil layers modelled as saturated, V_P was constrained to a minimum value equal to the P-wave velocity in saturated soil. For each analysis, the inversion scheme was initiated five times with 75,000 models sampled in each initiation. The misfit function (m), used to quantify the goodness of fit between a theoretical curve and the corresponding experimental data, is defined as (Wathelet et al., 2004; Hobiger et al., 2013)

$$m = \sqrt{\frac{1}{N}\sum_{i=1}^{N}\left(\frac{D_i - T_i}{E_i}\right)^2} \tag{1}$$

where D_i and T_i denote the experimental and theoretical values for the i-th data point ($1 \leq i \leq N$), respectively, and E_i is the associated measurement error, here specified as two standard deviations. Equation (1) was used to compute separate misfit values for the target dispersion and ellipticity curves. The sampled models were then ranked by the weighted average of the dispersion and ellipticity misfits ($\overline{m}$) by giving equal weights to both values. The lowest dispersion-ellipticity misfit achieved in each initiation is denoted as $\overline{m}_{min}$.

Figures 3cde give the results of the joint inversion for the Stóra-Laxá Bridge site. For inversion of ellipticity curves showing singularities, the peak frequency and the right flank of the ellipticity peak have been shown to carry the most valuable information on the stratigraphic structure (Hobiger et al., 2013). Hence, to constrain the frequencies of both ellipticity peaks, four segments of the experimental ellipticity curve were defined as inversion targets (Fig. 3e) resulting in a frequency gap between the ellipticity data and the target dispersion curve (Fig. 3d) of a factor of 1.2. For each of the five inversion initiations, 100 models were selected randomly from the subset of sampled models whose dispersion-ellipticity misfits satisfy $\overline{m} \leq 1.25 \cdot \overline{m}_{min}$. The resulting collection of interval V_S profiles is shown in Fig. 3c where the profiles are color-coded by $\overline{m}$. The associated theoretical dispersion and ellipticity curves are compared to the experimental data points specified as inversion targets in Figs. 3de. As shown, the theoretically computed dispersion curves fit the experimental average curve within ±2 standard deviations and the two ellipticity peaks are consistently well reproduced. The developed velocity profiles show an abrupt increase in V_S at 5–6 m depth, which matches the top of the scoria found in the borings at the site (Fig. 1b). The sharp velocity decrease at a depth of around 13 m is further consistent with the location of the layer interface between the scoria and the underlying gravelly silty sand. The second velocity increase at 35–40 m depth, related to the lower frequency ellipticity peak, is interpreted as depth to underlying rock. V_S of around 260–520 m/s is predicted for the sediments underlying the scoria. At depths of 15–20 m, measurements at normally dispersive, sandy, and gravelly sites in the SISZ have commonly indicated V_S of around 200–400 m/s, although examples of both higher and lower V_S exist (Erlingsson et al., 2022). Here, the overburden from the lava-rock is expected to somewhat increase the stiffness of the underlying soils, although the extent of this presumed effect is highly uncertain.

The inversion results for the Óseyri Bridge site are presented in Figs. 4cde. Following the same analysis process as described above, four segments of the experimental ellipticity curve were specified as inversion targets along with the broadband dispersion curve (Figs. 4de). As a result, the ellipticity and dispersion data overlap in the frequency range of 2.4–10.3 Hz. The theoretical dispersion and ellipticity curves fit the target curves well over their entire frequency range, and the observed ellipticity peaks and trough are well retrieved. The resulting interval V_S profiles (Fig. 4c) reveal a stiff layer embedded in the softer sediments between depths of 6 m and 12–15 m. A surficial sediment thickness of around 6 m is consistent with the boring log for the site (Fig. 1c). However, measurements of the lava-rock layer thickness are not available. The estimated V_S for the underlying sediments is around 300–550 m/s, which is comparable to the values predicted for the Stóra-Laxá Bridge site. The depth to underlying bedrock is established as around 80–85 m.

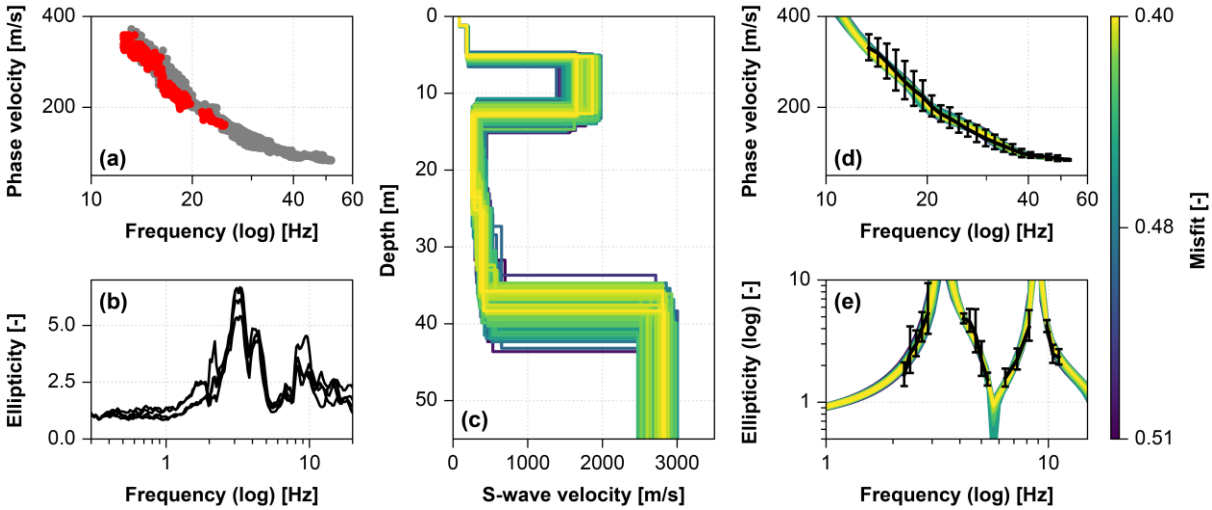

Figure 3. Joint dispersion-ellipticity curve inversion for the Stóra-Laxá Bridge site. (a) Dispersion curves obtained by active-source MASW (grey) and passive-source MAM (red) measurements. (b) Lognormal median R-wave ellipticity curves for individual stations of the passive-source array. (c) Set of V_S profiles whose misfit values satisfy $\overline{m} \leq 1.25 \cdot \overline{m}_{min}$. The associated theoretically computed dispersion and ellipticity curves are compared to the experimental data points specified as inversion targets in (d) and (e).

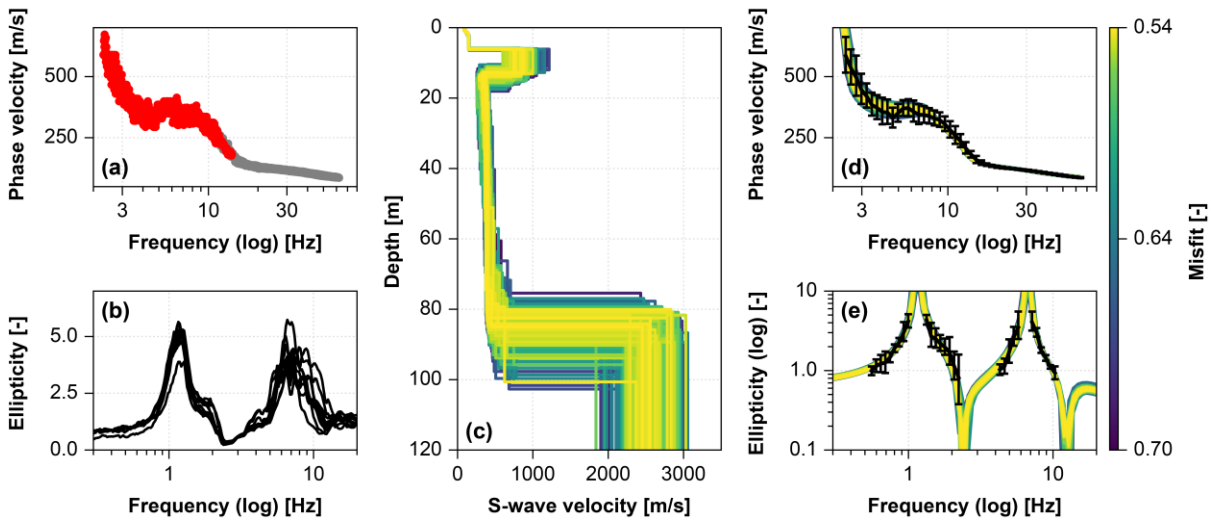

Figure 4. Joint dispersion-ellipticity curve inversion for the Óseyri Bridge site. The results are presented in the same manner as described for Fig. 3.

4 Numerical assessment of ground response

Equivalent linear and non-linear 1-D ground response analysis was conducted for the two sites described in preceding sections to study the effects of the granular sediments, underlying the lava-rock, on ground motion amplifications for different hazard scenarios. The EQL analysis was conducted using the STRATA code (Kottke

et al., 2008), while DEEPSOIL v7.0 (Hashash et al., 2020) was used for the NL analysis. EQL analysis has the advantage of being simple and computationally efficient. However, for strong input motions and/or soft soil profiles, leading to high shear strain levels, the suitability of EQL analysis has been questioned (e.g., Kaklamanos et al., 2013). In such cases, NL analysis can provide more reasonable results. Nevertheless, NL approaches suffer from lower numerical stability than EQL analysis and require a reliable constitutive material model, whose model parameters are often not as well established as the modulus reduction and damping (MRD) relationships required for EQL analysis. Hence, the code-to-code variability, related to the use of different numerical schemes, choice of constitutive models and model parameter calibration, adds to the uncertainty associated with NL analysis (Kramer, 2014; Régnier et al., 2018).

4.1 Definition of numerical soil models

The velocity models used for the EQL and NL analysis are shown in Figs. 5ab for the two sites, respectively. Consistent with conventional practice at building sites where a relatively thin surficial soil layer is found to overlie competent rock, it is assumed that the surficial soils would be removed prior to start of construction and structures founded on the underlying lava-rock. Therefore, the subsoil models are defined as 'stiff-soft-stiff' structures. Little information exists on typical V_S values for lava-rock in the South Iceland Lowland. However, as the lava-rock is typically highly fractured, its V_S is expected to be somewhat lower than that of basaltic rock. Resulting from the irregularity and inhomogeneity of igneous rock structures, a large variation is further expected. Prior studies have used estimated values of 1000 m/s (Bessason and Kaynia, 2002) and 1800 m/s (Rahpeyma et al., 2016). Here, the V_S and thickness of the lava-rock layer was specified based on the inverted velocity profiles (Figs. 3c, 4c) as 1650 m/s (8 m thickness) and 850 m/s (7.5 m thickness) for the Stóra-Laxá and Óseyri Bridge sites, respectively. However, an earlier study has indicated that the lava-rock V_S has minor influence on the estimated amplification effects, given that its value is considerably higher than that of the underlying soil (Bessason and Kaynia, 2002). For the granular sediments beneath the lava-rock, V_S is assumed to increase linearly with depth from 260 m/s to 520 m/s for the Stóra-Laxá Bridge site, and from 300 m/s to 550 m/s for the Óseyri Bridge site. At the base of the columns, bedrock is modelled by assigning a V_S value of 2800 m/s (at z = 33 m) and 2500 m/s (at z = 77.5 m) for the two locations, respectively.

In lack of site-specific data, the non-linear material behaviour is described using MRD relationships adopted from literature (Figs. 5cd) in the EQL analysis. The GeoIndex model (Roblee and Chiou, 2004) is used to describe the MRD behaviour of the sandy and gravelly soils underlying the lava-rock, specifically the depth-dependent curves for soil class 1-PCA (Primarily Coarse – All Plasticity Values). To account for the added confinement due to the lava-rock layer, reference depths for assignment of the GeoIndex MRD curves were based on the original (in-situ) soil profiles (in-situ depth in Figs. 5ab, right hand axes). The curves proposed for rock by Schnabel et al. (1972) were assumed for the lava-rock layer.

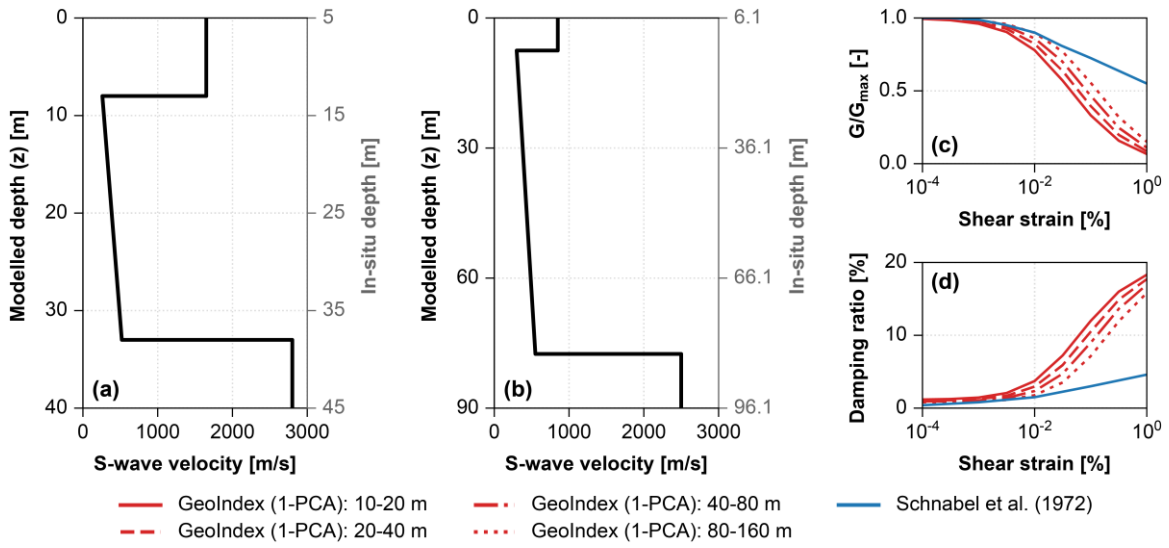

Figure 5. Velocity profiles defined for EQL and NL ground response analysis at the (a) Stóra-Laxá Bridge and (b) Óseyri Bridge sites. (c, d) Modulus reduction and damping curves specified for the lava-rock (Schnabel et al., 1972) and the underlying sediments (GeoIndex 1-PCA).

Two constitutive material models are implemented for NL analysis in DEEPSOIL v7.0. First, an extended version of the modified hyperbolic Kondner-Zelasko (MKZ) model (Matasovic, 1993) and, second, the generalized quadratic/hyperbolic (GQ/H) model with shear strength control (Groholski et al., 2016). As compared to the MKZ formulation, the GQ/H model was developed to better describe the large-strain shear strength of the soil, thus, reducing the risk of unrealistic shear stresses being predicted with increasing shear strains. Here, results obtained by specifying the MKZ and GQ/H models, respectively, for the granular sediments underlying the lava-rock are compared. In both cases, the constitutive model parameters are calibrated to fit the GeoIndex MRD curves using the reduction factor procedure (MRDF-UIUC) of Phillips and Hashash (2009). The surficial lava-rock layer is modelled as linear, assuming a strain-constant shear modulus $G_{max} = \rho \cdot V_S^2$ based on the estimated lava-rock S-wave velocity and a constant damping ratio of 0.5%.

4.2 Input motions

Three sets of strong ground motion records, recorded at rock sites during major earthquakes in the SISZ (M_w 5.4 to M_w 6.5), were specified as input motions for the EQL and NL analysis. Aiming to cover different hazard levels in the SISZ and the South Iceland Lowland, three PGA levels were considered: 0.1–0.2g (EQ-set I, mean 0.15g), 0.2–0.4g (EQ-set II, mean 0.3g), and ≥0.4g (EQ-set III, mean 0.53g, max 0.66g). The accelerograms assigned to each set (24 for sets I and II, 13 for set III) were scaled to provide an approximately even distribution of PGA over the respective interval, with the constant amplitude scaling factor restricted to the range of [0.5, 2]. Note that due to the limited amount of high PGA rock motions, some of the available accelerograms were assigned to more than one set. An overview of the selected input ground motions is provided in Table 1 and their acceleration response spectra (5% damping) are shown in Figs. 6abc. The mean and standard deviation normalized response spectra for the three EQ-sets all show comparable shapes as illustrated in Fig. 6d. The corresponding PGA distributions are shown in Figs. 6efg.

Table 1. Overview of strong ground motion records used for the EQL and NL ground response analysis.

Set	Event	Date	M_w	No. stations	No. records	Epicentral dist. [km]	PGA [g]	PGA [g] scaled
I	Mt. Hengill Area	04.06.98	5.4	1	2	6	0.14–0.17	0.17–0.18
I	South Iceland	17.06.00	6.5	7	7	5–41	0.07–0.32	0.11–0.20
I	South Iceland (aftershock)	17.06.00	6.0	3	5	10–18	0.05–0.15	0.10–0.15
I	South Iceland	21.06.00	6.4	5	6	14–24	0.11–0.18	0.12–0.20
I	Olfus	29.05.08	6.3	3	4	8–9	0.11–0.33	0.15–0.20
II	Mt. Hengill Area	04.06.98	5.4	1	2	6	0.14–0.17	0.23–0.29
II	South Iceland	17.06.00	6.5	5	7	5–41	0.11–0.34	0.20–0.36
II	South Iceland (aftershock)	17.06.00	6.0	1	1	10	0.15	0.24
II	South Iceland	21.06.00	6.4	5	7	6–24	0.11–0.57	0.20–0.40
II	Olfus	29.05.08	6.3	4	7	8–9	0.13–0.66	0.22–0.40
III	South Iceland	17.06.00	6.5	2	3	5–15	0.22–0.34	0.41–0.51
III	South Iceland	21.06.00	6.4	2	4	6	0.45–0.57	0.53–0.63
III	Olfus	29.05.08	6.3	3	6	8–9	0.22–0.66	0.40–0.66

4.3 Results of 1-D EQL and NL ground response analysis

The results of the 1-D EQL and NL ground response analysis are given in Figs. 7 and 8 for the Stóra-Laxá Bridge and Óseyri Bridge sites, respectively, in terms of acceleration response spectra (*SA*), surface-bedrock spectral amplification ratios (*SR,* Equation (2)), and maximum shear strain (γ_{max}) profiles. For clarity, only the mean response for each set of input motions is shown. The results obtained by utilizing the MKZ and GQ/H constitutive material models are distinguished as NL-MKZ and NL-GQ/H.

$$SR = \frac{SA_{surface}}{SA_{bedrock}} \quad (2)$$

where $SA_{surface}$ and $SA_{bedrock}$ are the acceleration response spectra at surface and that of reference bedrock.

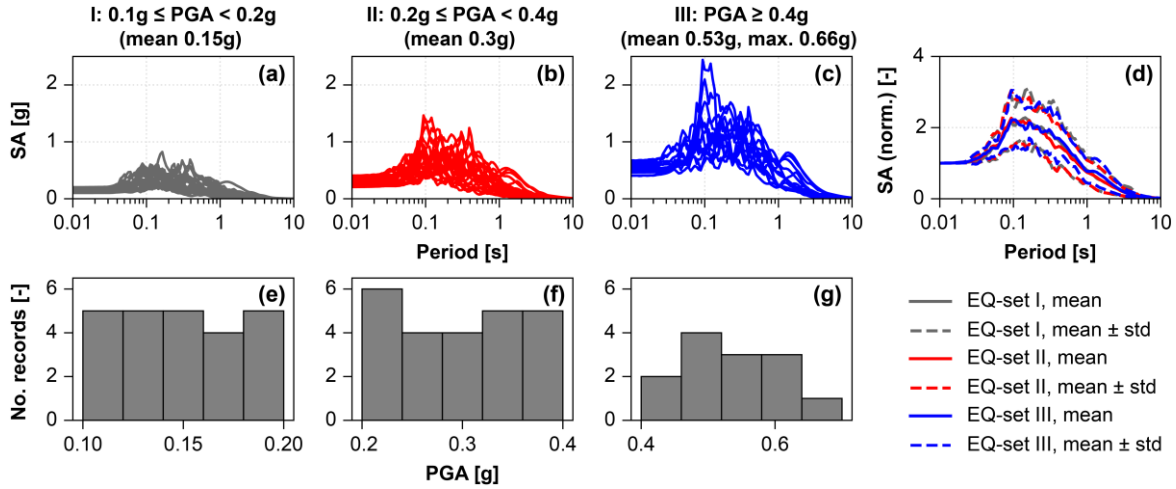

Figure 6. Acceleration response spectra (SA, 5% damping) for the input ground motions assigned to (a) EQ-set I, (b) EQ-set II, and (c) EQ-set III. (d) Mean plus/minus standard deviation (std) normalized SA for the three sets of input motions. Distribution of PGA values for (e) EQ-set I, (f) EQ-set II, and (g) EQ-set III.

The results in Figs. 7 and 8 illustrate a clearly intensity-dependent ground motion amplification behaviour, with the peak surface-bedrock amplification ratio (Figs. 7e, 8e) decreasing and occurring at longer periods with increased PGA level. For EQ-set III (PGA ≥ 0.4g), and to lesser extent EQ-set II (0.2g ≤ PGA < 0.4g), the numerical models indicate an attenuation of the input ground motions in the short period range (i.e., at periods shorter than 0.2–0.3 s). The amount of attenuation, and the width of the period interval where the attenuation effects are observed, further increases with PGA, showing mean amplification factors (*SR*) as low as 0.5–0.7, depending on the analysis approach (EQL, NL-MKZ, or NL-GQ/H). In the intermediate-to-long period range, amplification of the input ground motion is observed for both EQ-sets II and III, with the peak values of *SR* exceeding 2–3. For the EQ-set I input motions, the mean curves in Figs. 7ae and 8ae, indicate amplification effects over the entire period range.

The different analysis approaches (EQL, NL-MKZ, and NL-GQ/H) provide, overall, similar results for the EQ-set I input ground motions. For this set of motions, the mean values of γ_{max} are further at or below 0.1% (Figs. 7d, 8d), which is a strain level where EQL analysis may be expected to provide sufficient results (Kaklamanos et al., 2013) The differences between the EQL and NL approaches (especially NL-MKZ) become more apparent for the EQ-set II and III data, as higher shear strains are reached, with the EQL analysis generally predicting somewhat greater amplification and less attenuation, particularly near the resonant site frequency and in the short-to-intermediate period range (Figs. 7e, 8e). Such tendence of EQL analysis to show a stronger response near the site resonant frequency, as compared to NL approaches, is well reported (e.g., Kim et al. 2016). For the Stóra-Laxá Bridge site, where the shear strain level is found to exceed 0.4–0.6% for the granular materials underlying the lava-rock (Fig. 7d), the NL-MKZ ordinates (blue dashed line in Fig. 7e) are further noticeably lower at short-to-intermediate periods, and the peak response is shifted to higher periods, as compared to the NL-GQ/H results. This observation may be related to previously reported limitations of the MKZ model to accurately describe the material behaviour at large shear strains (Groholski et al., 2016).

5 Summary and concluding remarks

This work describes a non-invasive technique, utilizing a joint dispersion-ellipticity inversion, that has been found effective for V_S profiling at locations where a lava-rock layer is embedded in granular sediments at shallow depth ('soft-stiff-soft-stiff' sequence). It is applied at two sites in the SISZ where a 5–10 m thick layer of lava-rock is found within the top 10–20 m. The predicted depth and thickness of the lava-rock agrees with available geotechnical data and the V_S of the underlying sediments is consistent with measured values for comparable soil types in other locations in the SISZ. The results further indicate that MHVSR is a time- and cost-efficient tool for initial geological surveying; to identify sites where a lava-rock layer may overlie soft soils, or be embedded in the soil strata, thus, requiring further analysis.

To better understand the site amplification characteristics at locations in the SISZ where lava-rock overlies soft sediments, 1-D EQL and NL ground response analysis was conducted for the two sites considered in this

work. As any structures would conventionally be founded on the underlying lava-rock, the sites are treated as 'stiff-soft-stiff' structures, with the top-most soft layer 'removed'. Recorded accelerograms from major earthquakes in the SISZ were specified as input motions, considering three intensity levels defined in terms of PGA: (I) 0.1–0.2g, (II) 0.2–0.4g, and (III) ≥0.4g (max. 0.66g). The results show an amplification of the input motion at intermediate-to-long periods, with values of *SR* up to about 2–3.5 in the period range of 0.3–2 s. These values are though highly dependent on the ground motion intensity, and to a lesser extent, the numerical method adopted for the analysis. Attenuation effects were observed at periods shorter than 0.2–0.3 s for the two sets of higher intensity motions, showing levels of attenuation up to around *SR* = 0.5–0.7.

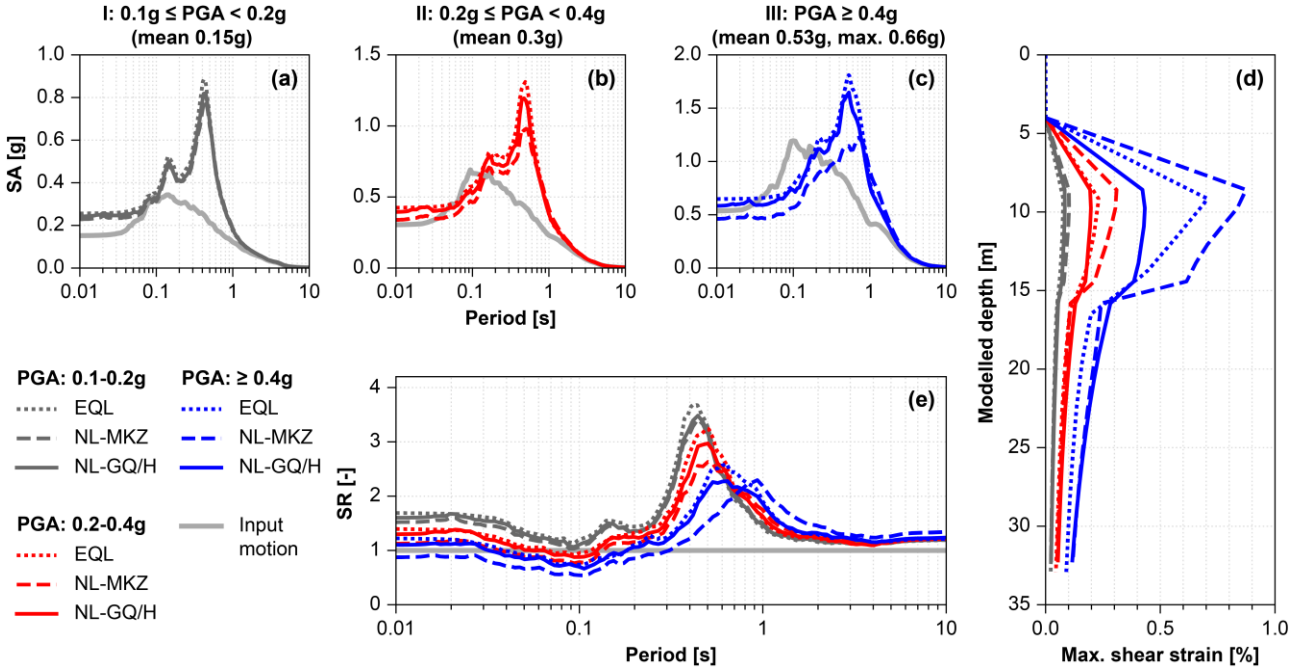

Figure 7. Stóra-Laxá Bridge site. Results of EQL and NL ground response analysis represented by the mean response for each set of input motions. Acceleration response spectra (SA, 5% damping) for (a) EQ-set I, (b) EQ-set II, and (c) EQ-set III. (d) Maximum shear strain profiles. (e) Spectral amplification ratio (SR).

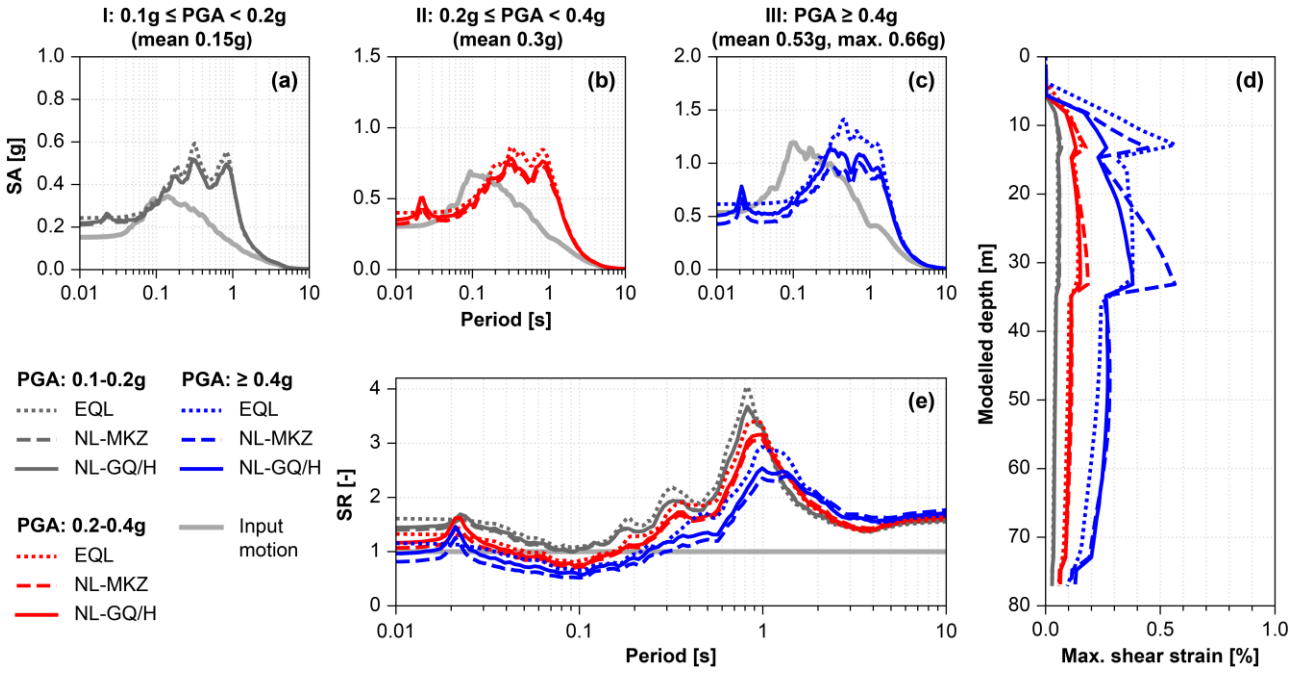

Figure 8. Óseyri Bridge site. Results of EQL and NL ground response analysis. The results are presented in the same manner as described for Fig. 7.

Large areas in the SISZ are characterized by fractured lava-rock overlying soft sediments. However, it can be challenging to identify such sites in practice, except by drilling sufficiently deep boreholes. Locations where a layer of lava-rock is embedded in soft sediments may, therefore, be misinterpreted as rock sites or as shallow sediments above competent bedrock. The current study provides an initial analysis of two well-characterized composite lava-rock/sedimentary sites in the SISZ using EQL and NL techniques. Compared to rock conditions, the results indicate that the amplification effects are considerable over certain period ranges. Hence, a presumption of rock conditions may underestimate the ground response for design. These findings agree with earlier studies (e.g., Bessason and Kaynia, 2002). Nevertheless, further work must be undertaken to better establish the amplification and attenuation effects in the context of the Icelandic geological and seismic framework, particularly with regard to the ongoing revision of EC8. These include extensive parametric studies assessing the effects of the lava-rock overburden and the S-wave velocity and thickness of the underlying granular sediments on the predicted ground response. Uncertainties related to assignment of non-linear material parameters, including selection of MRD curves and, in case of NL analysis, calibration of the adopted constitutive material models further have to be explored in a more comprehensive way.

6 Acknowledgements

This work was supported by the Icelandic Research Fund (grant no. 206793-053, 218149-053), the Icelandic Road and Coastal Administration, and the Energy Research Fund of the National Power Company of Iceland.

7 References

Atakan K., Brandsdóttir B., Halldórsson P., Friðleifsson G.O. (1997). Site response as a function of near-surface geology in the South Iceland Seismic Zone, *Natural Hazards*, 15(2-3): 139-164.

Bessason B., Kaynia A.M. (2002). Site amplification in lava rock on soft sediments, *Soil Dynamics and Earthquake Engineering*, 22(7): 525-540.

Bessason B., Rupakhety R., Bjarnason J.Ö. (2022). Comparison and modelling of building losses in South Iceland caused by different size earthquakes, *Journal of Building Engineering*, 46: 103806.

CEN (2004). *EN 1998-1:2004. Eurocode 8: Design of structures for earthquake resistance - Part 1: General rules, seismic actions and rules for buildings,* Comité Européen de Normalisation, Brussels.

CEN/TC 250/SC 8 (2021). *prEN 1998-1-1:2021 ENQ 2022-01-11. Eurocode 8: Design of structures for earthquake resistance - Part 1-1: General rules and seismic action.*

Einarsson P. (2008). Plate boundaries, rifts and transforms in Iceland, *Jökull*, 58: 35-58.

Erlingsson S. (2019). Geotechnical Challenges in Iceland, *Proceedings of the XVII European Conference on Soil Mechanics and Geotechnical Engineering*, Reykjavik, Iceland.

Erlingsson S., Olafsdottir E.A., Bessason B. (2022). Soil site stiffness categorization based on MASW field testing, *Proceedings of the 20th International Conference on Soil Mechanics and Geotechnical Engineering*, Sidney, Australia, pp. 371-376.

Groholski D.R., Hashash Y.M.A., Kim B., Musgrove M., Harmon J., Stewart, J.P. (2016). Simplified model for small-strain nonlinearity and strength in 1D seismic site response analysis, *Journal of Geotechnical and Geoenvironmental Engineering*, 142(9): 04016042.

Hashash Y.M.A., Musgrove M.I., Harmon J.A., Ilhan O., Xing G., Numanoglu O., Groholski D.R., Phillips C.A., Park, D. (2020). *DEEPSOIL 7.0, User Manual*. Board of Trustees of University of Illinois at Urbana-Champaign, Urbana, Illinois.

Hobiger M., Bard P.Y., Cornou C., Le Bihan N. (2009). Single station determination of Rayleigh wave ellipticity by using the random decrement technique (RayDec), *Geophysical Research Letters*, 36: L14303.

Hobiger M., Cornou C., Wathelet M., Di Giulio G., Knapmeyer-Endrun B., Renalier F., Bard P.Y., Savvaidis A., et al. (2013). Ground structure imaging by inversions of Rayleigh wave ellipticity: sensitivity analysis and application to European strong-motion sites, *Geophysical Journal International*, 192(1): 207-229.

IST. (2010). *Icelandic National Annexes to Eurocodes*, Staðlaráð Íslands, Reykjavík.

Jónasson K., Bessason B., Helgadóttir Á., Einarsson P., Gudmundsson G.B., Brandsdóttir B., Vogfjord K.S., Jónsdóttir K. (2021). A harmonised instrumental earthquake catalogue for Iceland and the northern Mid-Atlantic Ridge, *Natural Hazards and Earth System Sciences*, 21(7): 2197-2214.

Kaklamanos J., Bradley B.A., Thompson E.M., Baise L.G. (2013). Critical Parameters Affecting Bias and Variability in Site-Response Analyses Using KiK-net Downhole Array Data, *Bulletin of the Seismological Society of America*, 103(3): 1733-1749.

Kim B., Hashash Y.M.A., Stewart J.P., Rathje E.M., Harmon J.A., Musgrove M.I., Campbell K.W., Silva W.J. (2016). Relative Differences between Nonlinear and Equivalent-Linear 1-D Site Response Analyses, *Earthquake Spectra*, 32(3), 1845-1865.

Konno K., Ohmachi T. (1998). Ground-motion characteristics estimated from spectral ratio between horizontal and vertical components of microtremor, *Bulletin of the Seismological Society of America*, 88(1): 228-241.

Kottke A.R., Rathje E.M. (2008). *Technical manual for Strata. Report No.: 2008/10*, Pacific Earthquake Engineering Research Center, University of California, Berkeley.

Kramer S.L. (2014). *Geotechnical earthquake engineering*, Pearson Education Limited, Harlow, England.

Matasovic N. (1993). *Seismic Response of Composite Horizontally-Layered Soil Deposits*, Ph.D. Dissertation, University of California, Los Angeles.

Olafsdottir E.A., Erlingsson S., Bessason B. (2018). Tool for analysis of multichannel analysis of surface waves (MASW) field data and evaluation of shear wave velocity profiles of soils, *Canadian Geotechnical Journal*, 55(2): 217-233.

Olafsdottir E.A., Erlingsson S., Bessason, B. (2023). Hybrid non-invasive characterization of soil strata at sites with and without embedded lava rock layers in the South Iceland Seismic Zone, *Bulletin of Engineering Geology and the Environment*, 82: 146.

Phillips C., Hashash, Y.M.A. (2009). Damping formulation for nonlinear 1D site response analyses, *Soil Dynamics and Earthquake Engineering*, 29(7), 1143-1158.

Rahpeyma S., Halldorsson B., Olivera C., Green R.A., Jónsson S. (2016). Detailed site effect estimation in the presence of strong velocity reversals within a small-aperture strong-motion array in Iceland, *Soil Dynamics and Earthquake Engineering*, 89: 136-151.

Régnier J., Bonilla L.-F., Bard P.-Y., Bertrand E., Hollender F., Kawase H., Sicilia D., Arduino P. et al. (2018). PRENOLIN: International Benchmark on 1D Nonlinear Site-Response Analysis—Validation Phase Exercise, *Bulletin of the Seismological Society of America*, 108(2), 876-900.

Roblee C., Chiou B. (2004). A proposed geoindex model for design selection of non-linear properties for site response analysis, *International workshop on uncertainties in nonlinear soil properties and their impact on modeling dynamic soil response*.

Schnabel P.B., Lysmer J., Seed H.B. (1972). *SHAKE: A computer program for earthquake response analysis of horizontally layered sites. Report No. EERC 72-12*, Earthquake Engineering Research Center, University of California, Berkeley, California.

SESAME (2004). *Guidelines for the Implementation of the H/V Spectral Ratio Technique on Ambient Vibrations: Measurements, Processing, and Interpretations. SESAME European research project. WP12 – Deliverable D23.12*

Sigurðsson G.Ö., Rupakhety R., Ólafsson S. (2017). Site Response Evaluation in a Volcanic Area using H/V and 1 D wave Propagation Analysis, *Proceedings of the 16th World Conference on Earthquake Engineering*, Santiago, Chile.

Wathelet M., Jongmans D., Ohrnberger M. (2004). Surface wave inversion using a direct search algorithm and its application to ambient vibration measurements, *Near Surface Geophysics*, 2(4): 211-221.

Wathelet M., Chatelain J.L., Cornou C., Di Giulio G., Guillier B., Ohrnberger M., Savvaidis, A. (2020). Geopsy: A User-Friendly Open-Source Tool Set for Ambient Vibration Processing, *Seismological Research Letters*, 91(3): 1878-1889.

Viðauki C

Elín Ásta Ólafsdóttir, Sigurður Erlingsson og Bjarni Bessason. (2024). Database of measured shear wave velocity profiles for Icelandic soil sites. Birt í ráðstefnuriti *XVIII European Conference on Soil Mechanics and Geotechnical Engineering*, 26.–30. ágúst 2024, Lissabon, Portúgal.

Proceedings of the XVIII ECSMGE 2024
GEOTECHNICAL ENGINEERING CHALLENGES
TO MEET CURRENT AND EMERGING NEEDS OF SOCIETY

ISBN 978-1-032-54816-6
DOI 10.1201/9781003431749-627

ECSMGE 24
XVIII EUROPEAN CONFERENCE ON SOIL MECHANICS AND GEOTECHNICAL ENGINEERING

Database of measured shear wave velocity profiles for Icelandic soil sites

Base de données des profils de vitesse des ondes de cisaillement mesurés pour les sites de sols islandais

E.A. Olafsdottir*, S. Erlingsson, B. Bessason
Faculty of Civil and Environmental Engineering, University of Iceland, Reykjavik, Iceland
**elinasta@hi.is*

ABSTRACT: MASW (Multichannel Analysis of Surface Waves) is an active-source surface wave method that provides information on shear wave velocity (V_S) distribution down to 10–30 m depth. The technique has been found well-suited for profiling of Icelandic soil sites, including gravelly sites and sites with partly cemented materials or mixed soils containing cobbles or boulders. This paper introduces a database where results of MASW measurements conducted in Iceland can be accessed. The database is available in open-access online and provides the user with an interface which allows results from different sites to be viewed simultaneously and compared in terms of dispersion curves, V_S profiles and time-averaged V_S.

RÉSUMÉ: MASW est une méthode d'onde de surface à source active qui fournit des informations sur la distribution de la vitesse des ondes de cisaillement (V_S) jusqu'à 10 à 30 m de profondeur. La technique s'est avérée bien adaptée au profilage des sites de sols islandais, y compris les sites graveleux et les sites avec des matériaux partiellement cimentés ou des sols mixtes contenant des galets ou des rochers. Cet article présente une base de données où les résultats des mesures MASW effectuées en Islande peuvent être consultés. La base de données est disponible en libre accès en ligne et offre à l'utilisateur une interface permettant de visualiser simultanément les résultats de différents sites et de les comparer en termes de courbes de dispersion, de profils V_S et de V_S moyenné dans le temps.

Keywords: Iceland; shear wave velocity; surface wave analysis; MASW; database.

1 INTRODUCTION

Seismic site characterization is a fundamental aspect of engineering design of structures in seismically active areas. The seismic hazard in Iceland is considered moderate to high, with the largest earthquakes occurring within two complex fracture zones: the South Iceland Seismic Zone (SISZ) in the south and the Tjörnes Fracture Zone (TFZ) in the north (Einarsson, 2008). The soil site conditions in Iceland are shaped by a combination of volcanic activity, glacial drift, and sea level variations through the ages. The soil deposits largely consist of coarse-grained granular materials of basaltic origin (i.e., coarse silt, sand, gravel, and coarser grains), although thick peat deposits exist in some locations. Clayey materials are uncommon in Iceland (Erlingsson, 2019).

Surface wave methods have been found well-suited for profiling of Icelandic soil sites, including gravelly sites and sites characterized by conglomerated materials or mixed soils containing cobbles or boulders. From 2013 to 2021, MASW (Multichannel Analysis of Surface Waves) measurements were conducted in 19 areas in Iceland. Together, the tested sites represent the three most commonly encountered types of natural soil deposits in Iceland, in addition to engineered fills. This paper describes the first efforts made to create a database where the measurement results, along with supporting data, can be accessed. The database is accessible in open access at https://serice.hi.is. The user interface allows results from different sites to be viewed simultaneously and compared in terms of dispersion curves and measured shear wave velocity (V_S) profiles. The V_S profiles are further presented as time-averaged shear wave velocity ($V_{S,z}$) in line with the site categorization in the current Eurocode 8 [EC8] (CEN, 2004).

2 ANALYSIS PROCEDURE

The term MASW describes a linear data acquisition layout where a vertical impact source is applied in-line with an array of equally spaced receivers that are placed on the surface. The interval V_S profile of the underlying soil stratum is then obtained by inverting the dispersion characteristics of the recorded Rayleigh waves.

The same data acquisition and analysis approach was used for all the sites that are currently included in the database (Figure 1). The in-situ measurements were generally conducted using 24 vertical 4.5 Hz geophones with a spacing of 0.5 m, 1 m, and/or 2 m, depending on site conditions. In exceptional cases, the number of receivers was 12 or 16. Rayleigh waves were generated with a sledgehammer that was struck at various distances (usually in the range of 3–30 m) from one or both ends of each geophone array. Several shot gathers were recorded for each array length and impact point location. Each multi-channel record was analysed separately to quantify the variability of the dispersion curve estimates prior to the inversion. Comparison of dispersion curves obtained at different impact points (i.e., different source offset lengths and forward/reverse shot gathers) was further used during the data analysis for detection of possible near-field effects at certain source offsets and for validation of the 1D assumption adopted in the inversion process. For each test site, the resulting dataset was merged into a single composite curve by adding up the elementary dispersion curves within log-spaced wavelength bands. The composite experimental dispersion curve is subsequently referred to by the abbreviation EDC. A Monte Carlo global search process was then used to identify a set of V_S profiles that fit the observed data, given the uncertainty of the mean EDC and the assumed ground model. A comprehensive description of the data processing and inversion procedures is provided in Olafsdottir et al. (2023).

3 DATABASE OF MEASURED V_S PROFILES

The soil site database currently stores measured dispersion curves, V_S profiles and $V_{S,z}$ from 19 sites in Iceland. Between one and seven measurements are available for each site with an inter-profile distance below 1.1 km and an investigation depth between 10 m and 30 m (Olafsdottir et al., 2023).

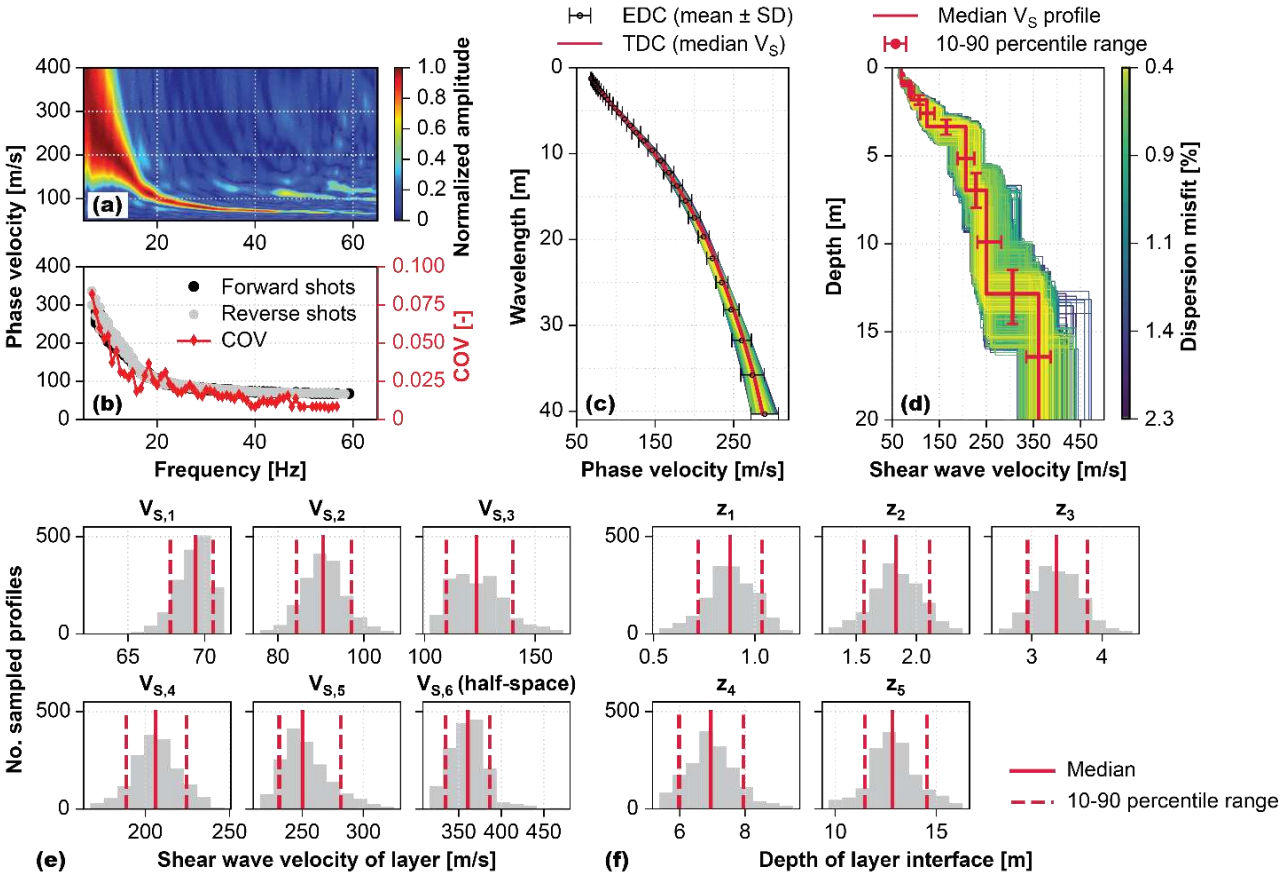

Figure 1. MASW survey by the Ölfus River in South Iceland, illustrating the workflow used for all sites. (a) Spectral image of a single shot gather. (b) Dispersion curves identified from repeated shot gathers (left-hand axis) and variation of the phase velocity values (right-hand axis). (c,d) Sampled V_S profiles (six-layered model) whose theoretical dispersion curves (TDC) fall within the boundary EDCs. The median and 10^{th} to 90^{th} percentile range of the V_S models, and the TDC corresponding to the median V_S profile, are shown in red. (e) Distribution of the shear wave velocity in the i-th layer, $i \in \{1, \dots, 6\}$, and (f) the depth of the i-th layer interface, $i \in \{1, \dots, 5\}$, for the set of velocity models shown in (d).

The user interface is based on an interactive map that shows the surveyed sites (Figure 2). By clicking on a specific map marker, the measurement locations at the given site are displayed (Figure 3a) and the profile(s) of interest can be selected by clicking their unique identifiers (IDs) (Figure 3b). The data are presented in figure form as shown in Figures 3d–f. Results from an unlimited number of measurements (from any survey sites) can be viewed simultaneously. The selected measurements are managed using the check boxes (view/hide) and cross marks (remove) by their profile IDs (Figure 3c).

The interval V_S profile shown for each measurement (Figure 3e) is the median of the subset of sampled V_S profiles whose associated theoretical dispersion curves fall within the boundary EDCs at all wavelengths. The 10th and 90th percentiles of $V_{S,i}$ and z_i are further provided (here $V_{S,i}$ and z_i denote the shear wave velocity in the i-th layer and the depth of the i-th layer interface, respectively).

The mean EDC and its boundary curves are presented as shown in Figure 3d. The boundary EDCs are defined as one standard deviation (SD) above and below the mean curve, except for measurements conducted on top of earth-rockfill dams with a central core, where they are specified as 1.5 SDs from the mean EDC. In those cases, the acquired multi-channel time series likely represent a mixture of the response of the core and shell materials. The theoretical dispersion curve of the median V_S profile is given, thus allowing the user to visually evaluate its fit to the EDC.

The median V_S profile is also given as time-averaged shear wave velocity ($V_{S,z}$, Figure 3f), defined by Eq. (1) where $V_{S,i}$ and h_i are the velocity and thickness of the i-th layer for a total of N layers down to depth z:

$$V_{S,z} = \frac{z}{\sum_{i=1}^{N}\left(\frac{h_i}{V_{S,i}}\right)} \quad (1)$$

Figure 2. The map interface of the soil site database. The current test sites are shown with red markers.

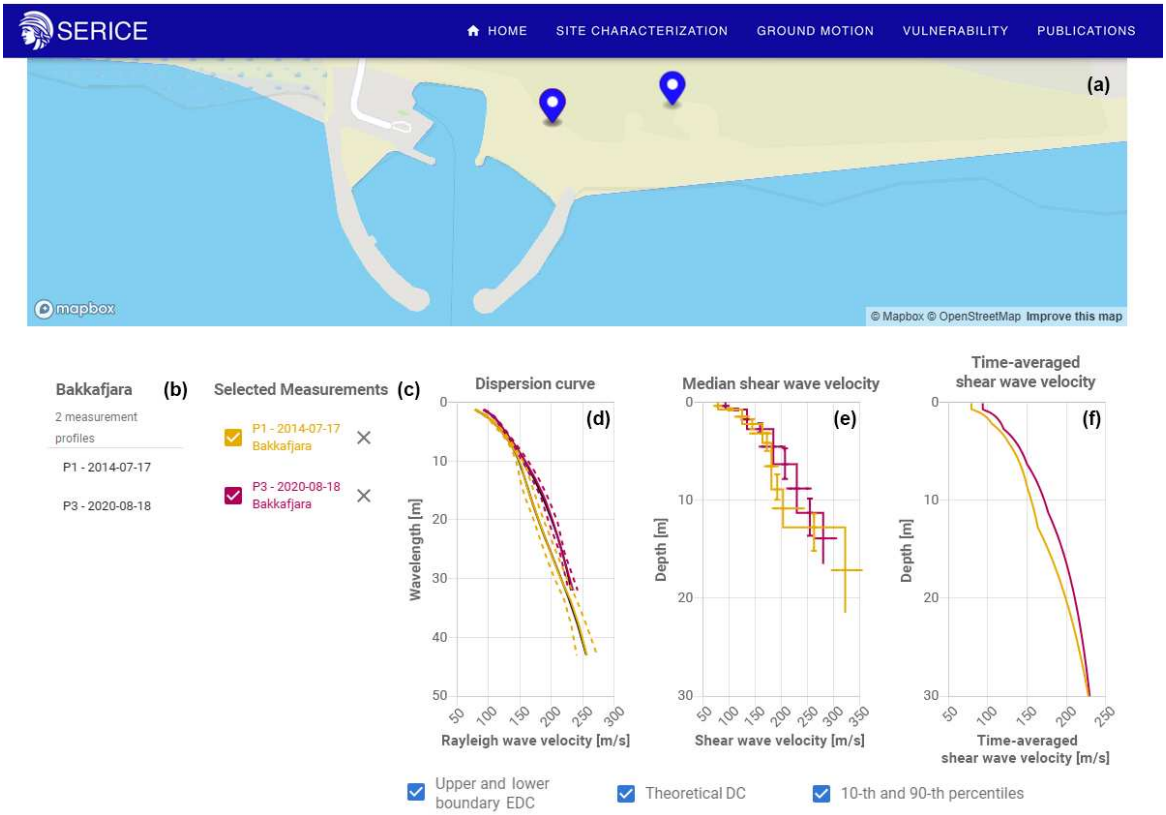

Figure 3. The user interface of the soil site database. (a) Measurement locations and (b) their profile IDs. (c) List of selected measurements. Results presented in terms of (d) dispersion curves, (e) median V_S profiles, and (f) time-averaged V_S.

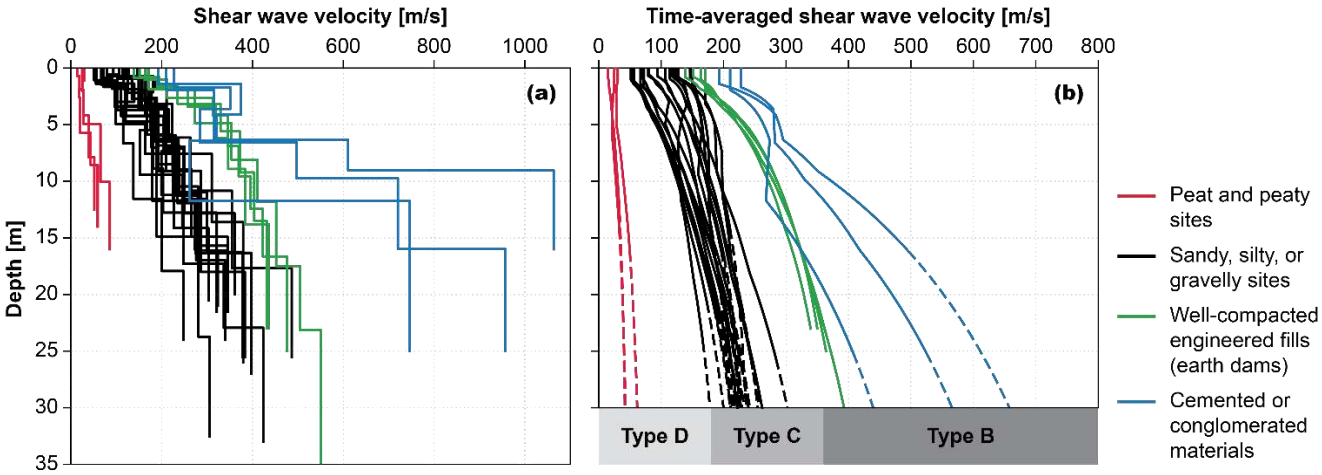

Figure 4. (a) Shear wave velocity (V_S) and (b) time-averaged shear wave velocity ($V_{S,z}$) profiles in the database. The $V_{S,z}$ profiles are shown with dashed lines at depths $z > z_{max}$ for natural sites with a survey depth of $z_{max} < 30$ m. The grey shaded areas in (b) illustrate the $V_{S,30}$ ranges defining ground types B, C, and D in the current EC8 (CEN, 2004).

The $V_{S,z}$ profile of each natural soil site is evaluated down to 30 m. In instances where the survey depth (z_{max}) is less than 30 m, the median V_S is extended to 30 m using the half-space velocity for calculation of $V_{S,z}$ at $z > z_{max}$. When V_S increases with depth, as is expected for all the sites currently included in the database, this approach provides a conservative estimate of $V_{S,30}$.

Figure 4 shows the current collection of median V_S profiles and the corresponding $V_{S,z}$. The tested sites are classified by general soil characteristics as (i) peat and peaty sites, (ii) silty, sandy, or gravelly sites, (iii) well-compacted engineered fills, and (iv) cemented or conglomerated materials. As shown, there is a distinct separation between the four classes. The estimated $V_{S,30}$ values further provide a general indication of the expected EC8 site category of sites within each class. It is though worth mentioning that a $V_{S,30}$ categorization of the peat and peaty sites included in this work is considered uncertain as they might also be categorized as type E or, in some cases, type S_1 or S_2.

4 CONCLUSIONS

Here we present a database (https://serice.hi.is) of surface wave measurements conducted in Iceland. The main purpose is to give researchers and professional engineers access to data and interpreted velocity profiles for design and further analysis.

Future work is aimed at extending the database by adding results from additional sites, as well as adding information on key site effect proxies. Future surveying efforts will also be aimed at assessing the depth of the seismic bedrock formation or the fundamental frequency of the soil deposits, which are required for site categorisation according to the 2nd gen. EC8 (CEN/TC250/SC8, 2021). Further research in this field is believed to be of high value for professional engineers to implement the new site classification scheme and aid simplified identification of site categories in cases where little (or no) site-specific information is available.

ACKNOWLEDGEMENTS

This work was supported by the Icelandic Research Fund (grant no. 206793-053, 218149-053), the Icelandic Road and Coastal Administration, and the Energy Research Fund of the National Power Company of Iceland.

REFERENCES

CEN (2004). *Eurocode 8: Design of structures for earthquake resistance. Part 1: General rules, seismic actions and rules for buildings*, European Committee for Standardization, Brussels, Belgium.

CEN/TC 250/SC 8 (2021). *Eurocode 8: Earthquake resistance design of structures. prEN_1998–1–1_2021_ENQ 2022-01-11*.

Einarsson, P. (2008). Plate boundaries, rifts and transforms in Iceland, *Jökull*, 58, pp. 35-58.

Erlingsson, S. (2019). Geotechnical Challenges in Iceland. *Proceedings of the XVII European Conference on Soil Mechanics and Geotechnical Engineering,* Reykjavik, Iceland, pp. 27-51. https://doi.org/10.32075/17ECSMGE-2019-1109.

Olafsdottir, E. A., Bessason, B., Erlingsson, S. (2023). Gagnagrunnur fyrir skúfbylgjuhraða í jarðsniðum byggður á yfirborðsbylgjumælingum, *Icelandic Journal of Engineering*, 29(1) [in Icelandic]. https://doi.org/10.33112/ije.29.3.

Viðauki D

Elín Ásta Ólafsdóttir, Bjarni Bessason og Sigurður Erlingsson. (2024). MASWavesPy: A Python package for analysis of MASW data. Birt í ráðstefnuriti *19th Nordic Geotechnical Meeting (NGM 2024)*, 18.–20. september 2024, Gautaborg, Svíþjóð.

MASWavesPy: A PYTHON PACKAGE FOR ANALYSIS OF MASW DATA

E.A. Olafsdottir[1], B. Bessason[1] and S. Erlingsson[1,2]

KEYWORDS

Surface wave analysis, MASW, Shear wave velocity, Open-source software

ABSTRACT

This paper presents MASWavesPy, an adaptable, open-source Python package to retrieve S-wave velocity (V_S) profiles from MASW-type active-source surface wave registrations. The data processing and forward modelling tools of MASWavesPy were validated by comparison with existing software. The analysis approach was then assessed by measurements at four geotechnical benchmark sites, where the retrieved V_S profiles were found to be consistent with existing in-situ and laboratory measurements.

1. INTRODUCTION

MASW (multichannel analysis of surface waves) is a non-invasive approach for in-situ evaluation of soil S-wave velocity (V_S) profiles. In the past two decades, surface wave methods (SWM), including MASW, have become increasingly more common in civil engineering practice as tools to retrieve the V_S distribution of soil sites down depths of a few tens of meters.

MASWavesPy is an open-source, adaptable Python package to process and analyze MASW-type active-source surface wave registrations and evaluate soil V_S profiles [1]. It presents an advancement of an earlier MATLAB tool created by the same authors [2,3] with more refined data processing and analysis methods for improved code usability and performance. Computationally intensive parts of the software are written in Cython for increased computational speed. The main aim of this paper is to present the new package and explain its main modules. The data processing and forward modelling tools of MASWavesPy are verified by comparison with existing software. The performance of the package as a whole is then assessed by measurements at four geotechnical benchmark sites in Norway, where V_S profiles obtained with MASWavesPy are compared with existing in-situ and laboratory data.

[1] Faculty of Civil and Environmental Engineering, University of Iceland
[2] VTI – The Swedish National Road and Transport Research Institute

2. METHOD

For MASW field testing (Fig. 1), a linear array of equally spaced receivers is placed on the soil surface and a vertical impact load is applied in-line with the receivers. The interval V_S profile of the underlying soil deposits is then retrieved by inverting the observed Rayleigh wave (R-wave) dispersion curve (DC). The inversion is conducted by modelling the subsurface as n homogeneous and isotropic linear elastic layers over a half-space. Each layer is described by its V_S, P-wave velocity (V_P) (or Poisson's ratio, ν), mass density (ρ) and thickness (h). In this work, the V_S and thickness of each layer are established by inverting the fundamental mode DC. Hence, the term 'dispersion curve' generally refers to its fundamental mode. In line with common practice [4], the values of V_P (or ν) and ρ for each layer are estimated based on available data and assigned fixed values during the inversion process.

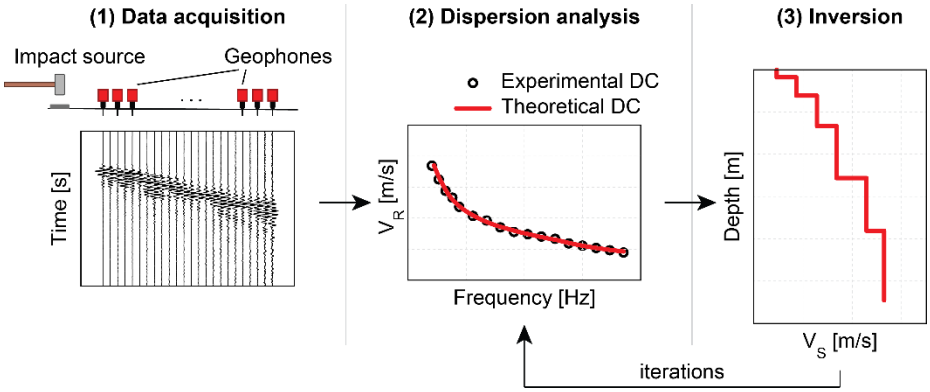

Figure 1. MASW surveying and analysis procedure. (1) Data acquisition: An impact load is applied on the soil surface and the wave propagation is recorded by an array of geophones. (2) Dispersion analysis: Data processing to retrieve the R-wave DC for the site. (3) Inversion: Evaluation of the V_S profile by inversion of the experimental DC.

A single shot gather may be sufficient to retrieve the V_S-depth distribution at a given site. However, to get a quality assessment of the V_S profile it is, in the authors' experience, important to collect multiple records with several impact locations (source offsets) and, in some cases, two or more receiver array lengths. This aligns with prior studies that advice collecting repeated forward and reverse shots to better assess the experimental DC and, consequently, the V_S profile [4-6]. The benefits of using multiple source-receiver configurations include mitigation of near- and far-field effects, the possibility of assessing DC uncertainty, and an extended DC frequency range providing both an improved survey resolution close to surface and an increased surveying depth.

MASWavesPy program structure

MASWavesPy is designed for processing and analyzing surface wave datasets that consist of multiple shot gathers. The package contains four main analysis

modules (`wavefield`, `dispersion`, `combination`, and `inversion`) and two supplementary modules (`dataset` and `select_dc`). MASWavesPy can be installed from the Python Package Index (PyPi) using the command `pip install maswavespy`. Its code, together with a quick start guide and sample data, can also be downloaded from Github (see further https://pypi.org/project/maswavespy/). The implementation described below refers to version v.1.0 (released 02.24). A more comprehensive description of the computational procedure is given in Olafsdottir et al. [1].

The `wavefield` module imports shot gathers as `RecordMC` objects (one object for each shot gather) and transforms each seismic record into the frequency-phase velocity (f–V_R) domain by using the phase shift method [7]. A DC obtained from a single shot gather is here referred to as an elementary DC. The supplementary `dataset` module can be used to batch import surface wave datasets, containing multiple shot gathers, as a `Dataset` object.

The `dispersion` module includes methods to visualize the f–V_R spectrum and identify the corresponding elementary DC. An `ElementDC` object stores the f–V_R domain representation of a given `RecordMC` and the identified elementary DC. In the f–V_R domain, the propagation of the fundamental R-wave mode (and higher modes, if excited) is revealed by the spectral amplitude maxima. Hence, the experimental DC is extracted by picking the relevant amplitude maxima over a range of frequencies. The `select_dc` module provides an easy-to-use graphical user interface (GUI) to aid the DC extraction. It also includes a function to automatically identify the absolute amplitude maxima at each frequency. It should, however, be noted that manual inspection of the spectral image, and the trend shown by the amplitude maxima with frequency, is a crucial aspect of the DC identification. Sometimes, the fundamental mode may be associated with a local maximum of the spectral image or masked by a higher mode or disturbances in the seismic data.

The `combination` module provides methods to combine elementary DCs, obtained from multiple shot gathers, into a composite DC with upper and lower boundaries [8]. It is, therefore, specifically intended for processing surface wave datasets. It further provides tools to assess the variation within the set of picked elementary DCs with wavelength or frequency. A `Dataset` object contains multiple `RecordMC` and `ElementDC` objects (one pair for each imported shot gather) and provides a routine for initializing a `CombineDCs` object for the set of records or a given subset of processed records.

Lastly, the `inversion` module provides routines to assess the V_S profile of the surveyed site by inverting the composite DC (as is recommended) or a particular elementary DC. The inversion methods, including methods for post-processing and visualizing the inversion results, are defined on an `InvertDC` object that is initialized using a given DC. The fast delta matrix algorithm [9]

is used for forward modelling (i.e., computation of theoretical DCs) and a Monte-Carlo global search algorithm [3] for searching the solution space for the optimal set of model parameters (V_S and h for each layer). A detailed description of the inversion process and recommended practices, e.g., related to model parameterization, is provided in Olafsdottir et al. [1,3].

3. EVALUATION OF MASWavesPy

Comparison with other computational methods

The wavefield transformation and DC extraction methods of MASWavesPy were verified by comparing their results with those of the Active FK toolbox of Geopsy [10]. Figure 2 shows spectral images that were obtained with the two programs using data from three locations in Iceland (one 24-channel shot gather for each site). The three sites are characterized by sediments of Holocene granular materials but have different surficial grain size distributions (silty sand to sandy gravel) and surficial compaction levels.

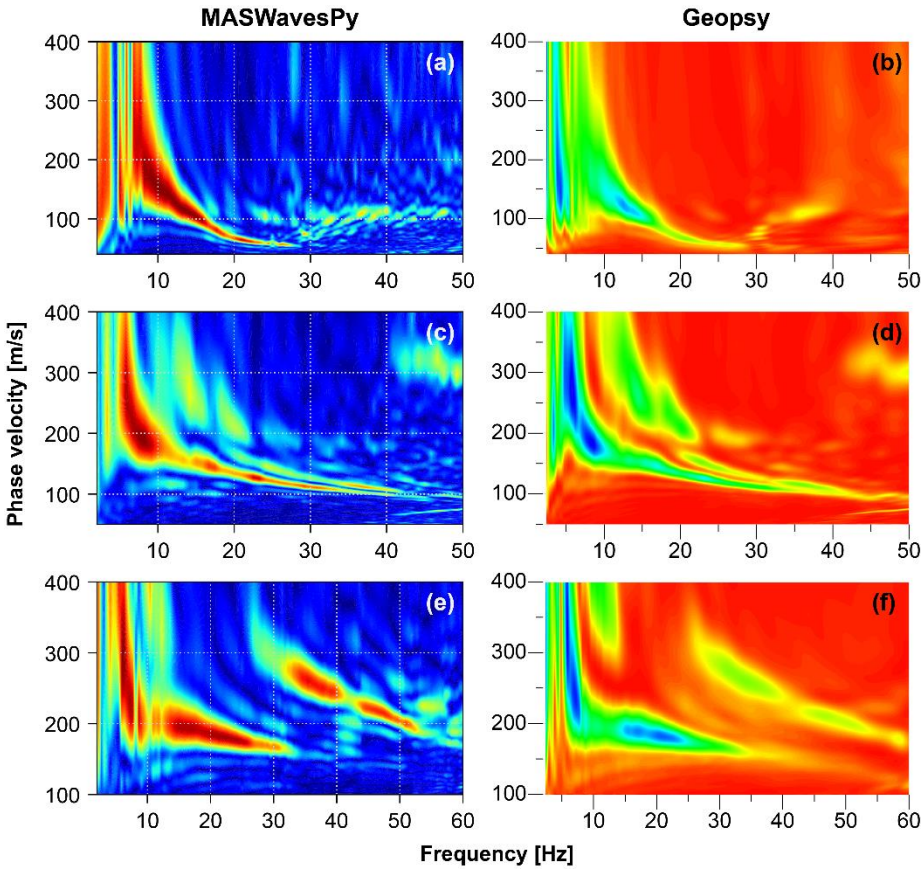

Figure 2. Spectral images obtained with MASWavesPy (left column) and Geopsy (right column). (a,b) Site I. (c,d) Site II. (e,f) Site III.

The corresponding elementary DCs are given in Fig. 3, where they are presented in the phase velocity-wavelength (V_R–λ) domain. Also shown is the composite DC for each site with experimental boundaries defined as one standard deviation of the mean curve. Each composite DC was retrieved using a variety of receiver array lengths and source offsets. Therefore, its wavelength range is wider than that of the two elementary DCs.

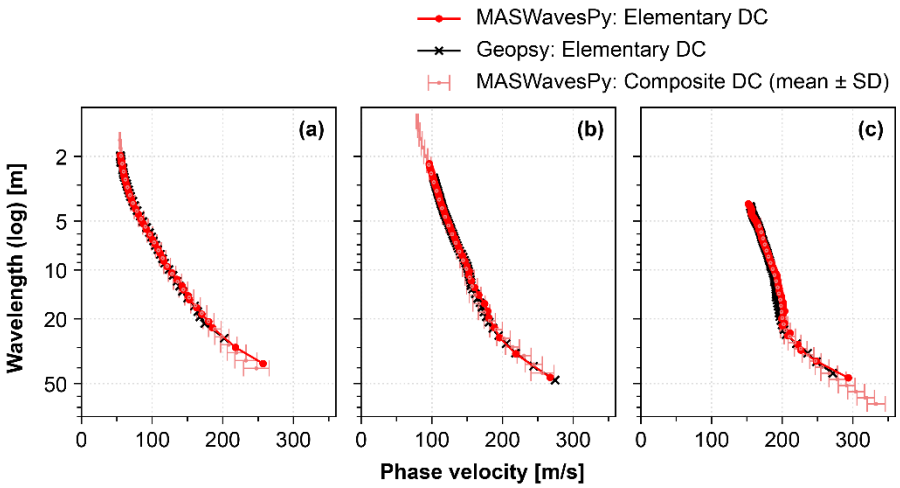

Figure 3. Comparison of experimental DCs obtained with MASWavesPy and Geopsy for (a) site I, (b) site II, and (c) site III. The elementary DCs are extracted from the spectral images shown in Fig. 2. The composite DC (obtained with MASWavesPy) for each site is shown with upper and lower boundaries corresponding to one standard deviation (SD) of the mean curve.

As shown in Figs. 2 and 3, there is a good agreement between Geopsy and MASWavesPy. Each pair of spectral images shows the same dispersion characteristics. The extracted DCs also agree well, with the observed inter-code differences being smaller than, or comparable to, the estimated uncertainty of the composite DC. The fundamental R-wave mode dominated the surface wave signal at sites I and II. At site III, a higher mode was found to dominate at frequencies exceeding 30 Hz (Figs. 2ef), therefore limiting the maximum frequency (minimum wavelength) of the extracted DCs (Fig. 3c). For site II, the spectral imaging routines of both programs revealed higher mode propagation between approximately 12 Hz and 40 Hz (Figs. 2cd). The effects of this on the identification of the fundamental mode DC were though minimal (Fig. 3b).

The forward modelling tool of MASWavesPy was evaluated by comparing its results to those of the gpdc module in Geopsy [10]. Figure 4 shows theoretical dispersion curves (TDCs) that were obtained using the two programs for three soil layer models of varying complexity (Table 1). The models, initially defined by Tokimatsu et al. [11], all present values of V_S that are consistent with

those commonly measured in the upper-most 15–20 m at granular soil sites. Model A represents a normally dispersive soil profile. The S-wave velocity varies more irregularly in models B and C, with a stiff surficial layer in model B and a low-velocity layer at depths of 6–14 m in model C. The TDCs were computed over a frequency range of 3–100 Hz, as commonly retrieved in active-source surveys. As shown in Fig. 4, the results show excellent agreement between the two programs, with the TDCs in all cases being nearly identical.

Table 1. Definition of soil layer models A, B and C.

Layer	h [m] (All)	V_P [m/s] (All)	ρ [kg/m^3] (All)	V_S [m/s] Model A	Model B	Model C
1	2.0	360	1800	80	180	80
2	4.0	1000	1800	120	120	180
3	8.0	1400	1800	180	180	120
4	(infinite)	1400	1800	360	360	360

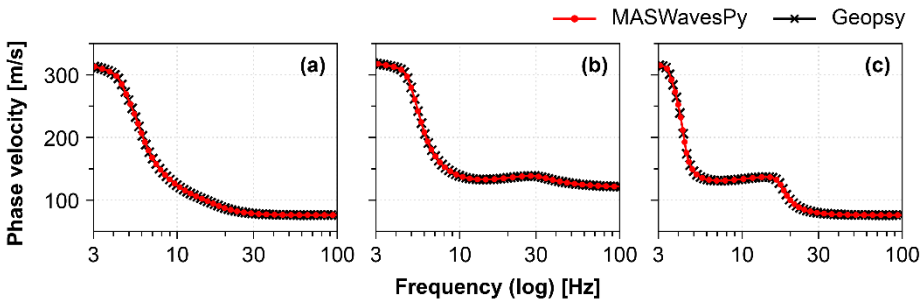

Figure 4. Comparison of theoretical dispersion curves computed with MASWavesPy and Geopsy for (a) model A, (b) model B, and (c) model C.

Comparison with invasive and non-invasive measurements of V_S

For further evaluation of the package, velocity profiles obtained using MASWavesPy were compared with results of invasive, non-invasive, and laboratory-scale measurements of V_S at four well-established geotechnical research sites in Norway. The Halden, Øysand and Tiller-Flotten sites were developed in the Norwegian GeoTest Site (NGTS) project [12]. The research site at Onsøy was established in the late 1960s [13]. The four sites are characterized by deposits of silt, soft clay, silty sand, and quick clay [12-16]. They are, therefore, considered representative of soft soil conditions commonly encountered in engineering practice.

The MASW data was acquired using a set of 24 vertical 4.5 Hz geophones with the receiver arrays placed as close as possible to the relevant invasive measurements. However, some differences may be expected in the V_S assessments as the invasive tests are point measurements whilst SWMs average the soil stiffness properties over a larger area. A certain degree of variability is further associated with inverted V_S profiles, e.g., resulting from the non-

uniqueness of the R-wave DC inversion and the choice of layering parameterization. The MASWavesPy data processing and analysis is described in Olafsdottir et al. [1]. An example illustrating the analysis process is given in Fig. 5, showing data and results from Tiller-Flotten.

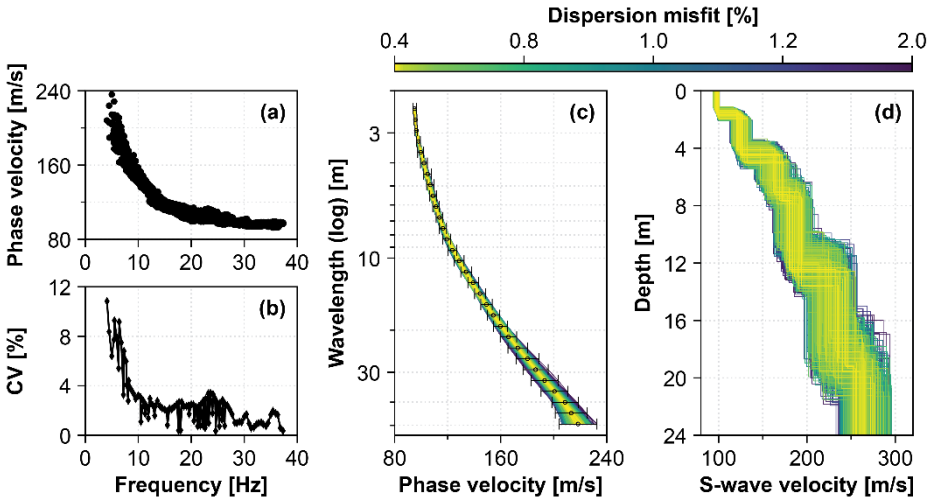

Figure 5. MASW survey at the Tiller-Flotten geotechnical research site. (a) Set of elementary DCs retrieved by processing repeated shot gathers collected at the site. (b) Coefficient of variation (CV) of the identified elementary DCs. (c,d) Sampled V_S profiles whose TDCs fall within one standard deviation (SD) of the composite DC at all wavelengths. The V_S profiles and associated TDCs are color-coded by dispersion misfit values. In (c), the composite DC (mean ± SD) is shown in black.

Figure 6 compares the resulting velocity profiles with the independent assessments of V_S for each of the four sites. The MASWavesPy results are summarized by the median of the set of sampled V_S models whose TDCs fall within one standard deviation of the composite DC. The lowest misfit V_S profile for each site is also shown. The comparison in Fig. 6 reveals that the V_S profiles obtained with MASWavesPy are, overall, consistent with those established with invasive techniques (SCPT and SDMT) and MASW surveys conducted with other hardware and software. They further show comparable values as the laboratory assessments of V_S available for the Halden, Onsøy and Øysand sites.

4. CONCLUSIONS

This paper presents MASWavesPy, an adaptable, open-source Python package to establish soil V_S profiles from MASW-type surface wave data. It is based on an earlier MATLAB tool created by the same authors, with more refined data processing and analysis methods for improved code usability. Furthermore, efforts were made to improve the computational performance of the

forward modelling to decrease the run-time of global search approaches in the inversion.

The wavefield transformation, DC extraction and forward modelling tools of MASWavesPy were verified by comparing their results with those of Geopsy, a widely known software for active-source and ambient vibration processing. The performance of the package as a whole was subsequently assessed by measurements at four geotechnical benchmark sites in Norway, where velocity profiles obtained with MASWavesPy were found to be consistent with those previously obtained at the same locations with a variety of in-situ and laboratory techniques.

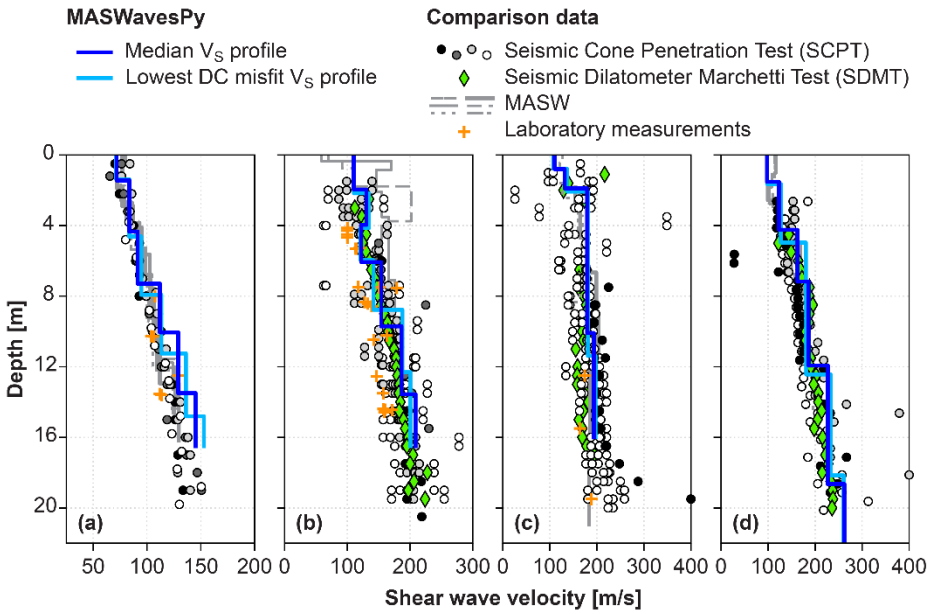

Figure 6. Comparison of inverted V_S profiles (MASWavesPy) and results of invasive, non-invasive and laboratory measurements of V_S for (a) Onsøy, (b) Halden, (c) Øysand, and (d) Tiller-Flotten. SCPT, SDMT, MASW and laboratory results from Blaker et al. [14], Quinteros et al. [15], L'Heureux, Lindgård, and Emdal [16], Long and Donohue [17], Bazin et al. [18], NGI [19], and NGTS data. Figure altered from Olafsdottir et al. [1].

ACKNOWLEDGEMENTS

This work was supported by the Icelandic Research Fund (grants no. 206793-053, 218149-053), the Icelandic Road and Coastal Administration, the Energy Research Fund of the National Power Company of Iceland, and the University of Iceland Research Fund (grant no. 94242). The authors thank the organizers of the NGTS project (www.geotestsite.no) for assistance prior to and during the data acquisition at the Norwegian research sites, and for providing access to results of in-situ and laboratory measurements conducted at the sites.

REFERENCES

[1] E. A. Olafsdottir, B. Bessason, S. Erlingsson and A. M. Kaynia: A Tool for Processing and Inversion of MASW Data and a Study of Inter-Session Variability of MASW. Geotechnical Testing Journal, vol. 47, no. 5, 2024. doi:10.1520/GTJ20230380

[2] E. A. Olafsdottir, S. Erlingsson and B. Bessason: Tool for analysis of multichannel analysis of surface waves (MASW) field data and evaluation of shear wave velocity profiles of soils. Canadian Geotechnical Journal, vol. 55, no. 2, pp. 217–233, 2018. doi:10.1139/cgj-2016-0302

[3] E. A. Olafsdottir, S. Erlingsson and B. Bessason: Open-Source MASW Inversion Tool Aimed at Shear Wave Velocity Profiling for Soil Site Explorations. Geosciences, vol. 10, no. 8, 2020. doi:10.3390/geosciences10080322

[4] S. Foti et al.: Guidelines for the good practice of surface wave analysis: a product of the InterPACIFIC project. Bulletin of Earthquake Engineering, vol. 16, no. 6, pp. 2367–2420, 2018. doi:10.1007/s10518-017-0206-7

[5] C. M. Wood and B. R. Cox: A comparison of MASW dispersion uncertainty and bias for impact and harmonic sources. Proc. of GeoCongress 2012, pp. 2756–2765, 2012. doi:10.1061/9780784412121.282

[6] J. P. Vantassel and B. R. Cox: SWprocess: a workflow for developing robust estimates of surface wave dispersion uncertainty. Journal of Seismology, vol. 26, pp. 731–756, 2022. doi:10.1007/s10950-021-10035-y

[7] C. B. Park, R. D. Miller and J. Xia: Imaging dispersion curves of surface waves on multi-channel record. SEG Technical Program Expanded Abstracts 1998, pp. 1377–1380, 1998. doi:10.1190/1.1820161

[8] E. A. Olafsdottir, B. Bessason and S. Erlingsson: Combination of dispersion curves from MASW measurements. Soil Dynamics and Earthquake Engineering, vol. 113, pp. 473–487, 2018. doi:10.1016/j.soildyn.2018.05.025

[9] P. W. Buchen and R. Ben-Hador: Free-mode surface-wave computations. Geophysical Journal International, vol. 124, no. 3, pp. 869–887, 1996. doi:10.1111/j.1365-246X.1996.tb05642.x

[10] M. Wathelet et al.: Geopsy: a user-friendly open-source tool set for ambient vibration processing. Seismological Research Letters, vol. 91, no. 3, pp. 1878–1889, 2020. doi:10.1785/0220190360

[11] K. Tokimatsu, S. Tamura and H. Kojima: Effects of multiple modes on Rayleigh wave dispersion characteristics. Journal of Geotechnical Engineering, vol. 118, no. 10, pp. 1529–1543, 1992. doi:10.1061/(ASCE)0733-9410(1992)118:10(1529)

[12] J.-S. L'Heureux et al.: Norway's National GeoTest Site Research Infrastructure (NGTS). Proc. of the 19th Int. Conf. on Soil Mechanics and Geotechnical Engineering, pp. 611–614, 2017.

[13] T. Lunne, M. Long and C. F. Forsberg: Characterisation and engineering properties of Onsøy clay. Characterisation and Engineering Properties of Natural Soils, vol. 1, pp. 395–428, 2003.

[14] Ø. Blaker et al.: Halden research site: geotechnical characterization of a post glacial silt. AIMS Geosciences, vol. 5, no. 2, pp. 184–234, 2019. doi:10.3934/geosci.2019.2.184

[15] S. Quinteros et al.: Øysand research site: Geotechnical characterisation of deltaic sandy-silty soils. AIMS Geosciences, vol. 5, no. 4, pp. 750–783, 2019. doi:10.3934/geosci.2019.4.750

[16] J.-S. L'Heureux, A. Lindgård and A. Emdal: The Tiller-Flotten research site: Geotechnical characterization of a very sensitive clay deposit. AIMS Geosciences, vol. 5, no. 4, pp. 831–867, 2019. doi:10.3934/geosci.2019.4.831

[17] M. Long and S. Donohue: In situ shear wave velocity from multichannel analysis of surface waves (MASW) tests at eight Norwegian research sites. Canadian Geotechnical Journal, vol. 44, no. 5, pp. 533–544, 2007. doi:10.1139/t07-013

[18] S. Bazin et al.: Geophysical characterisation of marine and quick clay sites: field and laboratory tests. Proc. of the 5th Int. Conf. on Geotechnical and Geophysical Site Characterisation, vol. 2, pp. 831–836, 2016.

[19] NGI: Field and laboratory test results Halden. Norwegian GeoTest Sites (NGTS). Factual report 20160154-04-R, Norwegian Geotechnical Institute (NGI), 2018.